SUPPORTING INFORMATION

Single-step Ugi Multicomponent Reaction for the Synthesis of Phosphopeptidomimetics

Andrea F.G. Gargano[†], Stefanie Buchinger[†], Michal Kohout[†], Wolfgang Lindner[†], Michael Lämmerhofer[‡*]

[†] Department of Analytical Chemistry, University of Vienna, Waehringer Strasse 38, 1090 Vienna, Austria

[‡] Institute of Pharmaceutical Sciences, University of Tübingen, Auf der Morgenstelle 8, 72076 Tübingen, Germany

Correspondence:
Michael Lämmerhofer
Institute of Pharmaceutical Sciences
University of Tübingen
Auf der Morgenstelle 8
72076 Tübingen, Germany
T +49 7071 29 78793
F +49 7071 29 4565
mail to:michael.laemmerhofer@uni-tuebingen.de

Table of contents

Section S1: X-Ray crystallography structure

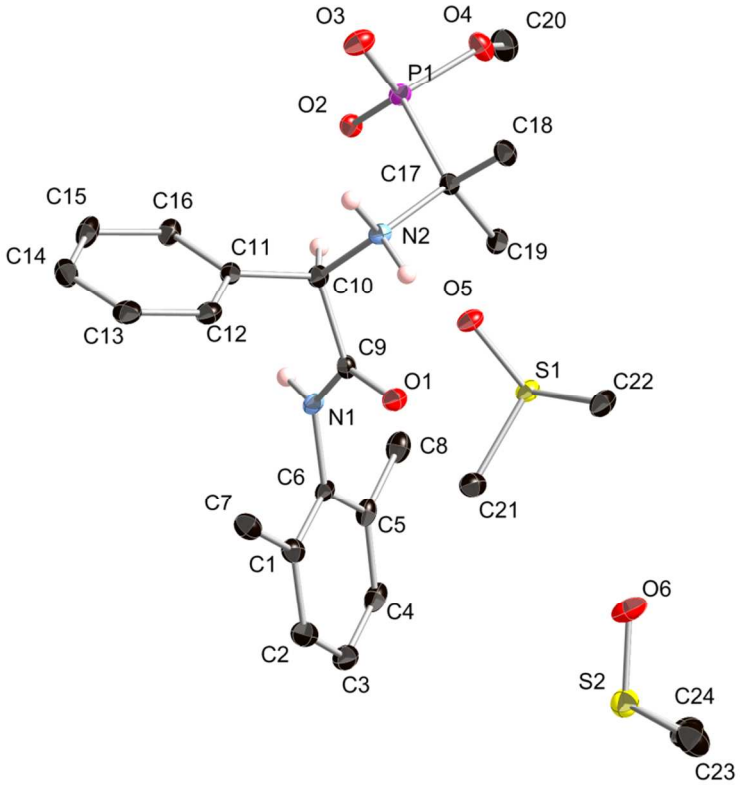

Figure S1: Crystallographic structure of *Table 3* compound **1**. Thermal ellipsoids drawn at the 35% probability level, selected hydrogens omitted for clarity. Empirical formula: $C_{20}H_{27}N_2O_4P$, $2(C_2H_6OS)$. Formula weight: 546.66 g/mol. Temperature: 100(2) K. Wavelength: 0.71073 Å. Crystal system: Triclinic. Space group: *P*-1. Unit cell dimensions: a = 9.373(3) Å, α = 108.637(5)°b = 12.019(4) Å β = 95.801(6), c = 13.078(4) Å, γ = 95.605(4)°. Z = 2. Goodness-of-fit on F2: 1.093. Final R indices [I > 2σ(I)]: R1 = 0.0691, wR2 = 0.1179. R indices (all data): R1 = 0.1056, wR2 = 0.1320. The crystal structure has been deposited in the Cambridge Structural Database (CCDC 940294).

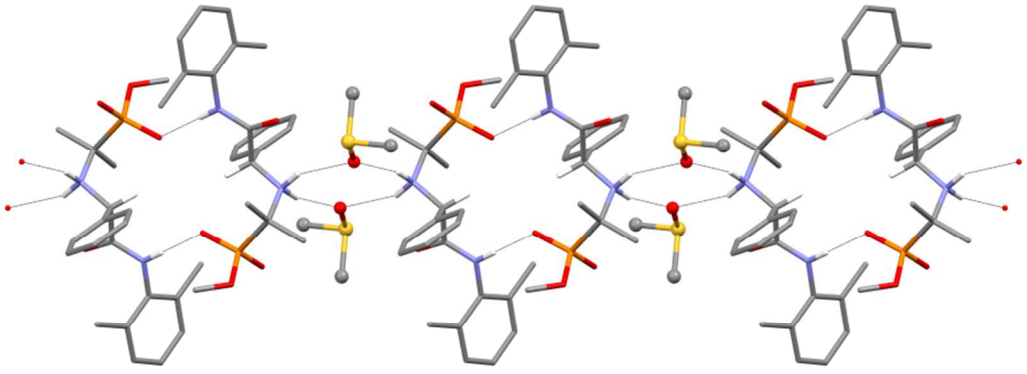

Figure S2: Crystallographic structure **1** *Table 3:* Formation of hydrogen-bonded chains along the b axis.

Section S2: Chromatographic characterization

*Example of reversed-phase characterization of the reaction mixture from Table 3 product **1***

a)

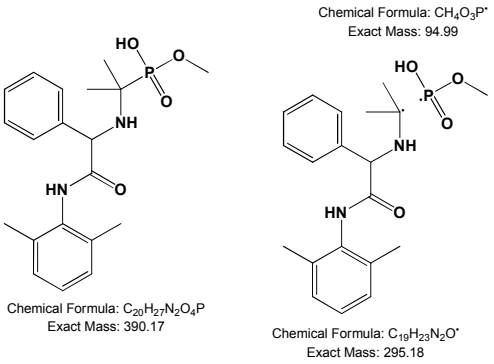

b)

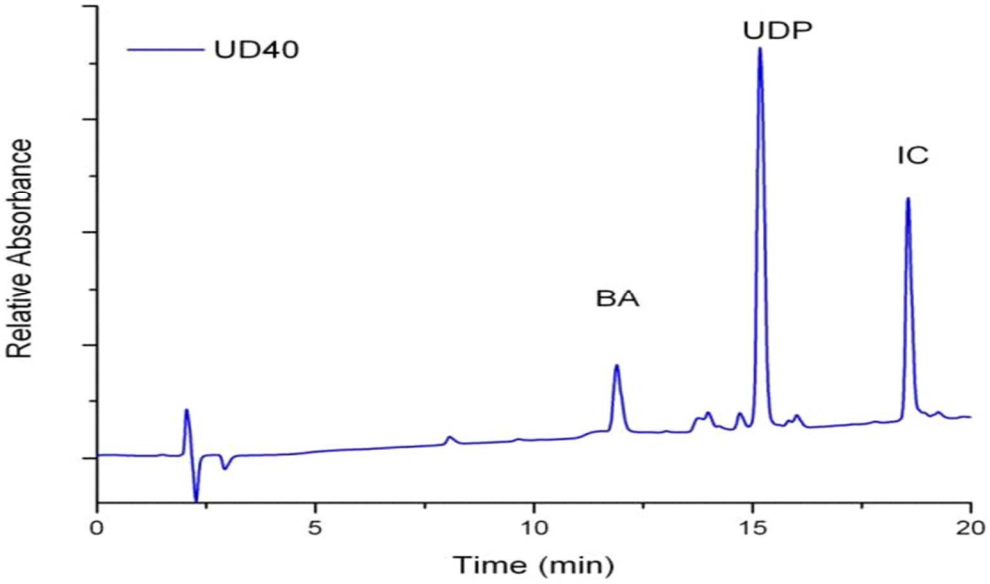

c)

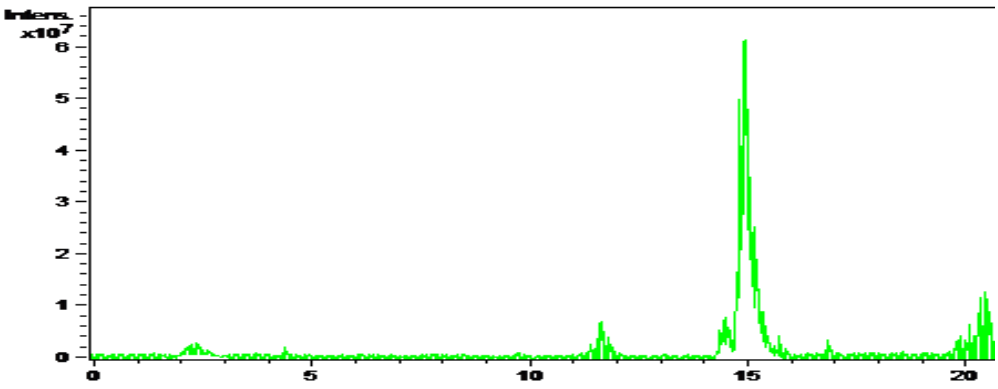

d)

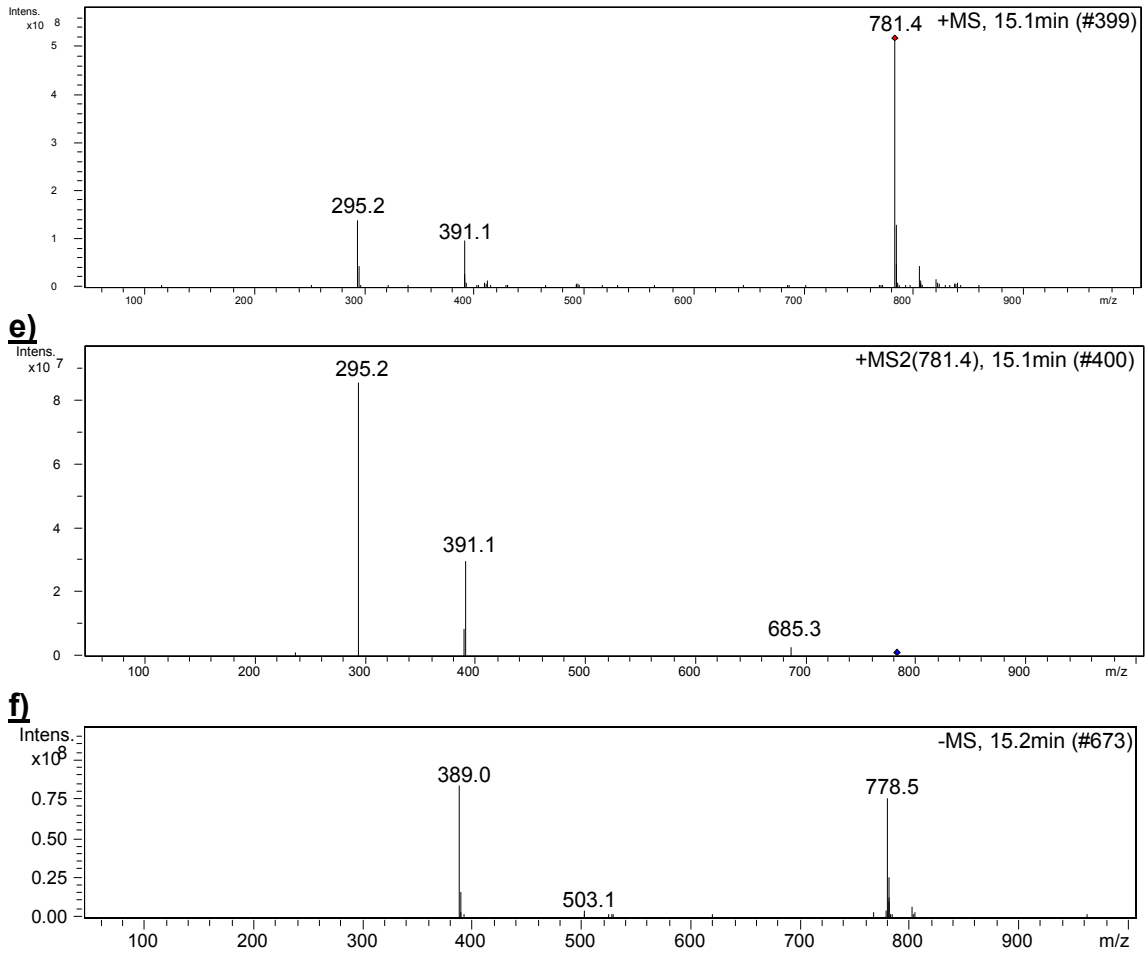

Figure S3: **a)** Chemical structure, Mw and fragmentation of *Table 3* product **1**, used as target compound during the synthesis optimization. **b)** RPLC-UV chromatogram of the crude product of *Table 3* product **1** (BA= benzaldehyde, IC= 2,6-dimethylphenyl isocyanide; UDP = product code). **c)** Total Ion Current (TIC) chromatogram (50-1000 m/z) of the RP analysis of the crude product of *Table 3* product **1**. **d)** MS spectrum in positive mode of product peak (UDP, retention time: 15 min), the compound in ESI generate dimers. **e)** MS/MS of the dimer of product peak (781), resulting in the MS of the product (391) and a specific product fragment (295, see Fig. S1 a). **f)** MS spectrum of product peak in negative mode (UDP, retention time = 15.1 min).

Chromatographic enantioseparation

The compounds of *Table 3* entry **1**-**5** and **7**-**15** as well as the compounds reported in *Table 4* were purified adopting a weak chiral anion-exchanger based on carbamoylated quinidine or quinine stationary phases (CHIRALPAK QD-AX or QN-AX™).
Figure S4 depicts an example of a preparative enantioseparation on CHIRALPAK QD-AX, namely of *Table 3* product **5**. Detailed mechanistic descriptions of the enantioseparation as well as results obtained for various amido-aminophosphonate compounds are available in the following reference. [1]
Typically, enantioseparations were performed adopting mobile phases composed of methanol-acetic acid-ammonium acetate (98/2/0.5; v/v/m) for analytical separations or methanol-formic acid with apparent pH in the mixture adjusted typically to 4 with ammonia for preparative separations. Molar concentrations of formic acid (formate represents counterion in this system) were adjusted to achieve elution in reasonable time. Column dimension was 150 x 4 mm ID (analytical) or 250 x 16 mm ID (for preparative separations). Detection for aromatic compounds performed at λ= 254 nm and 214 for non-aromatic amido-aminophosphonates. For analytical separations flow-rate was 1 mL/min and injection volume 5 µL.

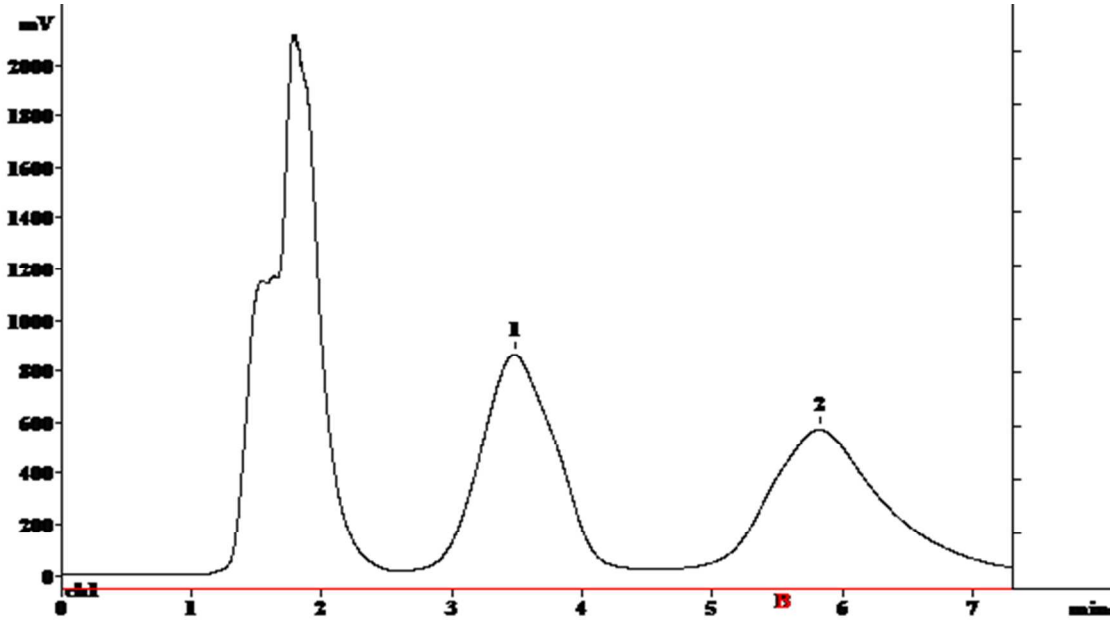

Figure S4: Chromatogram of preparative enantioseparation of *Table 3* product **5** (1 and 2 in the figure indicates corresponding enantiomers; the front peak contains unreacted reactants). Mobile phase composed of MeOH containing 75 mM formic acid with the apparent pH adjusted to 4 using ammonium hydroxide. Stationary phase, CHIRALPAK QD-AX™, 250 x 16 mm ID packed with 100 Å, 10 µm silica gel-based particles. Detection performed at λ=310 nm, flow-rate of 15 mL/min and an injection volume of 1 mL (25 mg per injection).

Optimization of hydrolysis procedure

In order to evaluate the possibility of generating a phosphonic acid derivative from the obtained phosphonate compounds without hydrolysis of amide bond and racemization of stereogenic center in case of enantiomeric substances, we investigated several hydrolysis approaches (*Figure S5 and Table S1).* Phosphonic acid monoesters are commonly transformed into the corresponding acids by adopting acidic or basic media, like aqueous HCl or NaOH. [2] Such conditions were not suitable for the hydrolysis of our target compound (*Table 3* product **1***)*. Therefore, other methods had to be selected; amongst those trimethylsilylbromide (TMSBr) seemed the most promising. This result was confirmed by our findings. Quantitative yields were furnished by hydrolysis with TMSBr in dichloromethane (*Figure S6)*.The optimized reaction protocol was also tested with an isolated enantiomer and no racemization was observed (*Figure S7)*.

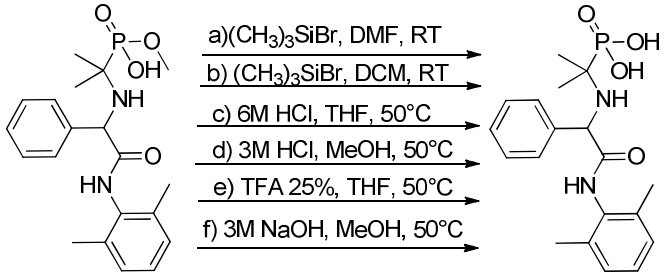

Figure S5: Optimization of hydrolysis procedure

Table S1: All the reactions were performed starting from 2 mg of *Table 3* compound **1** and left to react overnight

	% free acid	% methyl ester
a	40	60
b	100	0
c	40	60
d	23	77
e	4	96
f	4	96

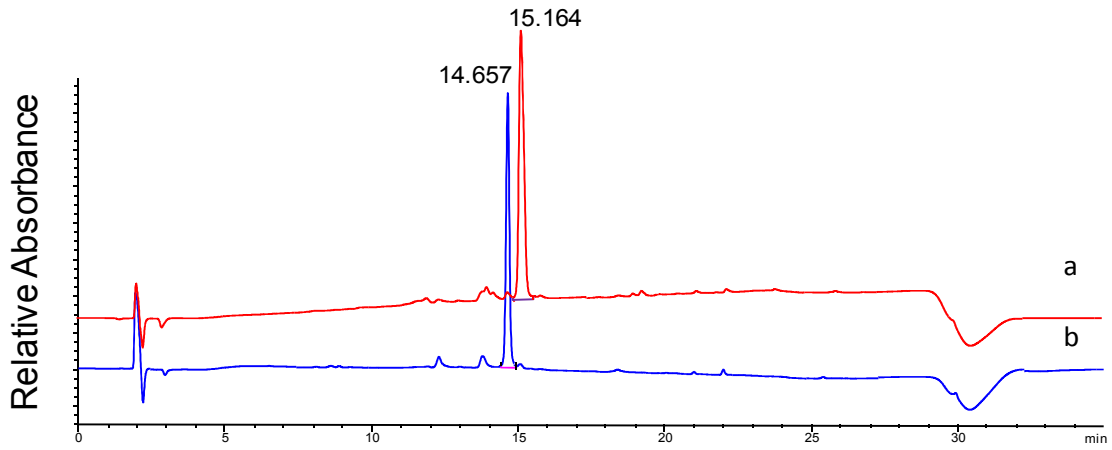

Figure S6: Overlay of RP-HPLC chromatograms of Table 3 compound 1 a) before (red trace) and b) after hydrolysis with TMSBr in dichloromethane (blue trace).

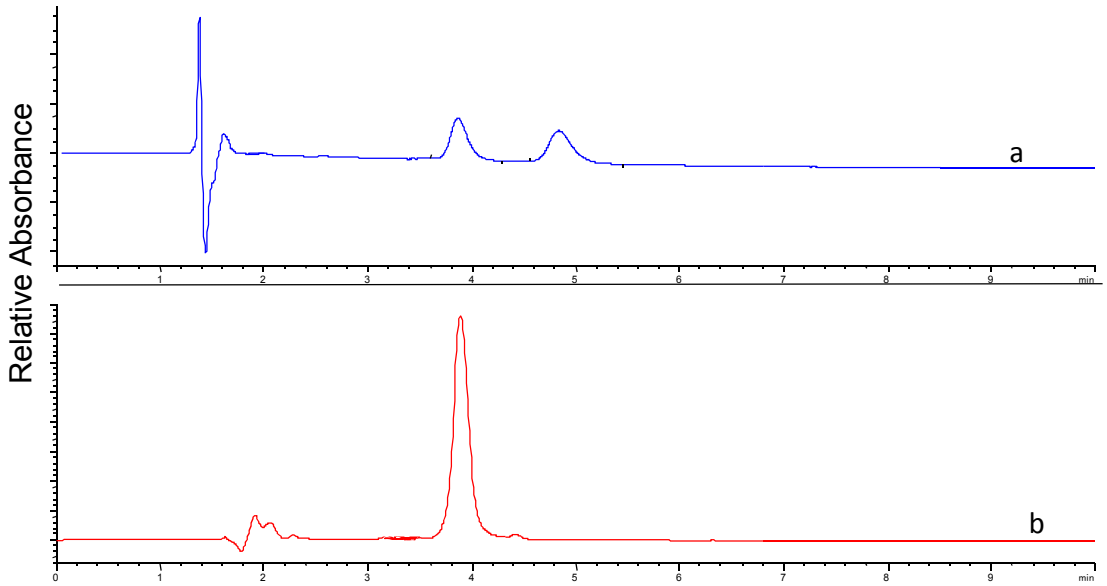

Figure S7: Chiral anion-exchange chromatograms of hydrolysis reaction products using TMSBr in DCM performed a) with racemate (blue trace) and b) single enantiomer (red trace) of *Table 3* compound **1** entry (b, ee before and after hydrolysis >98%).

Section S3: NMR Spectra

Table 3 product **1** has been purified by different purification procedures, in order to examine the effect on the form in which the zwitterionic amido-aminophosphonic acid compound is obtained: in free zwitterionic form (*Figure N1,a*), as formate salt (*Figure N1,b*), or as tetrabutylammonium salt (*Figure N1,e*).

Interesting to note is the difference in shape and position of the dimethyl signals in the ^{1}H-NMR spectra of *Table 3* compound **1**. When different purification procedures were employed and different forms of compound **1** were ^{1}H-NMR spectroscopically investigated. In the zwitterionic form of *Figure N1, (a)* The dimethyl aromatic signal of compound **1** exists as a broad peak, since such residue in its rotation along the N-C bond is present in different spatial distances from the amide group. The bulkiness of the residue hinders the free rotation to an extent that under NMR experiment time it is possible to identify such phenomena as band broadening.
A possible explanation for the difference in shape and position of this signal when compound **1** is purified by chiral chromatography or crystallization could be found in the presence/absence of counterion in the product. The counterions might lead to different supramolecular structure which would explain the different position and shape of the dimethyl signals. The compound purified by crystallization is in fact obtained as racemate while the one purified by chromatography is obtained as a single enantiomer. In highly concentrated solution, such as the one for the NMR measurement (20 mg/mL), the racemic amido-aminophosphonate molecule can undergo hydrogen bonding between the amide portion of one molecule and the acidic residue of another similarly to what is observed in its crystal structure (Figure S2 of supporting information). This circumstance constrains the rotation of the dimethyl phenyl residue and therefore a sharper peak is observed.
When formic acid is present and acts as counter-ion, it may disturb the formation of the above described supramolecular system or yields a different one, which may impact the freely rotating system of the dimethyl phenyl residue leading to different shape and position of the dimethyl signals.

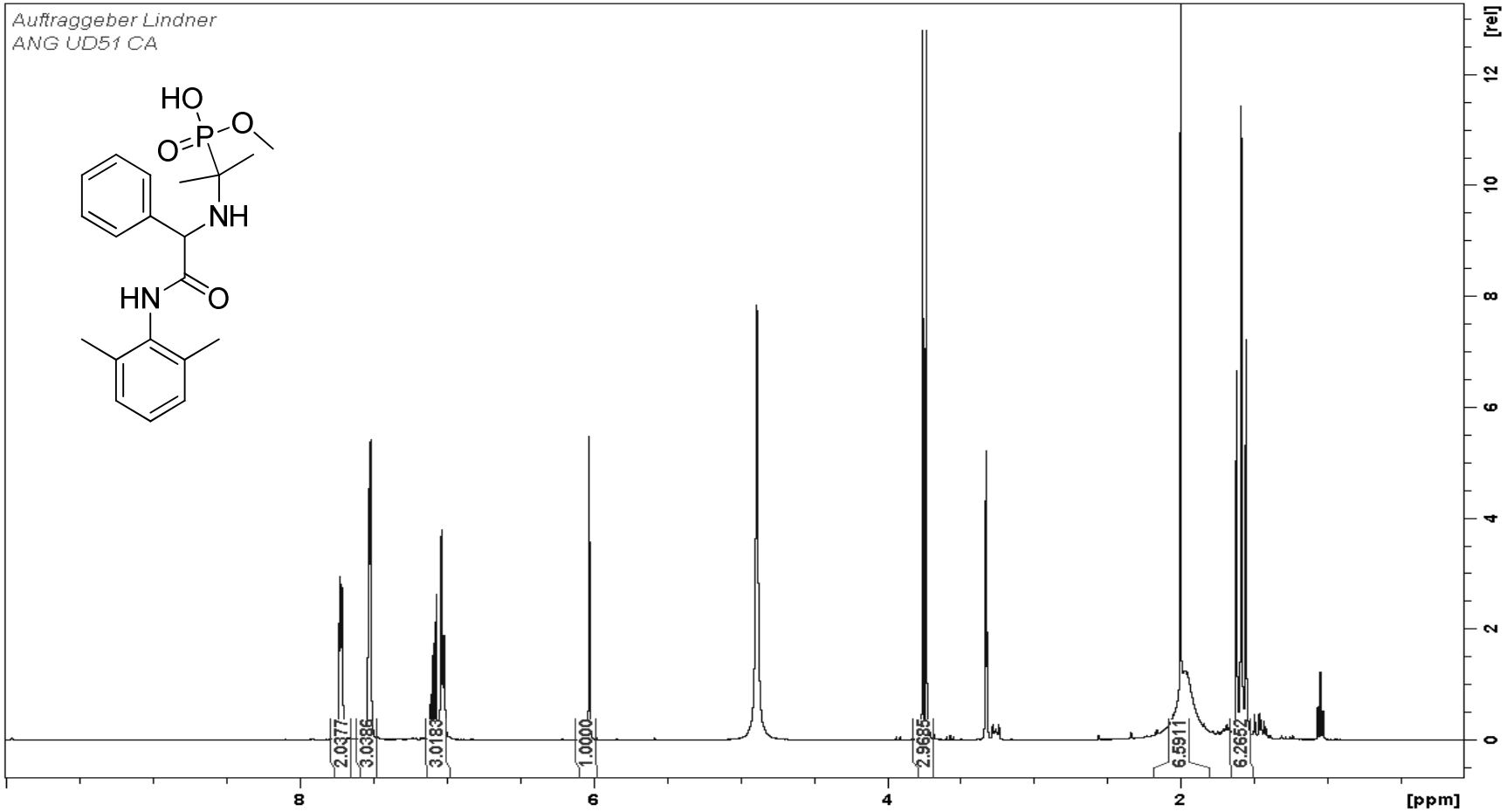

Figure N1, (a): ^{1}H NMR spectrum of *Table 3* compound **1** purified by crystallization (NMR solvent: in CD_3OD)

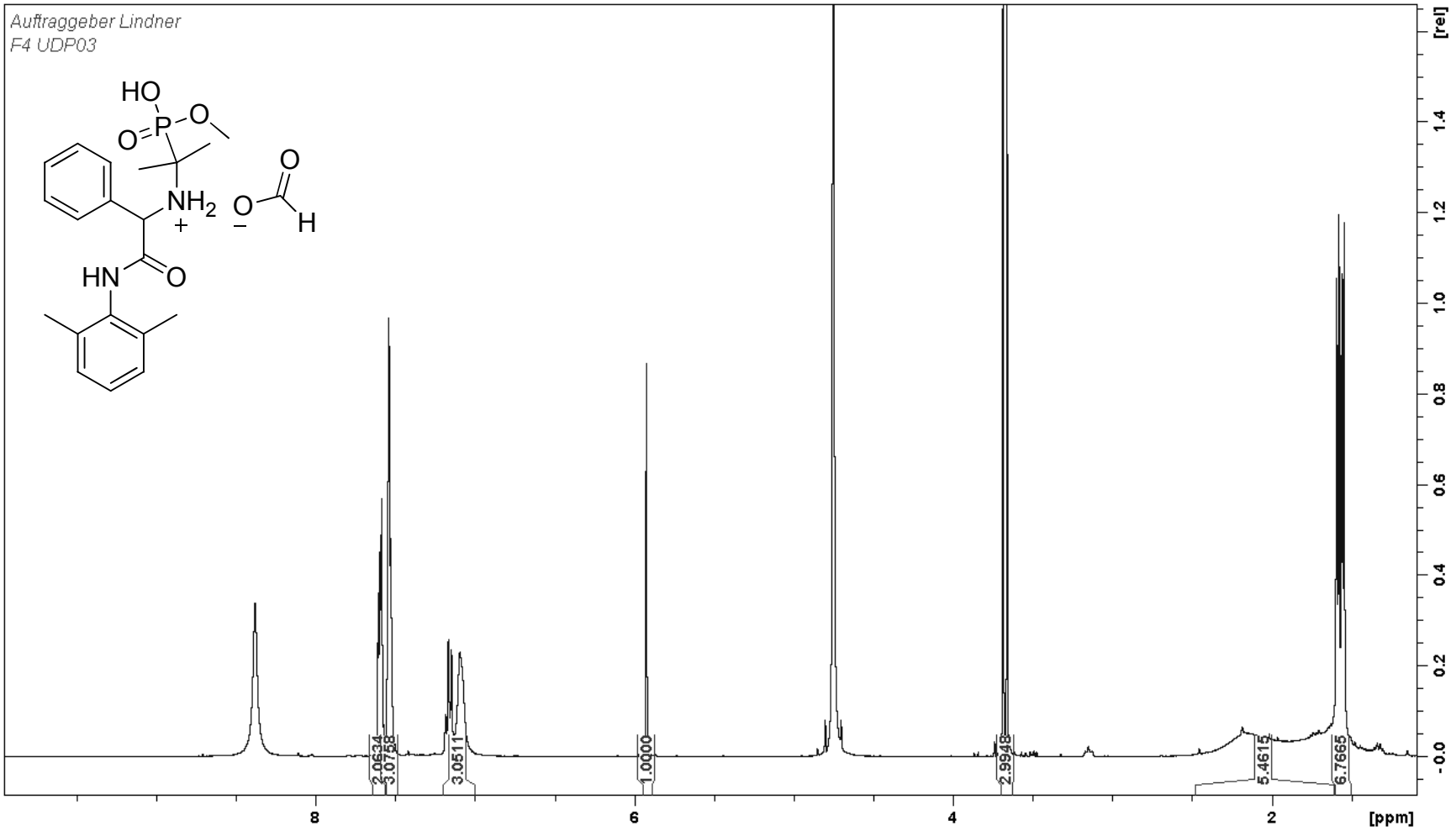

Figure N1, (b): ^{1}H-NMR spectrum of *Table 3* compound **1** as formate salt in CD_3OD. Compound **1** purified by chiral anion-exchange chromatography with excess of formic acid in mobile phase; evaporation of eluent after isolation of product peaks results compound **1** with formate as counterion. ∫ of FA peak = (8.4 ppm) 2.74

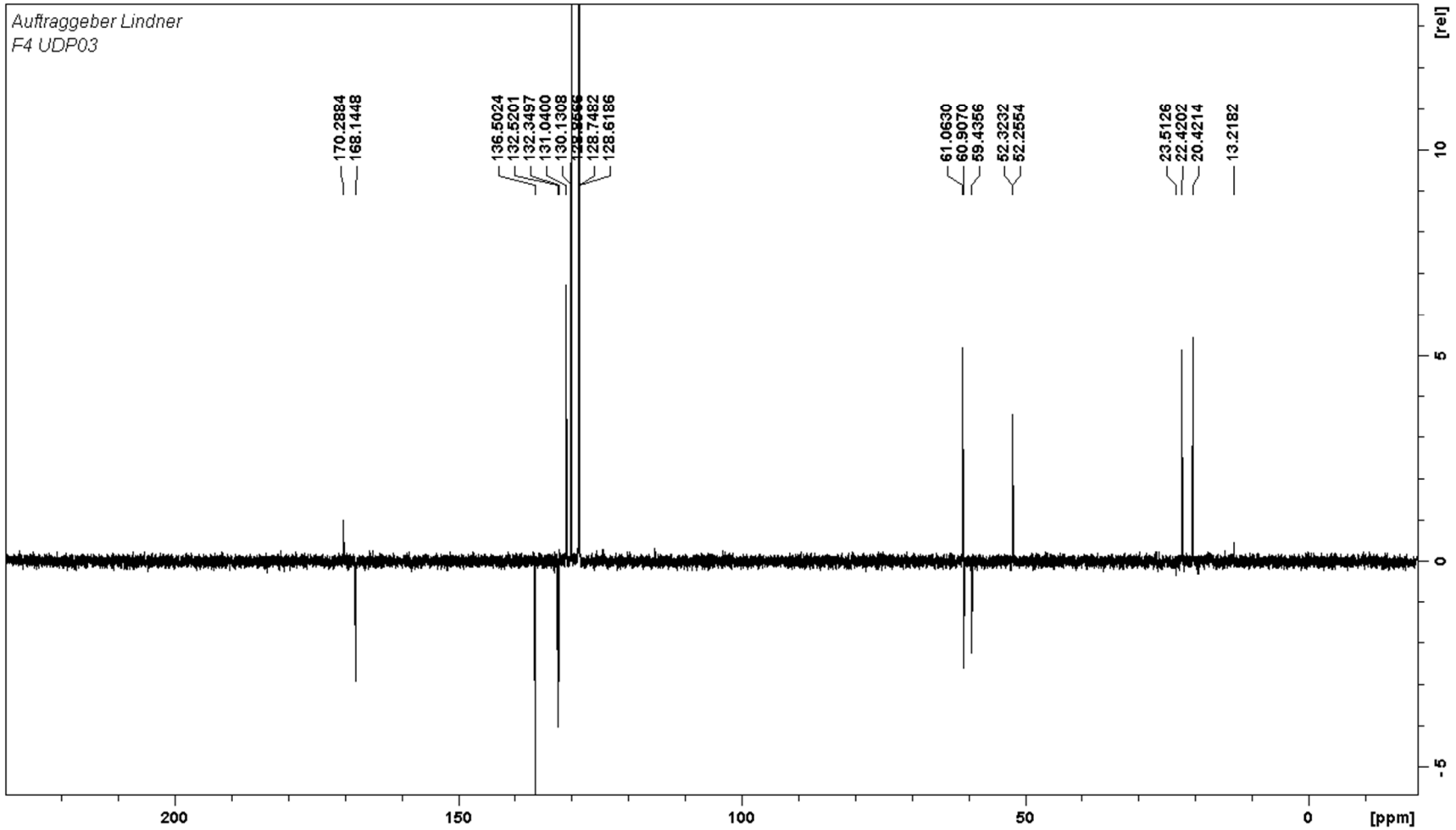

Figure N1, (c): ^{13}C-NMR spectrum of *Table 3* compound **1** (as formate salt) in CD_3OD.

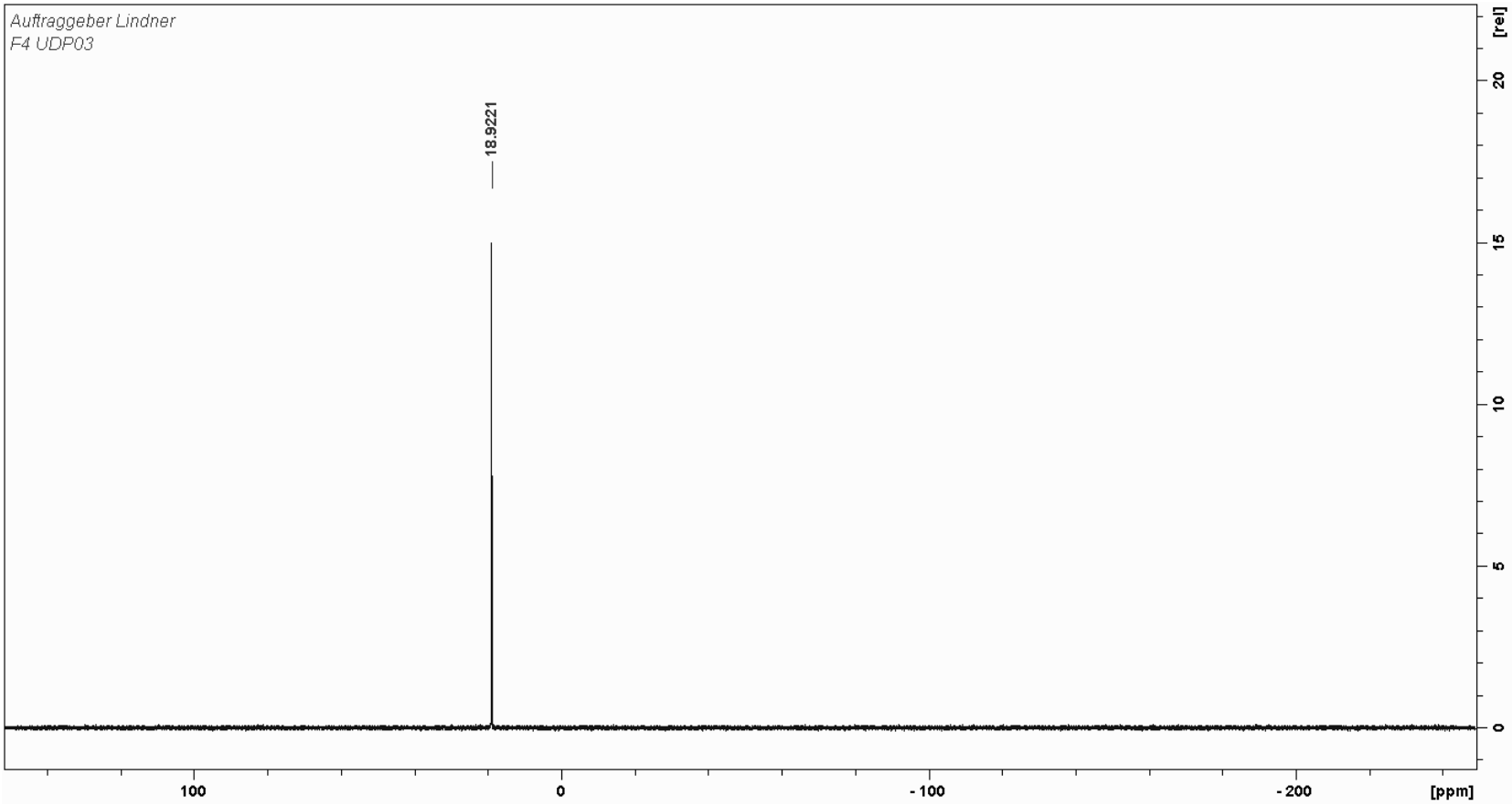

Figure N1, (d): ^{31}P-NMR spectrum of *Table 3* compound **1** (as formate salt) in CD_3OD.

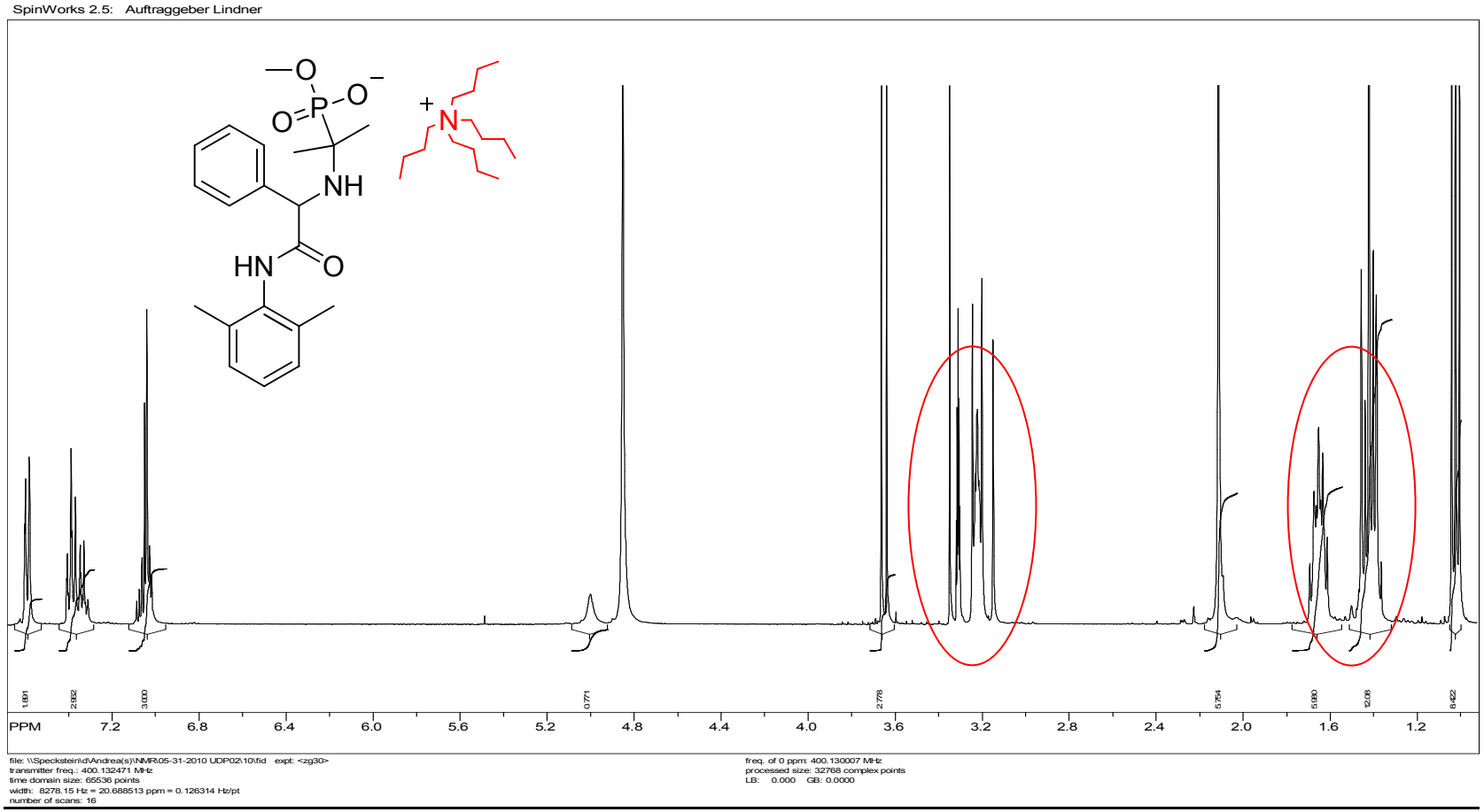

Figure N1, (e): ^{1}H NMR spectrum of *Table 3* compound **1** (as tetrabutylammonium salt) in CD_3OD. Compound obtained by liquid-liquid extraction with $CHCl_3$ / water (target compound in water fraction).

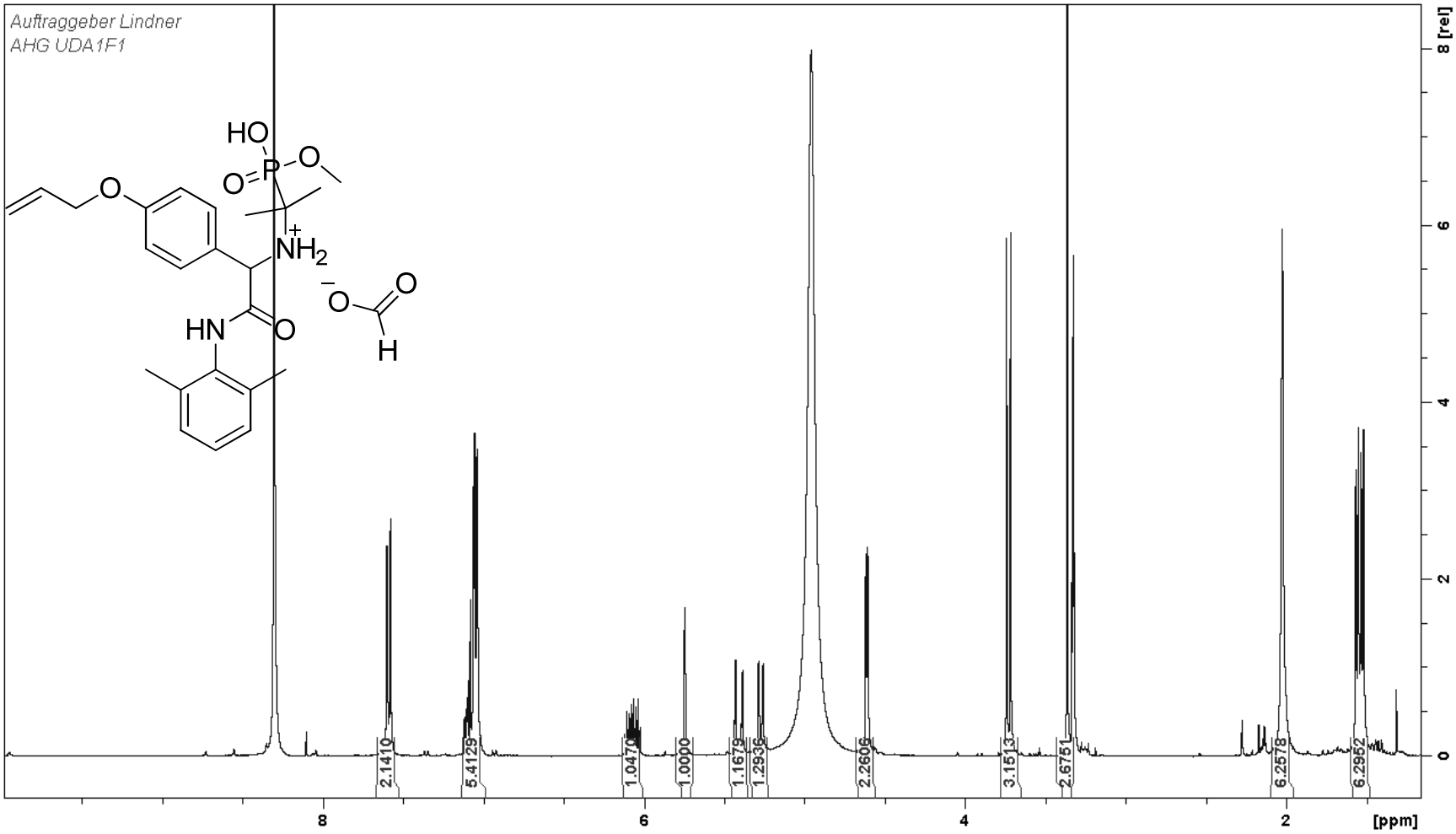

Figure N2, (a): ^{1}H NMR spectrum of *Table 3* compound **2** (as formate salt) in CD_3OD. . ∫ of FA peak = 5

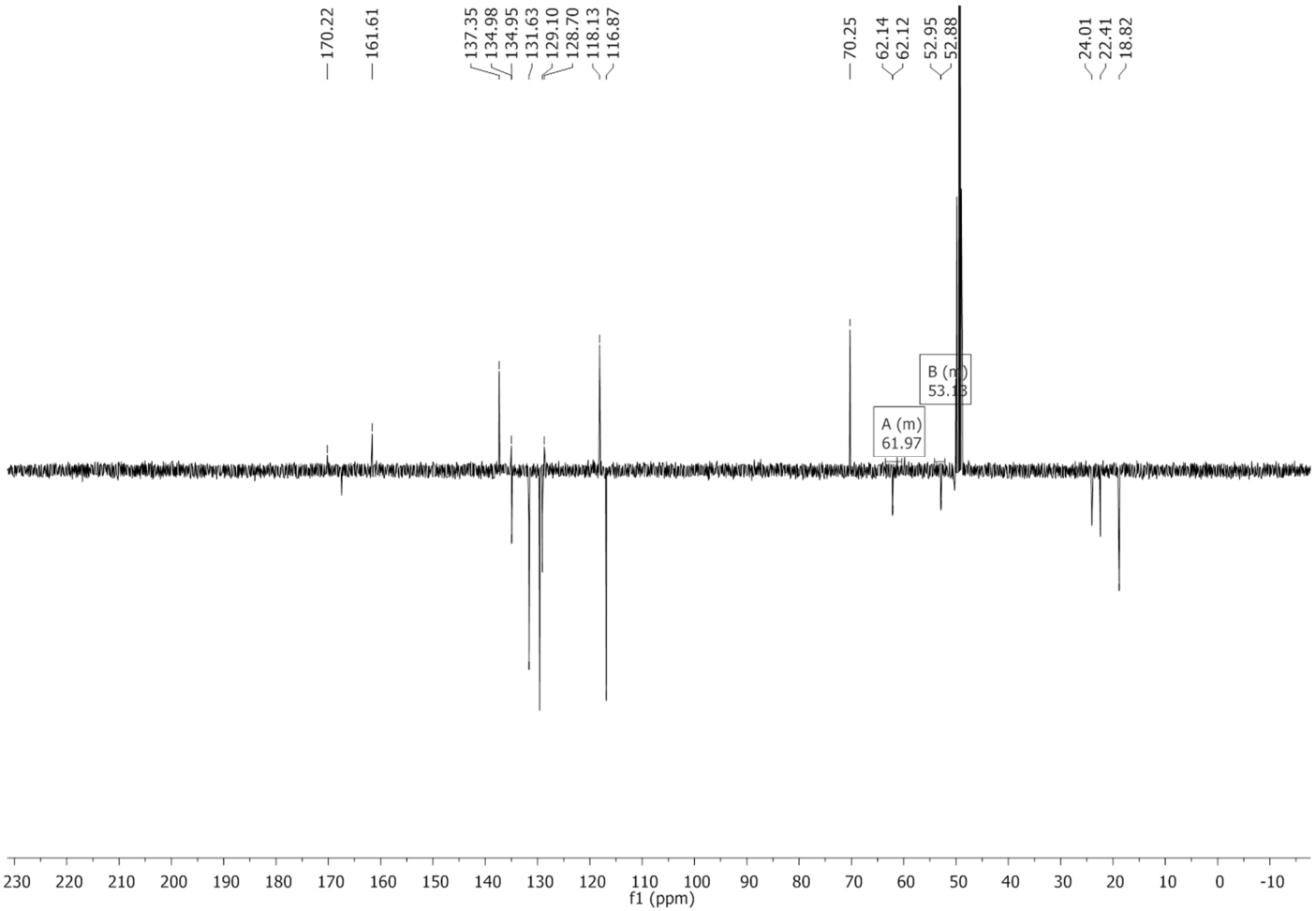

Figure N2, (b): ^{13}C NMR spectrum of *Table 3* compound **2** (as formate salt) in CD_3OD..

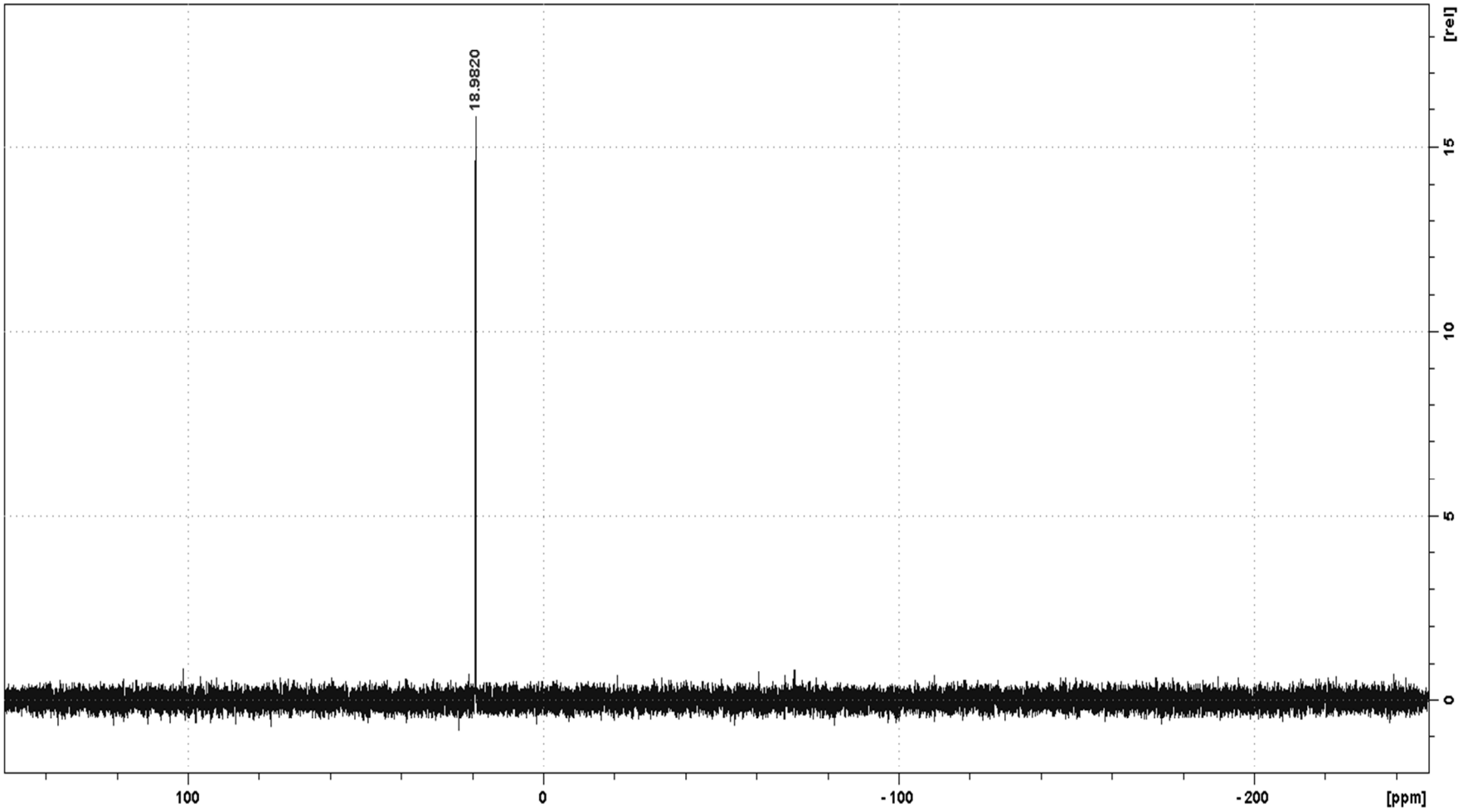

Figure N2, (c): ^{31}P NMR spectrum of *Table 3* compound **2** (as formate salt)

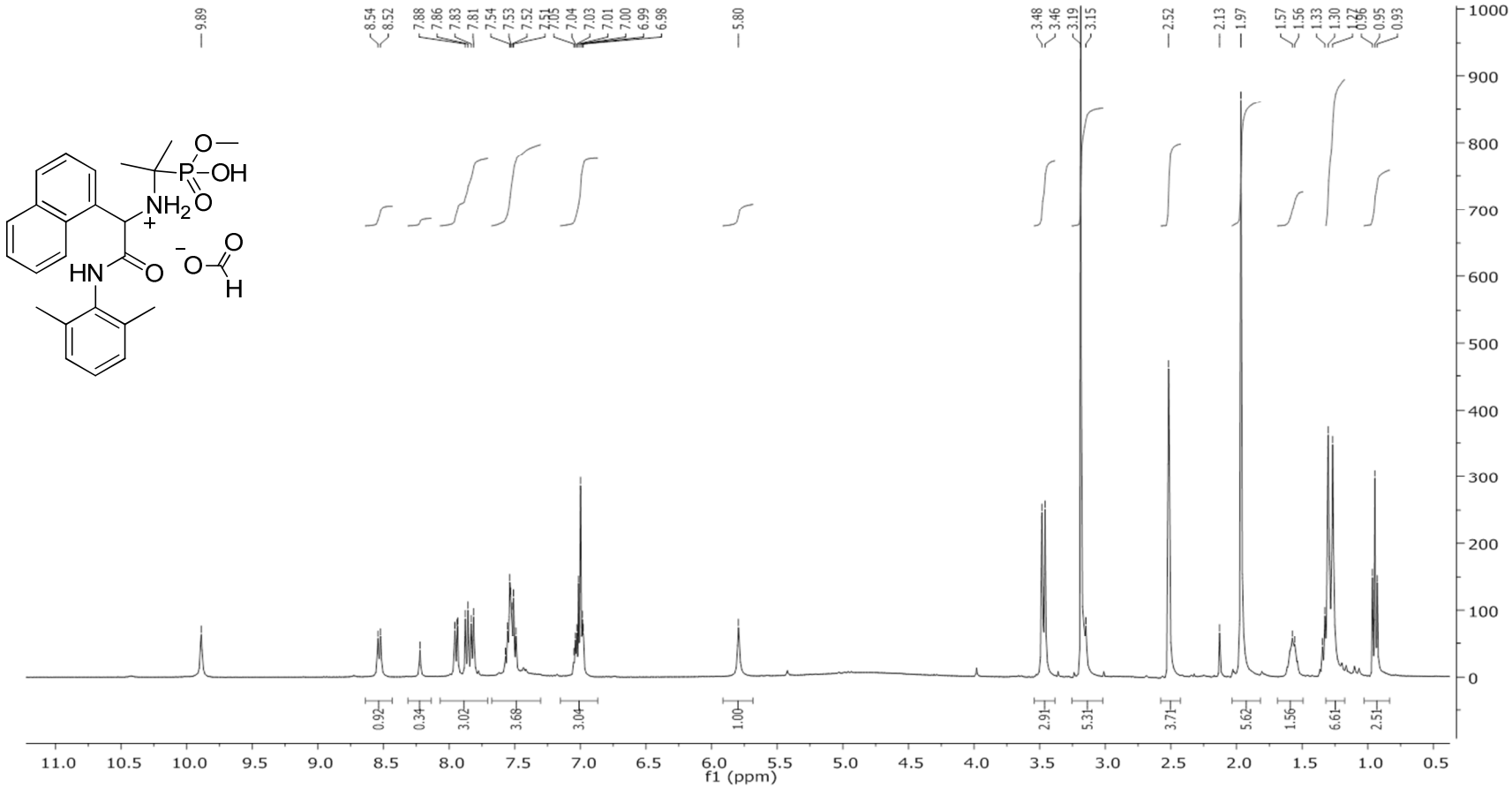

Figure N3, (a): ^{1}H spectrum of *Table 3* compound **3** (as formate salt) in d6-DMSO. . ∫ of FA peak = 0.73

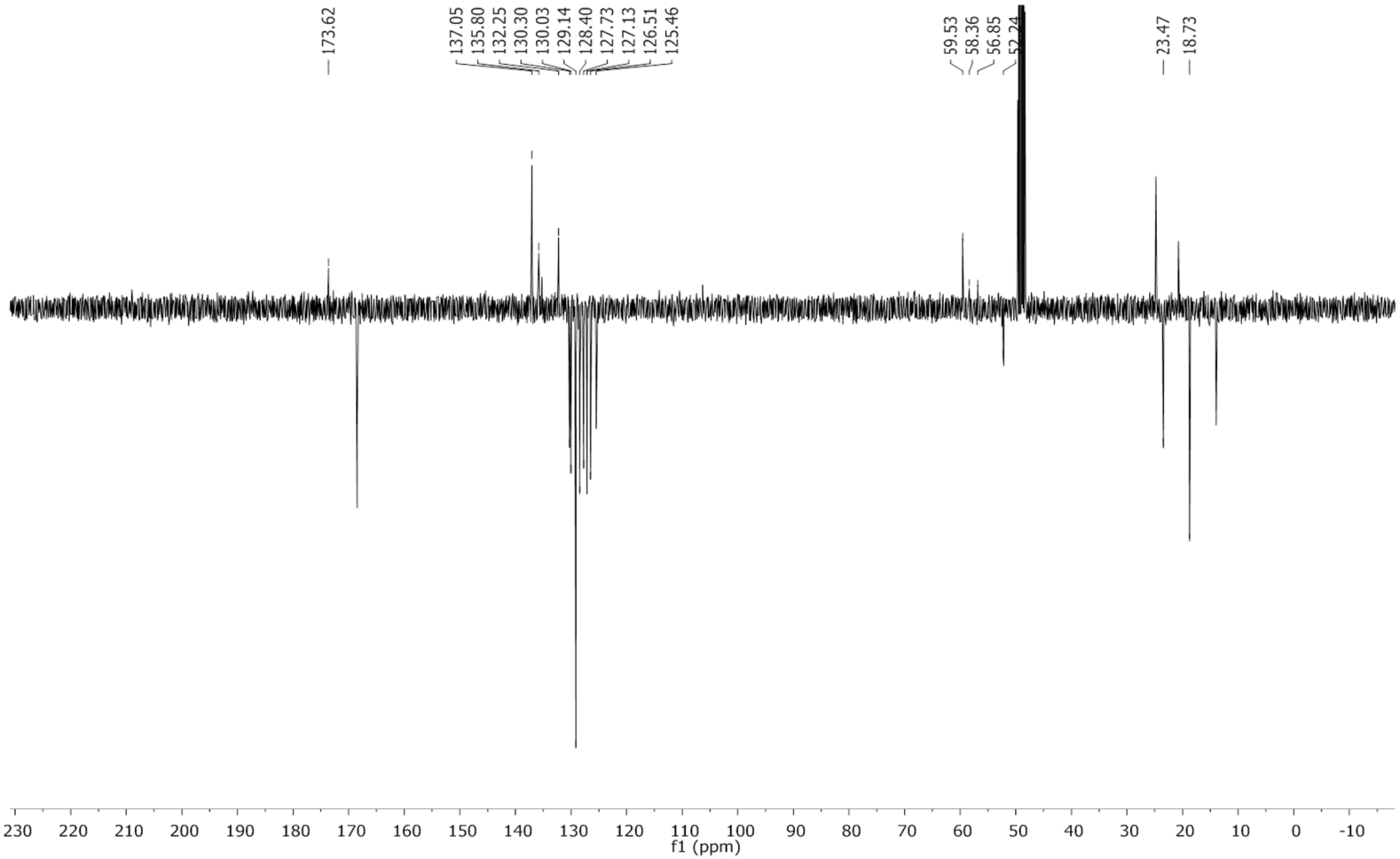

Figure N3, (b): ^{13}C NMR spectrum of *Table 3* compound **3** (as formate salt) in d6-DMSO.

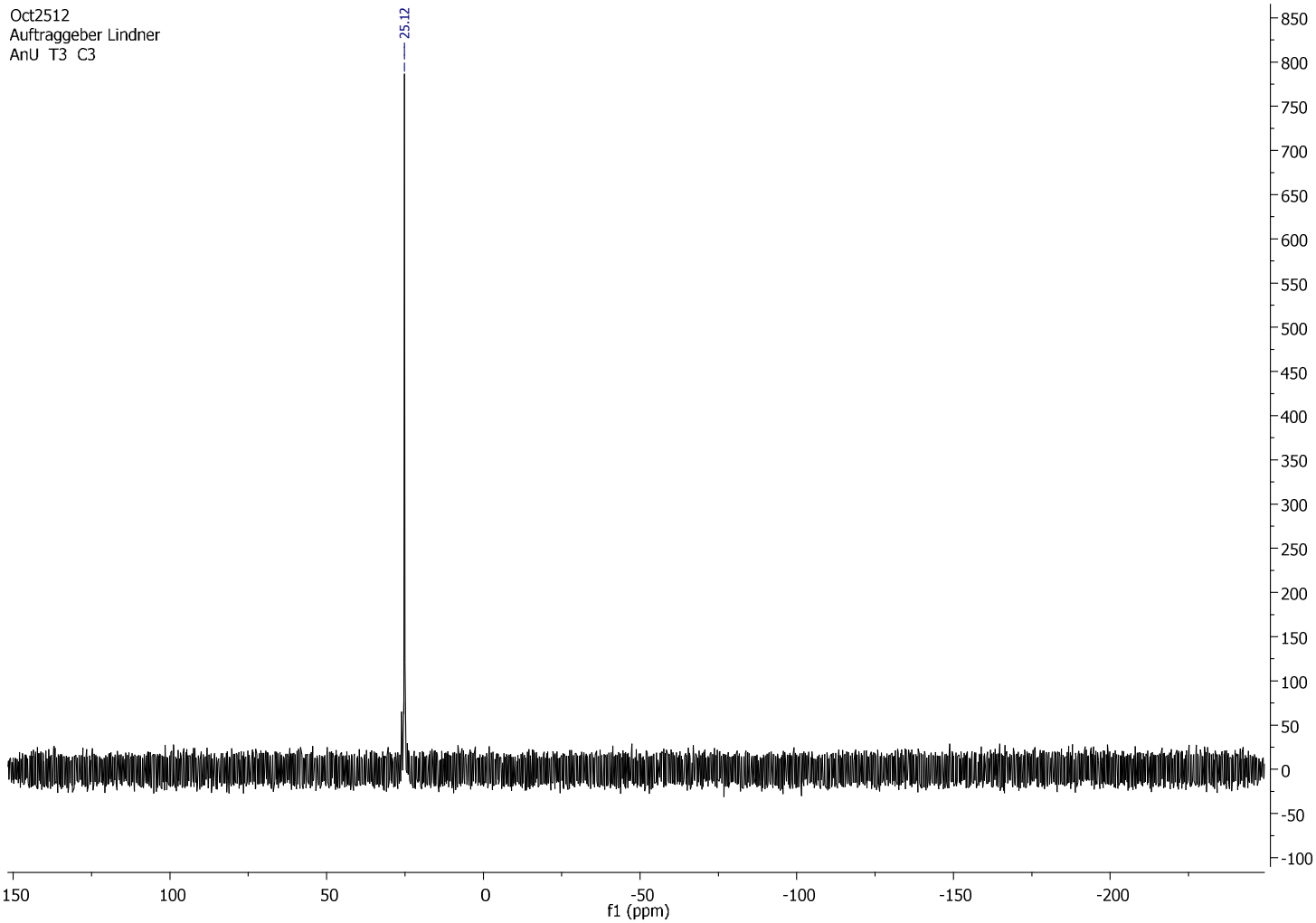

Figure N3, (c): ^{31}P-NMR spectrum of *Table 3* compound **3** (as formate salt) in d6-DMSO.

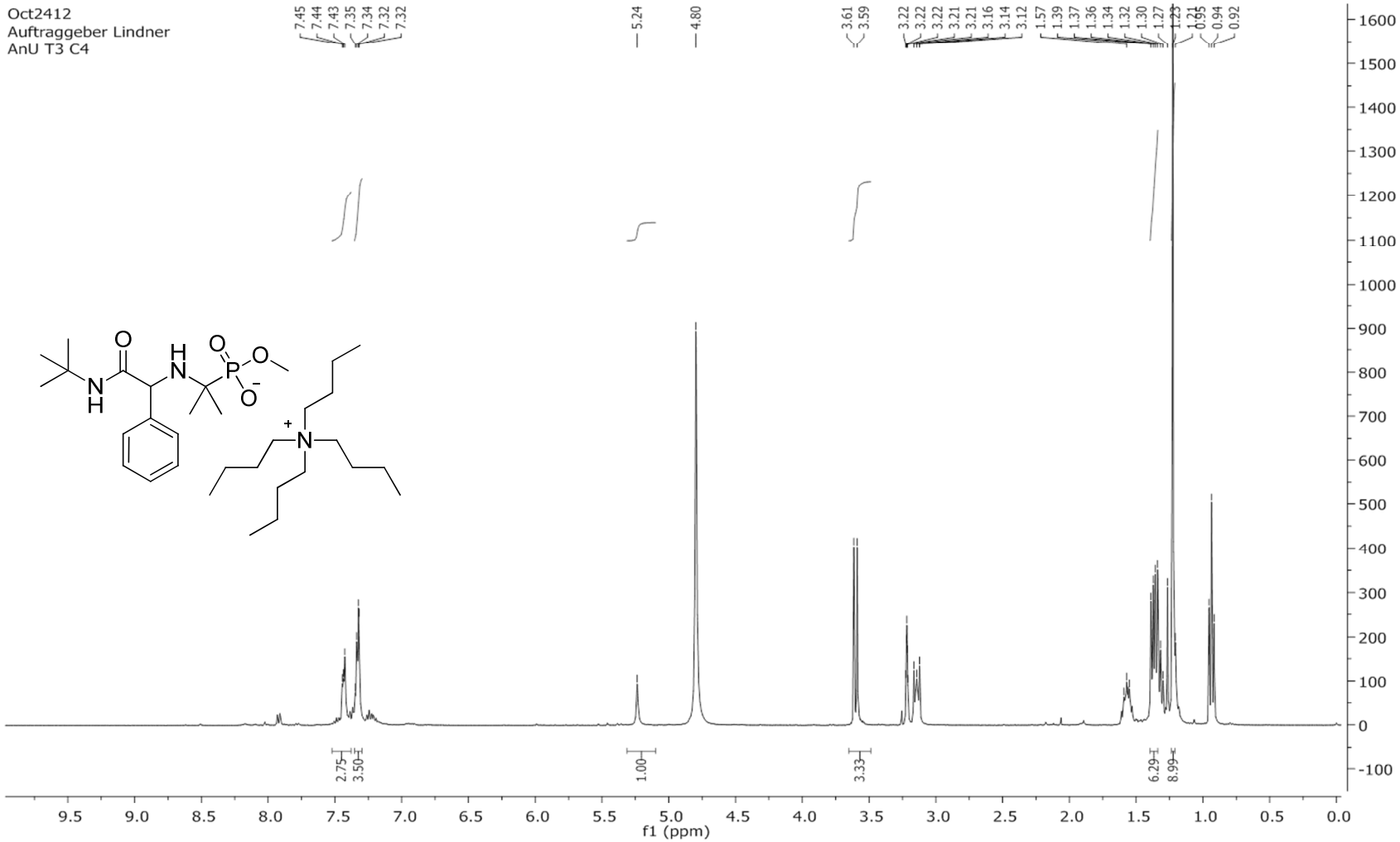

Figure N4, (a): ^{1}H NMR spectrum of *Table 3* compound **4** (as tetrabutylammonium salt) in CD_3OD. . ∫ of TBAOH peaks =(3.2 ppm) 1.3 , (1.4 ppm) 4.5, (0.9 ppm) 3.4.

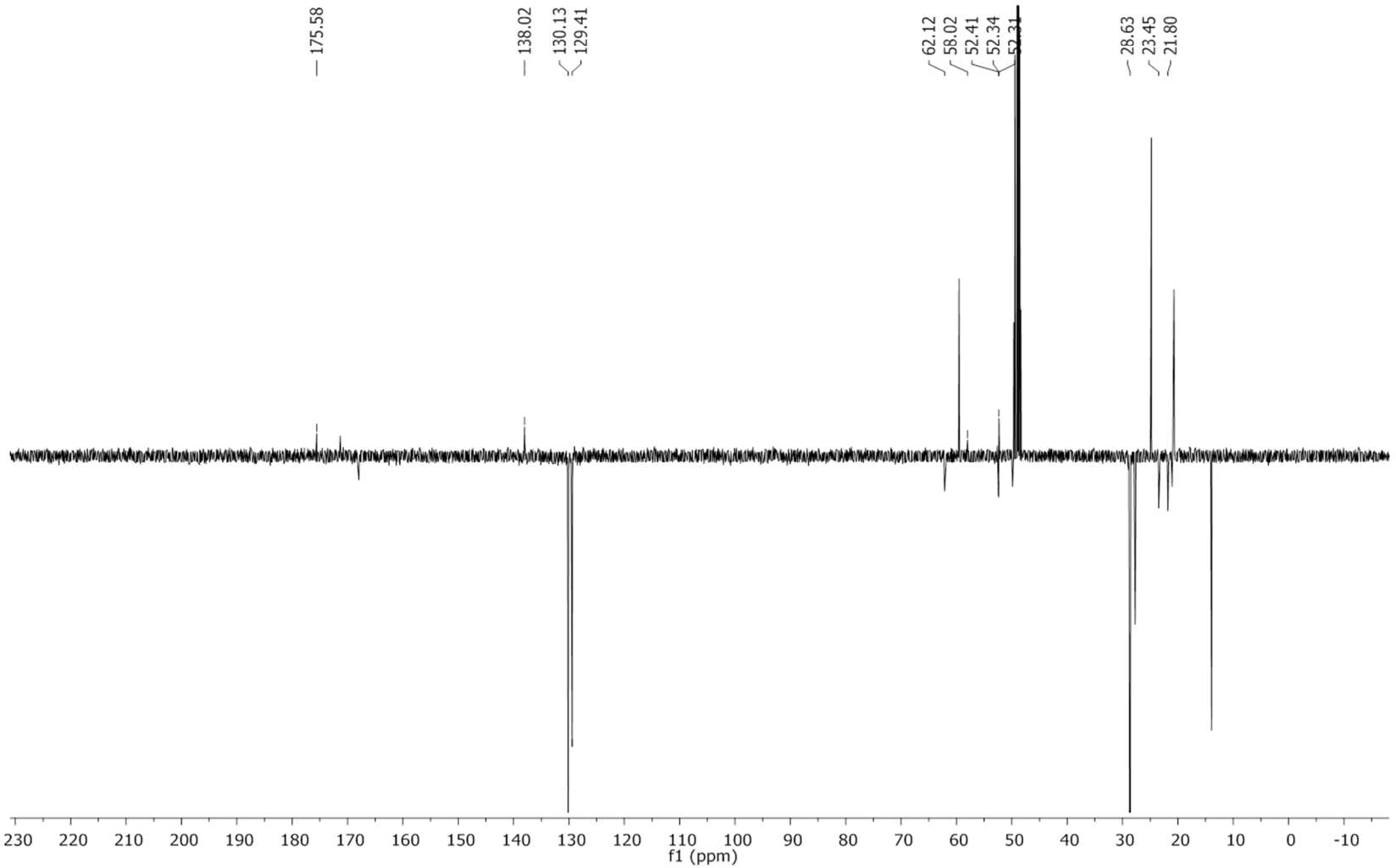

Figure N4, (b): ^{13}C-NMR spectrum of *Table 3* compound **4** (as tetrabutylammonium salt) in CD_3OD.

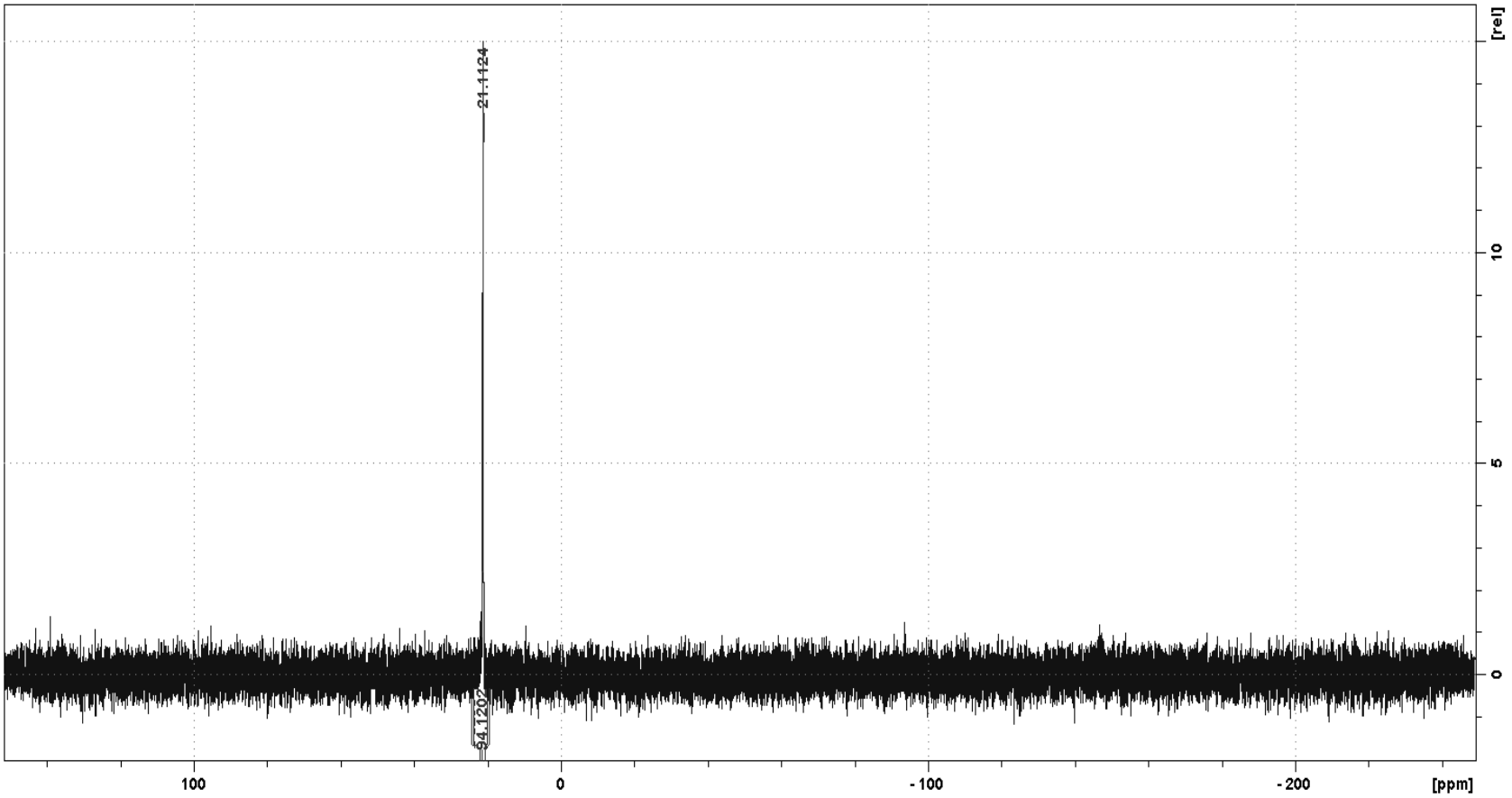

Figure N4, (c): ^{31}P-NMR spectrum of *Table 3* compound **4** (as tetrabutylammonium salt) in CD_3OD.

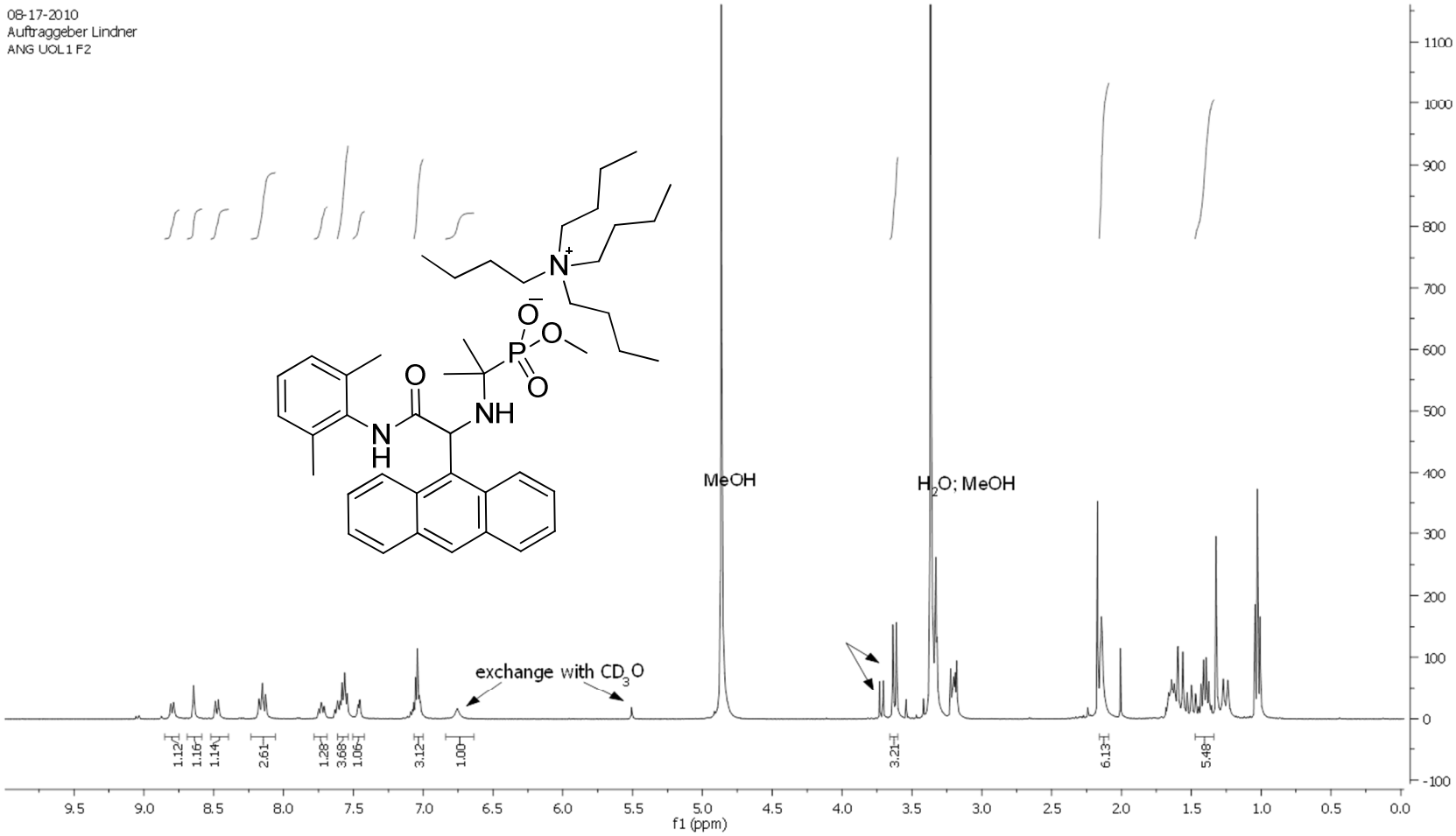

Figure N5, (a): ^{1}H NMR spectrum of *Table 3* compound **5** (as tetrabutylammonium salt) in CD_3OD. . ∫ of TBAOH peaks =(3.3 ppm) 1.5 , (1.6 ppm) 6, (1 ppm) 4.

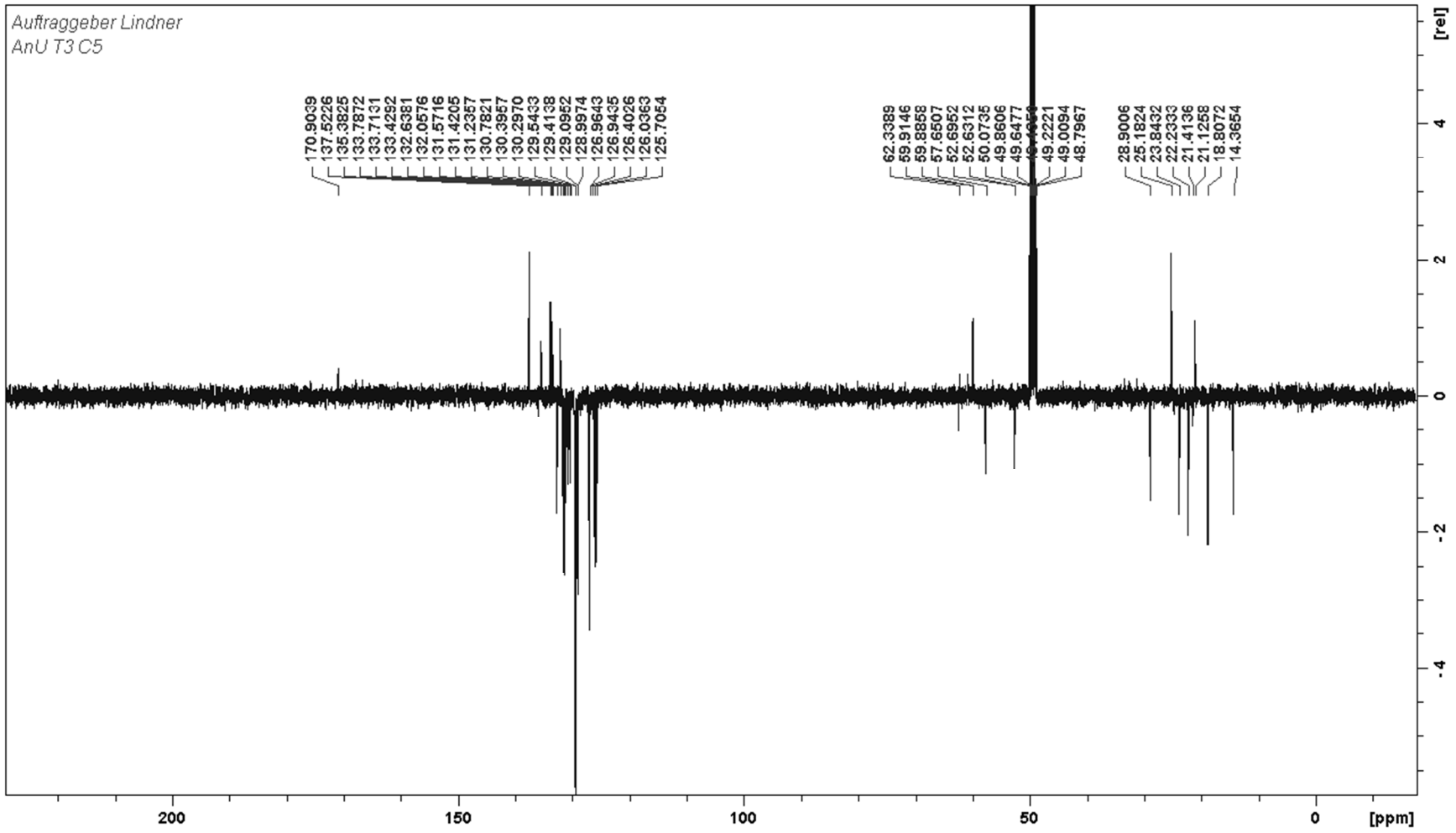

Figure N5, (b): ^{13}C-NMR spectrum of *Table 3* compound **5** (as tetrabutylammonium salt) in CD_3OD.

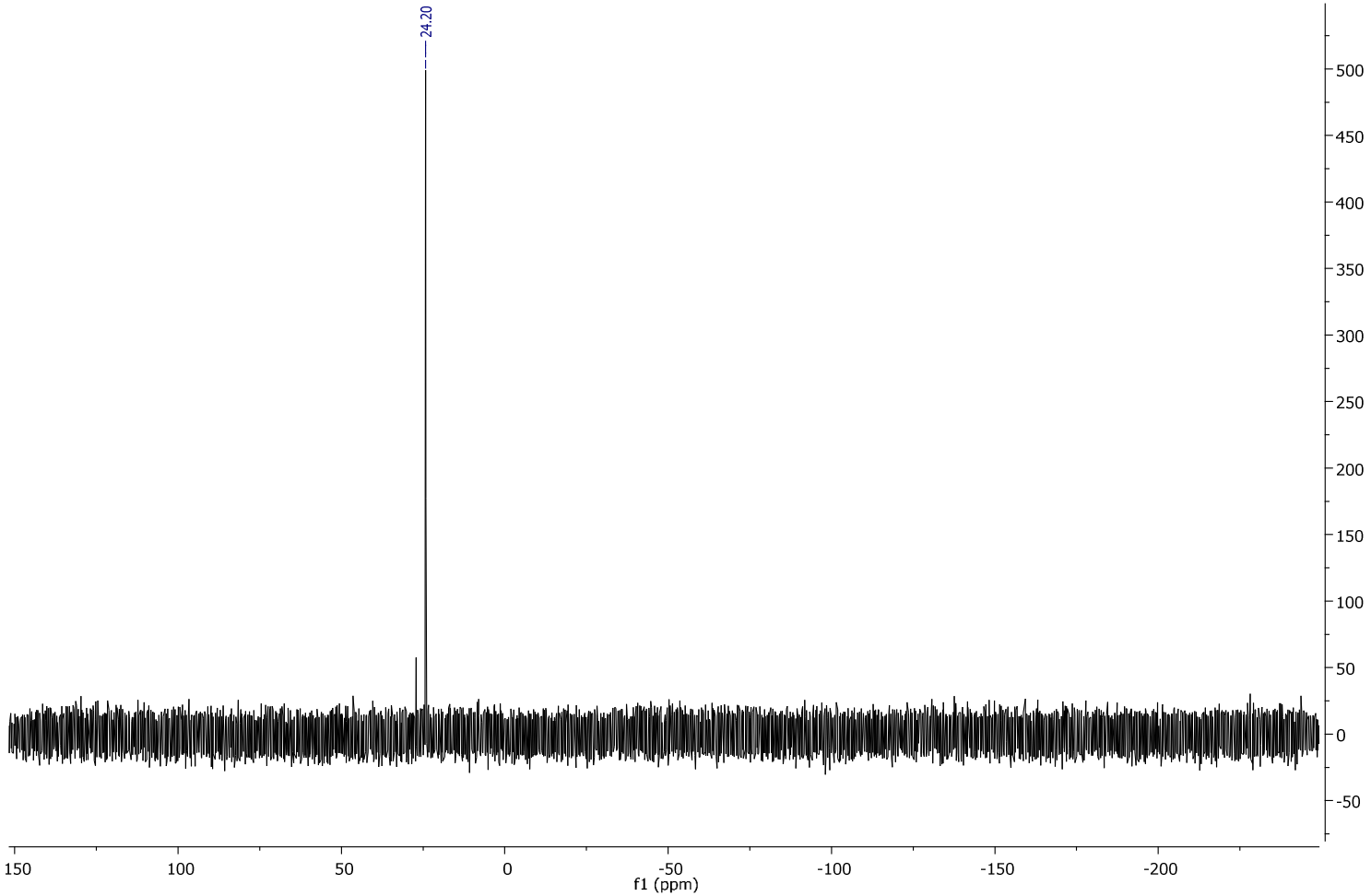

Figure N5, (c) : ^{31}P-NMR spectrum of *Table 3* compound **5** (as tetrabutylammonium salt) in CD_3OD.

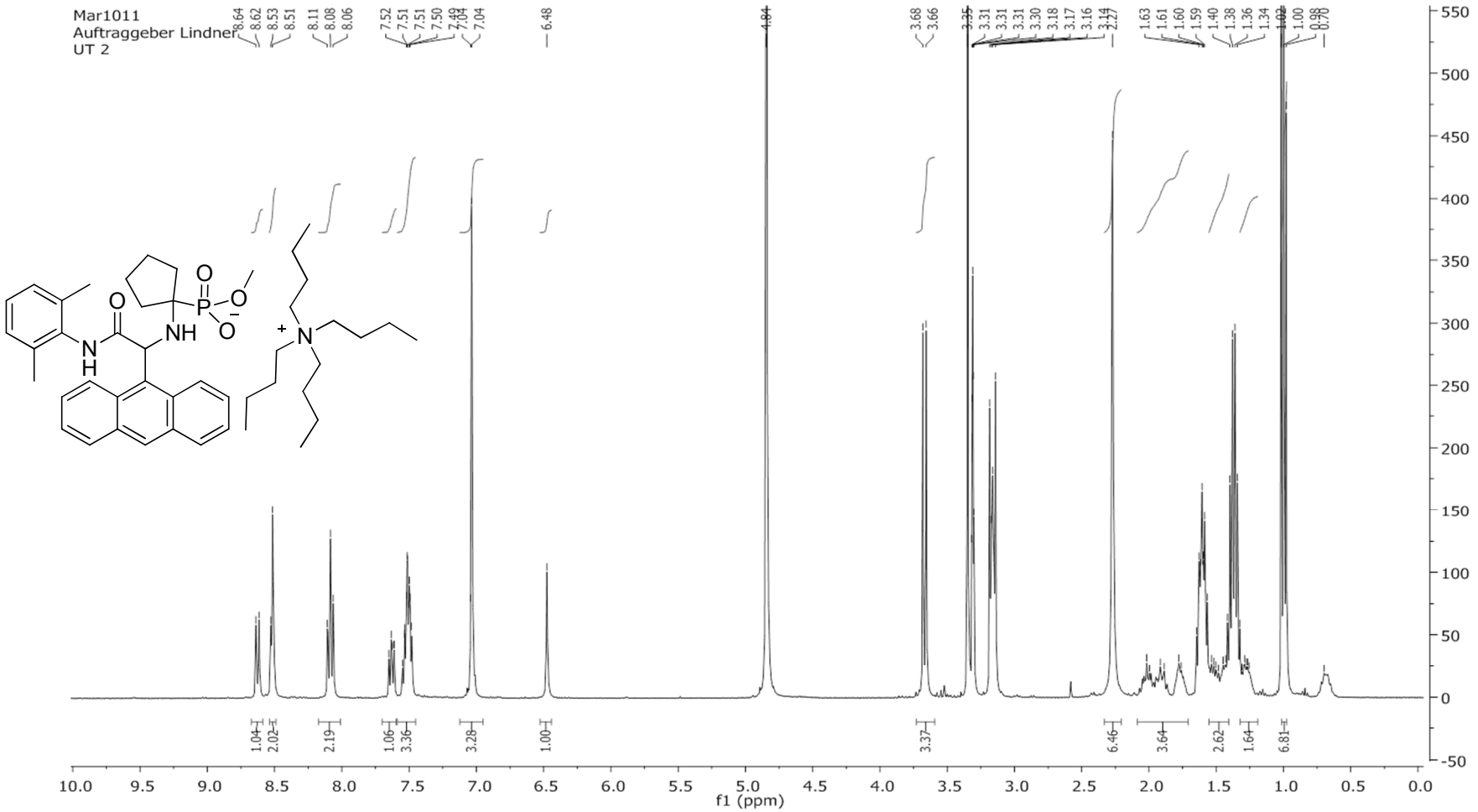

Figure N6, (a): ^{1}H NMR spectrum of *Table 3* compound **6** (as tetrabutylammonium salt) in CD_3OD. ∫ of TBAOH peaks =(3.3 ppm) 5 , (1.5 ppm) 15, (1 ppm) 12.3. Ratio TBAOH- target compound ~1:1.

.

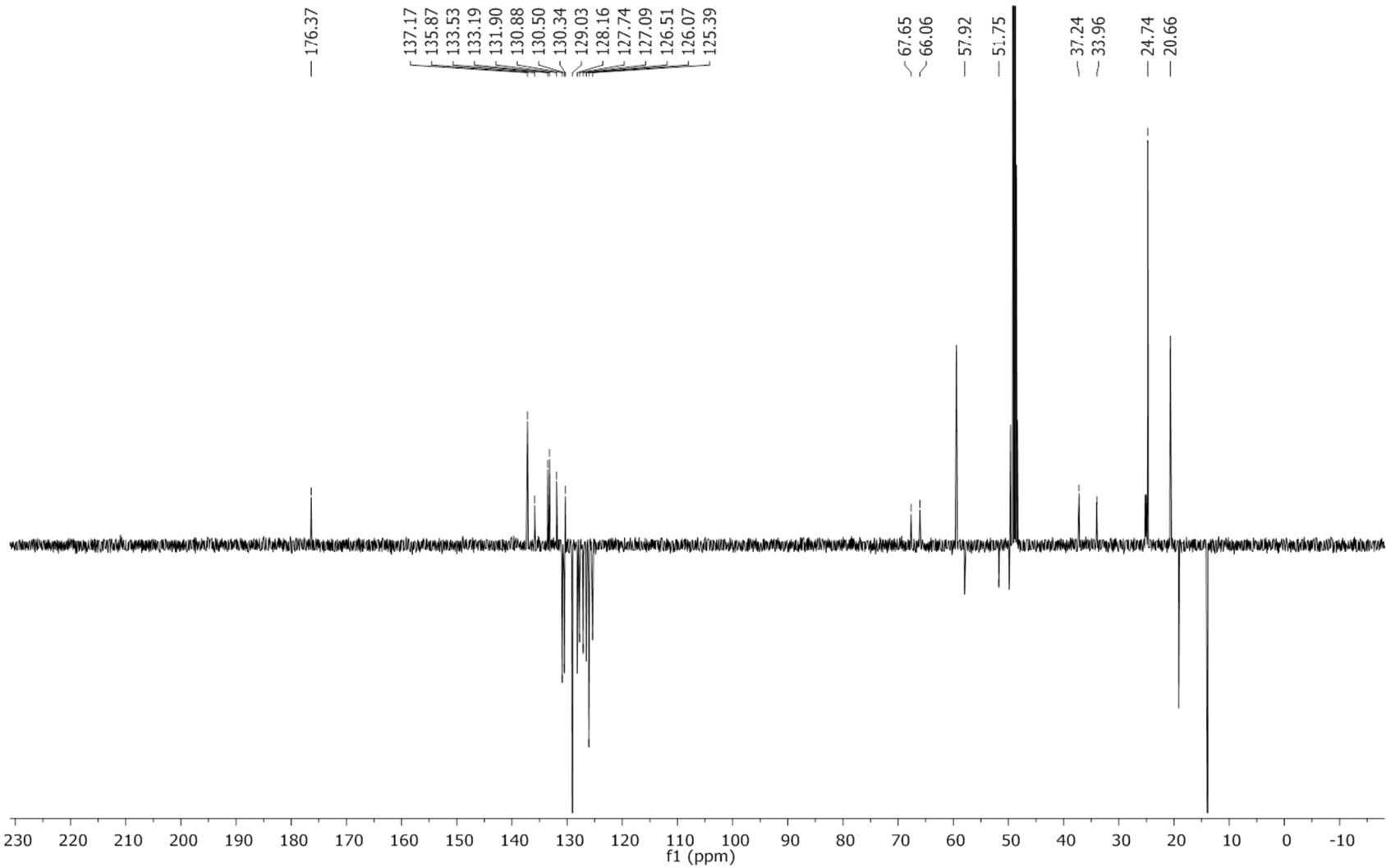

Figure N6, (c) : ^{13}C-NMR spectrum of *Table 3* compound **6** (as tetrabutylammonium salt) in CD_3OD.

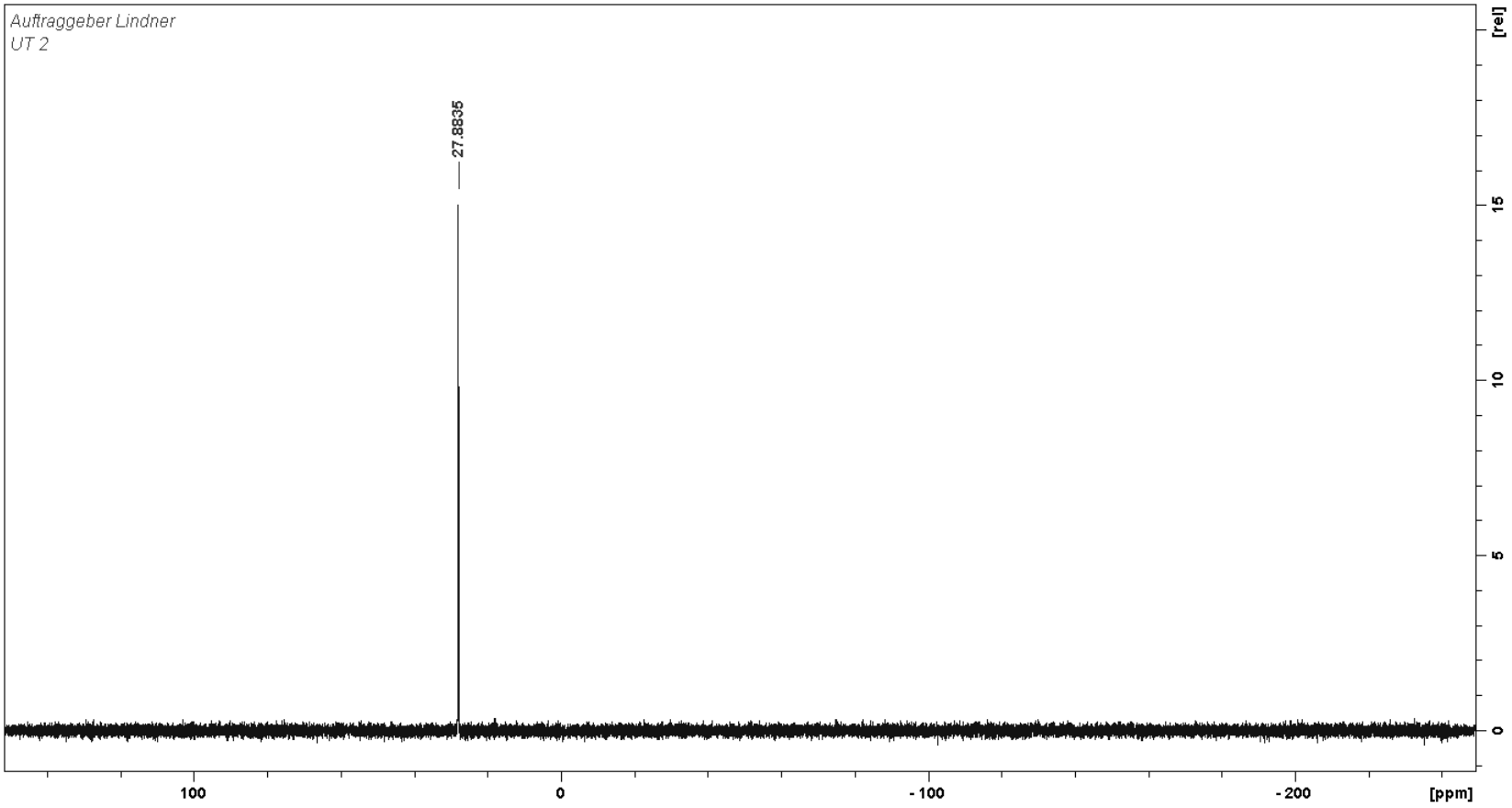

Figure N6, (c): ^{31}P NMR spectrum of *Table 3* compound **6** (as tetrabutylammonium salt) in CD_3OD.

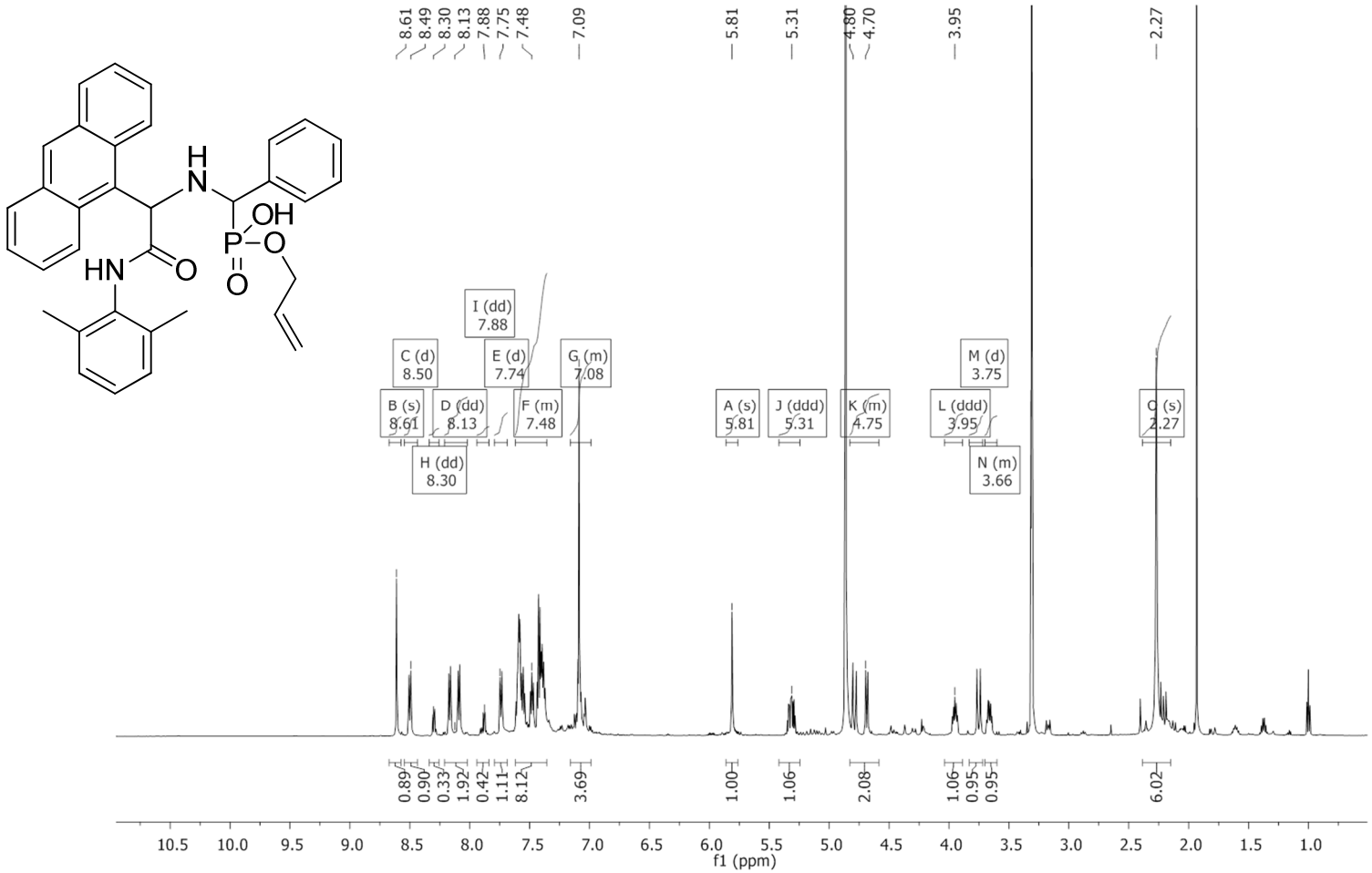

Figure N7, (a): ^{1}H NMR spectrum of *Table 3* compound **7** in CD_3OD.

.

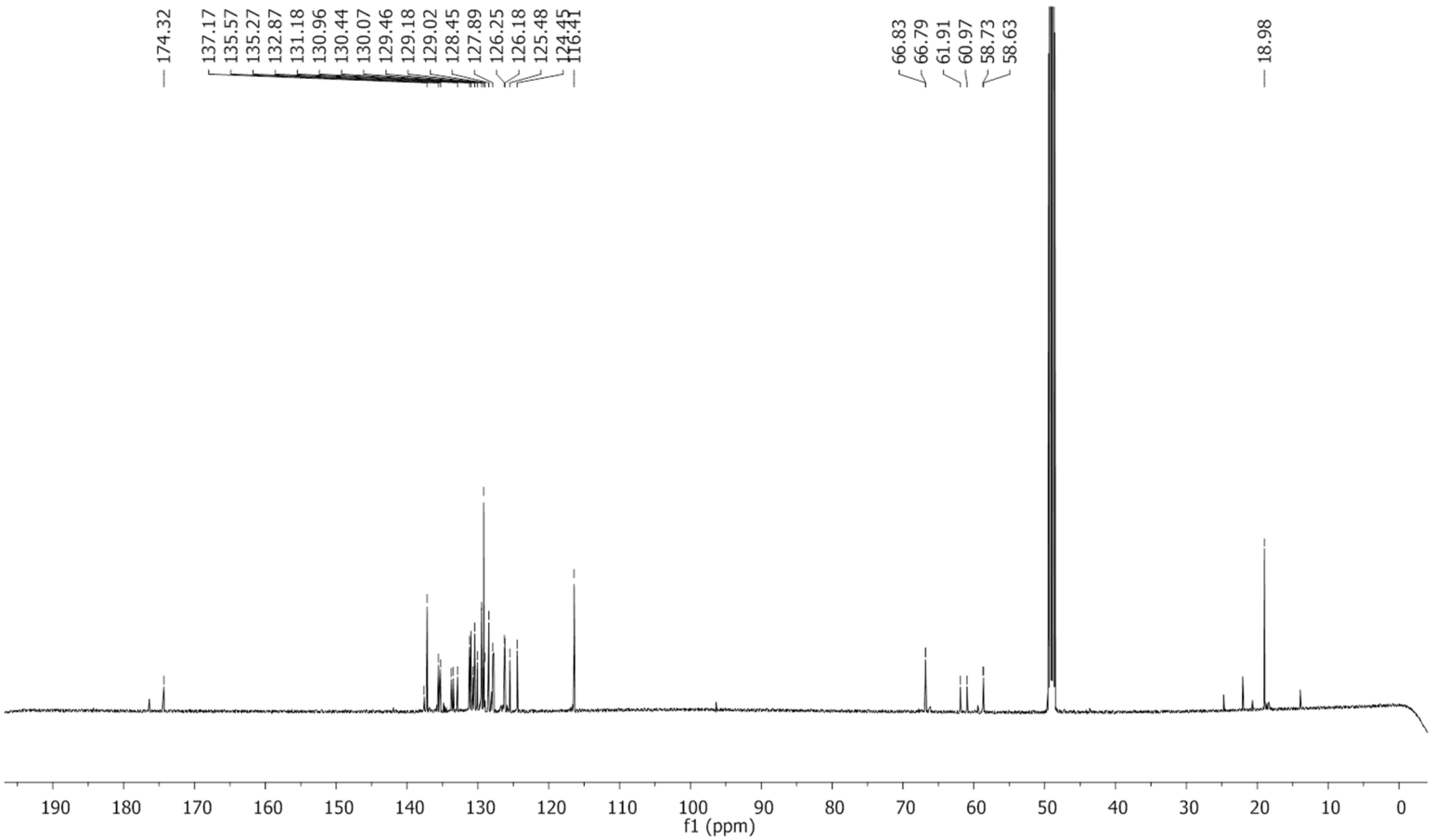

Figure N7, (b): ^{13}C-NMR spectrum of *Table 3* compound **7** in CD_3OD.

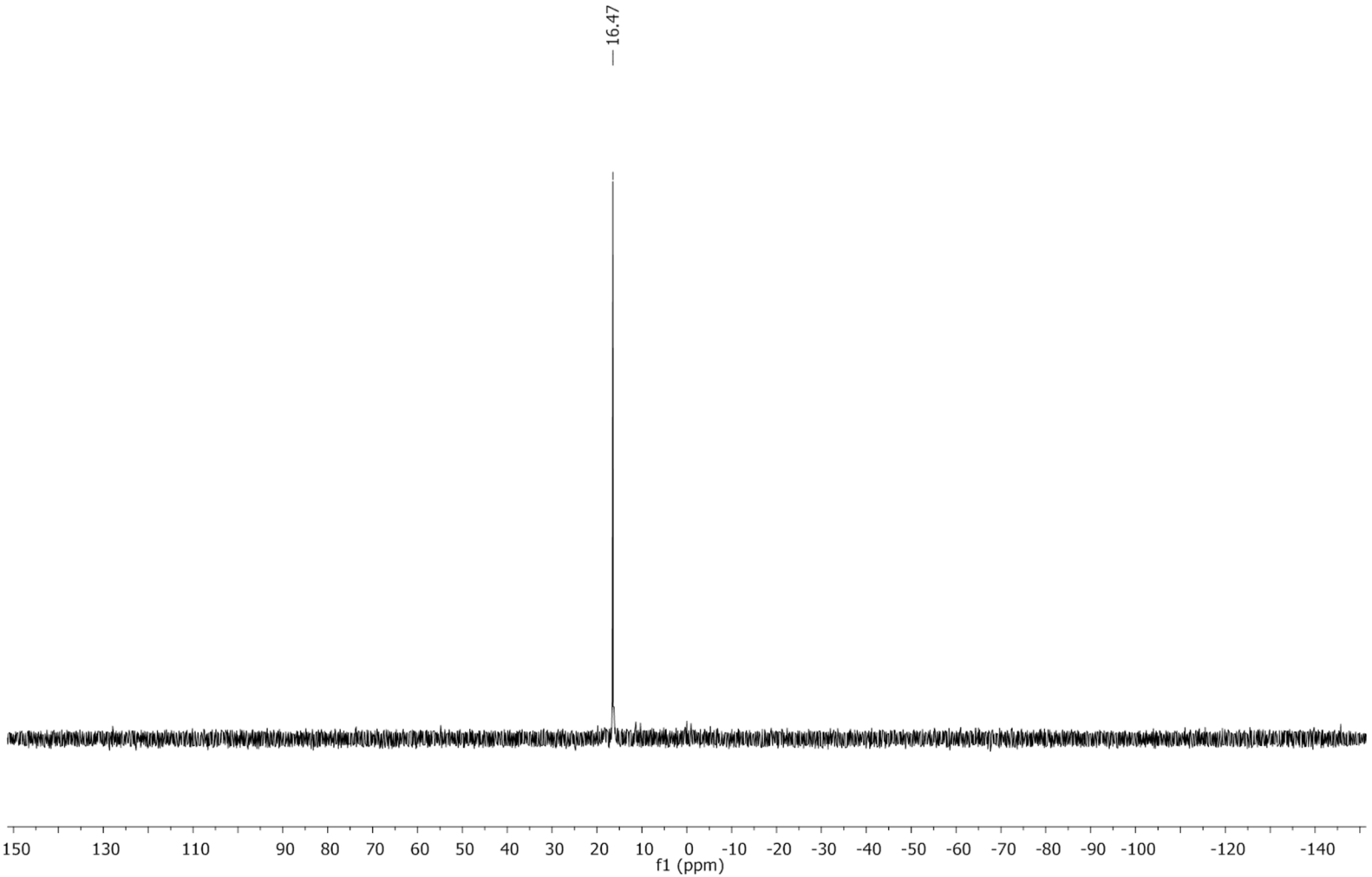

Figure N7, (c): ^{31}P-NMR spectrum of *Table 3* compound **7** in CD_3OD.

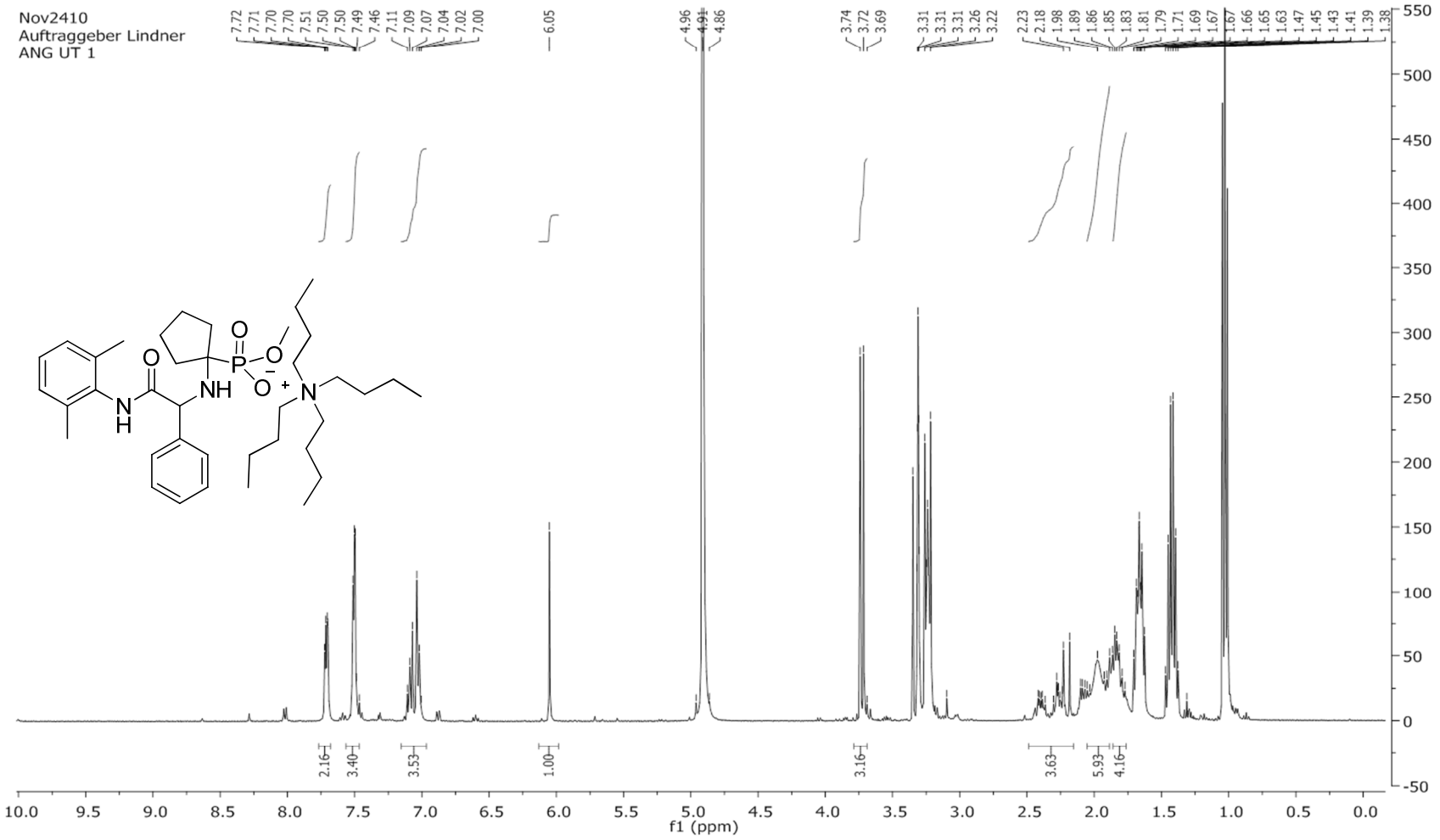

Figure N8, (a): ^{1}H NMR spectrum of *Table 3* compound **8** (as tetrabutylammonium salt) in CD_3OD. ∫ of TBAOH peaks =(3.3 ppm) 5 , (1.6 ppm) 4, (1.4 ppm) 6, (1 ppm) 12. Ratio TBAOH- target compound ~1:1.

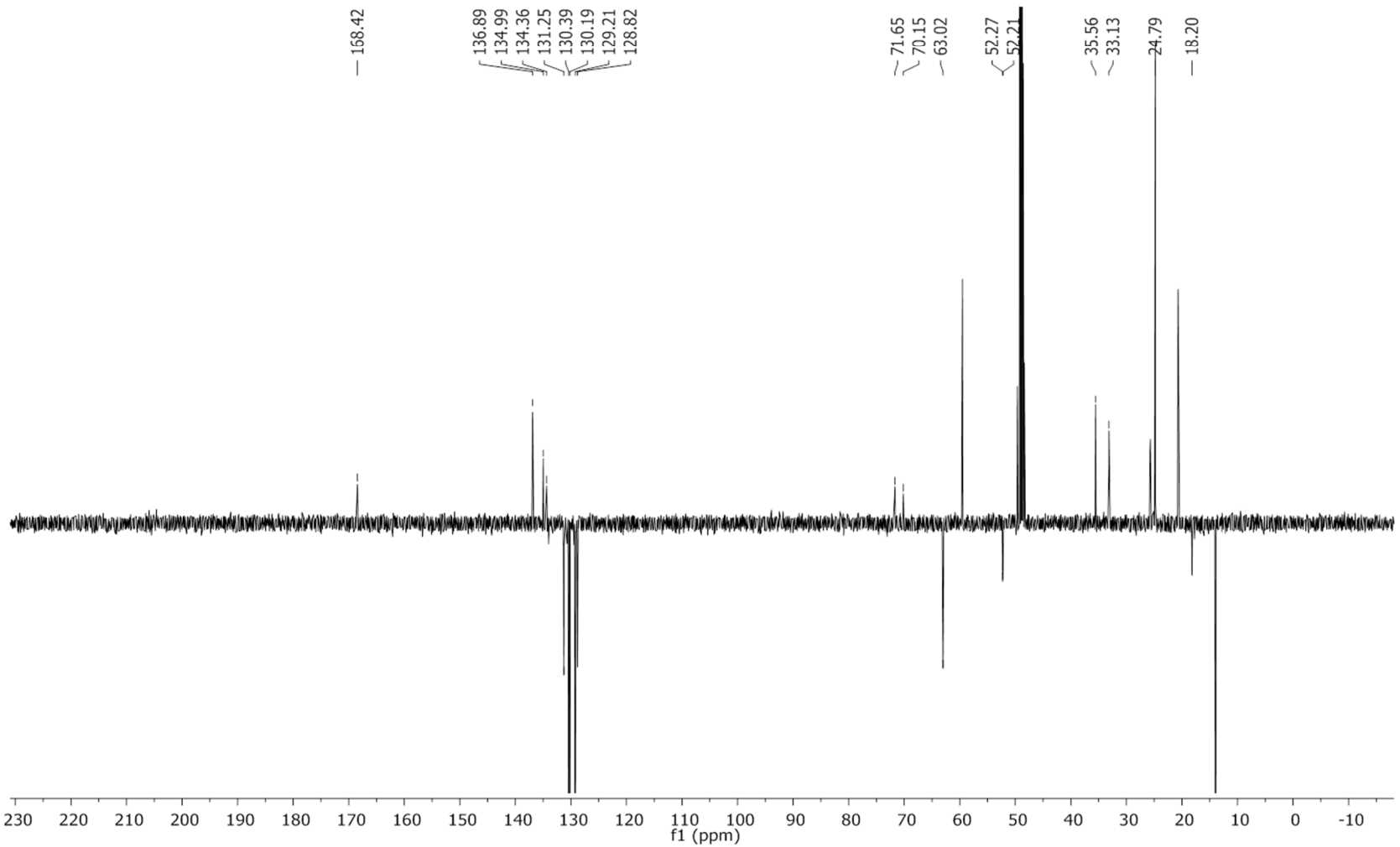

Figure N8, (b): ^{13}C NMR spectrum of *Table 3* compound **8** (as tetrabutylammonium salt) in CD_3OD.

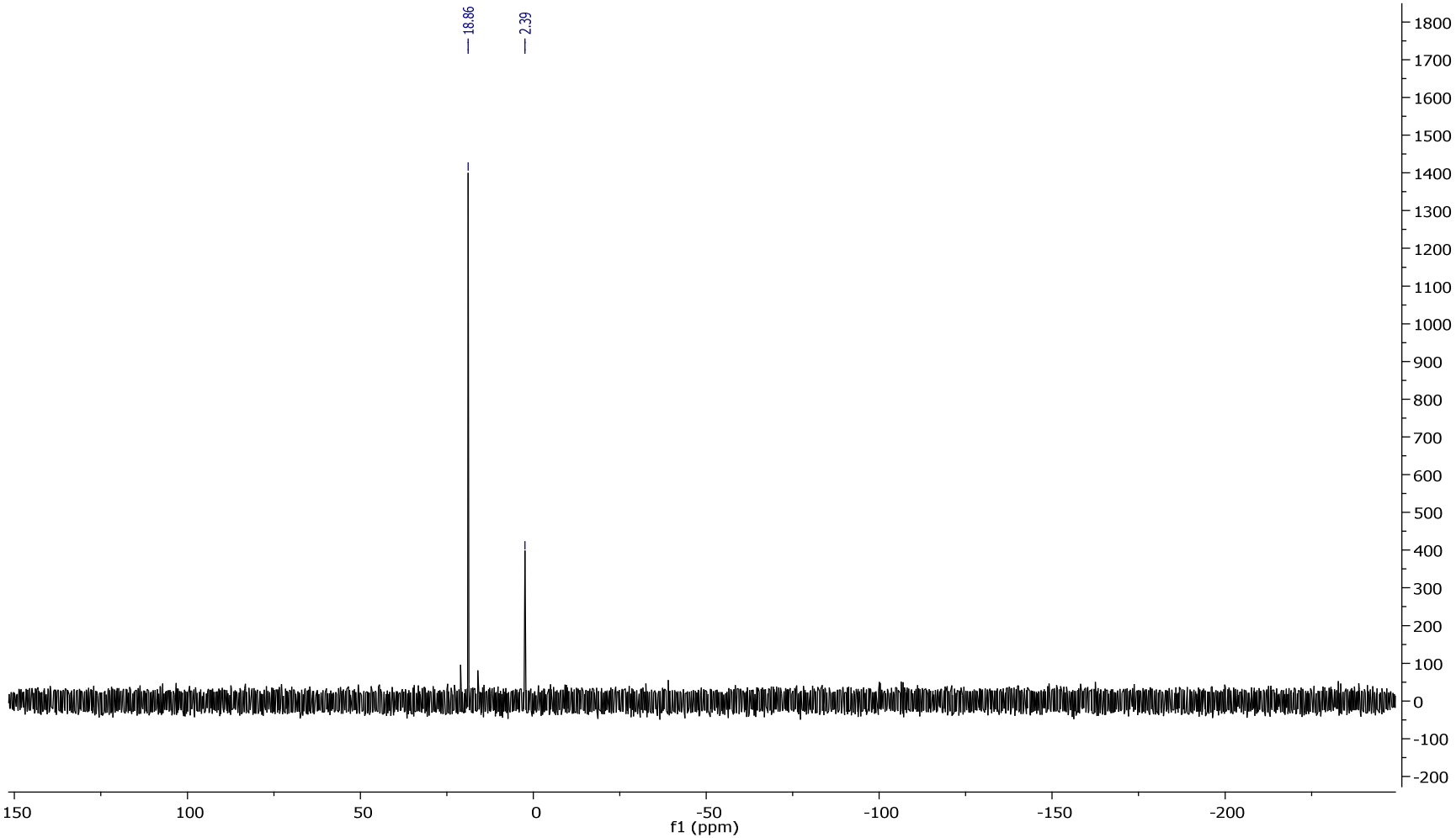

Figure N8, (c): ^{31}P NMR spectrum of *Table 3* compound **8** (as tetrabutylammonium salt) in CD_3OD. The peak at δ 2.39 ppm represent the unreacted aminophosphonic acid.

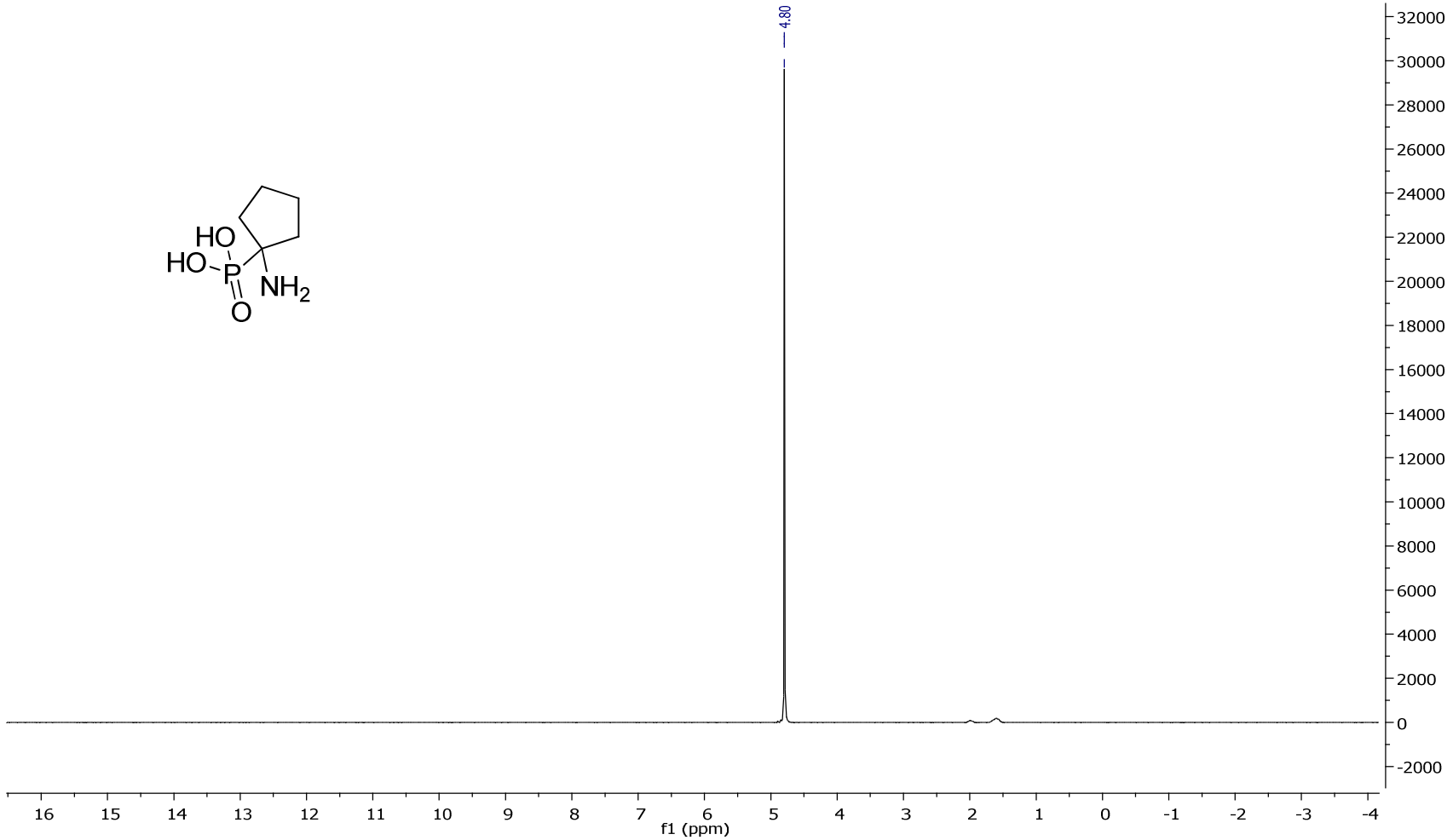

Figure N8, (d): ^{31}P NMR spectrum of aminocyclohexyl phosphonic acid, reagent used for the synthesis of compound **8** in CD_3OD.

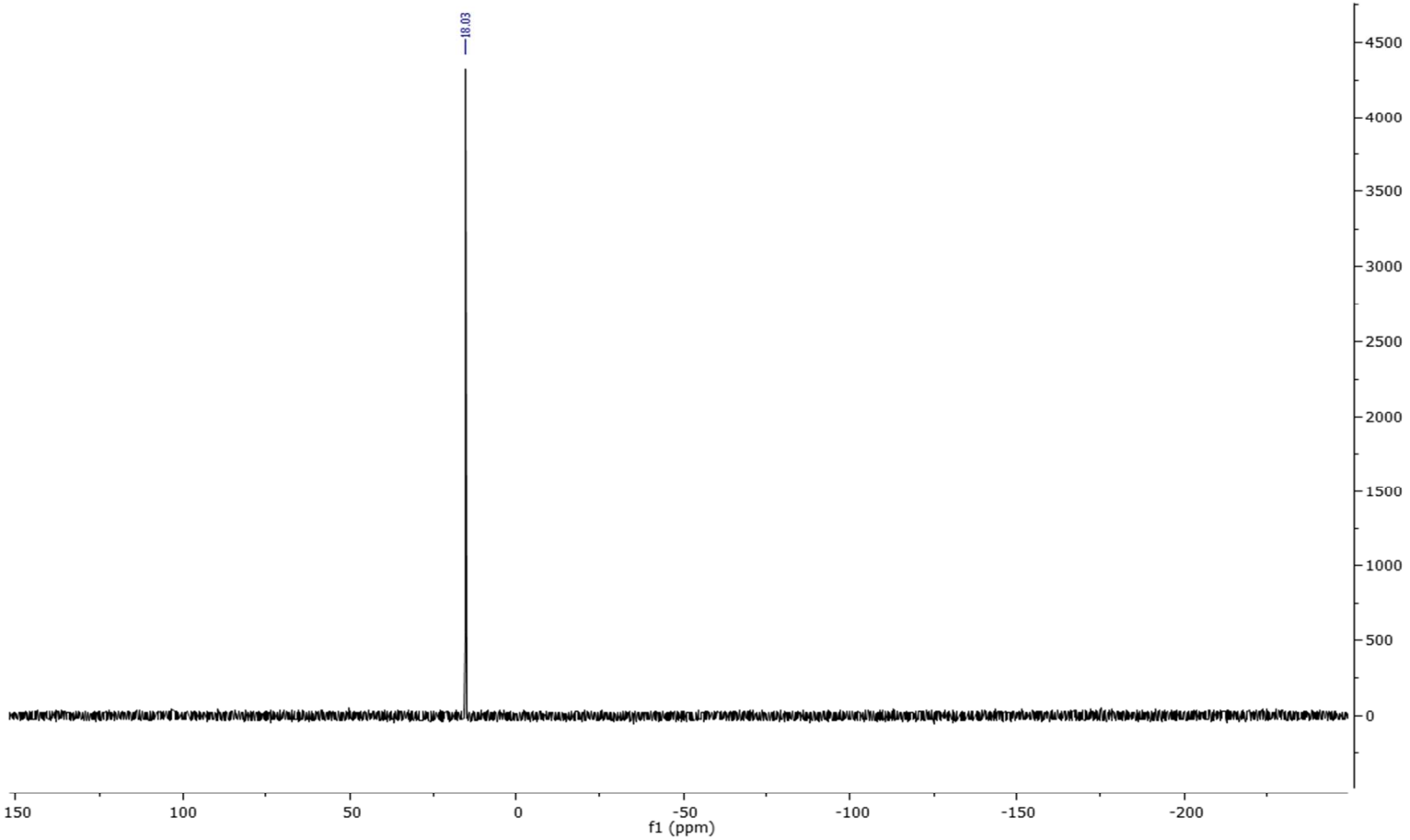

Figure N8, (e): ^{31}P NMR spectrum of *Table 3* compound **8** (as tetrabutylammonium salt) in CD_3OD after C18-SPE trapping of the target compound.

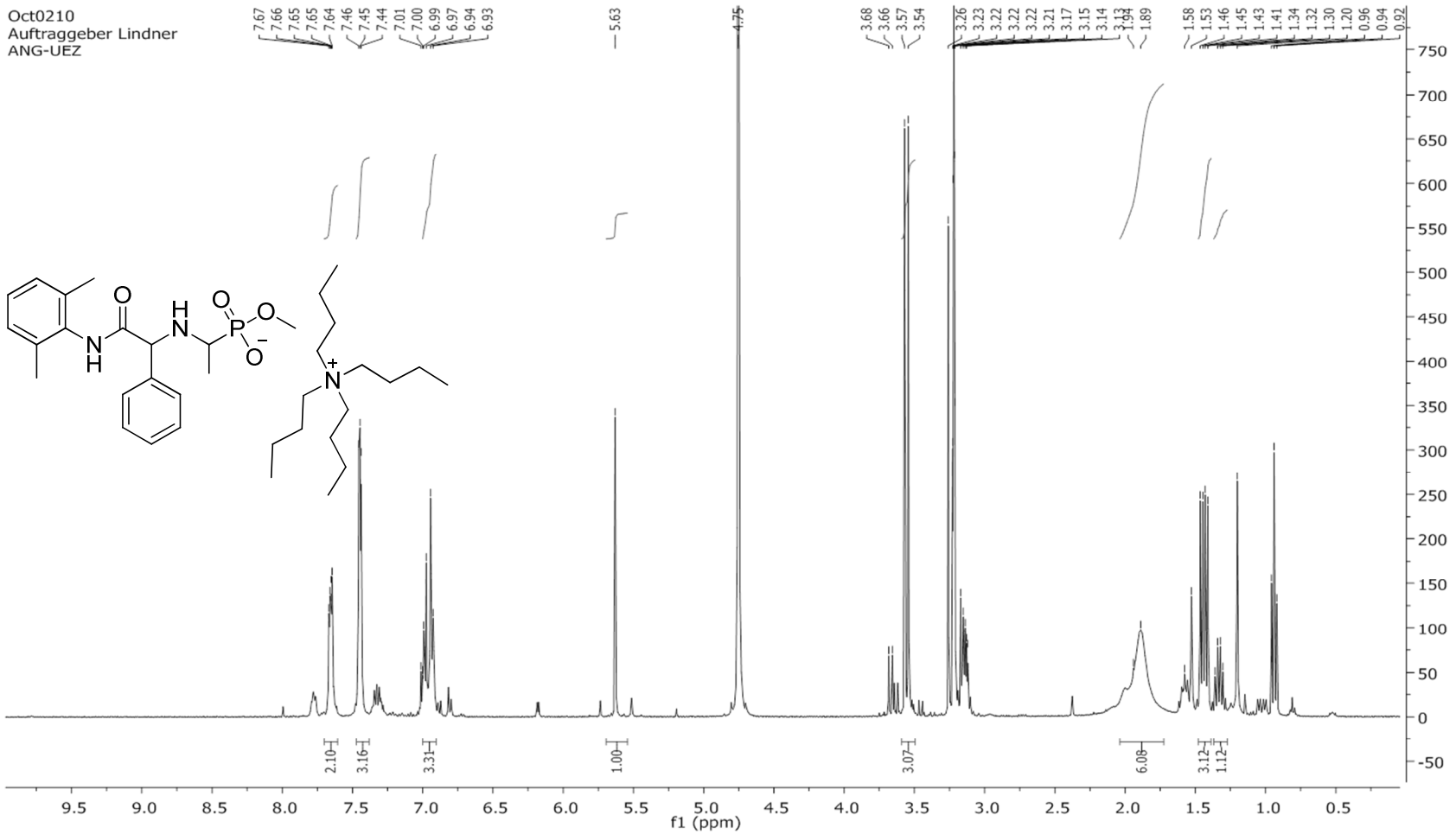

Figure N9, (a): ^{1}H NMR spectrum of *Table 3* compound **9** (as tetrabutylammonium salt, mixture 1:6 of the first and second eluting diasteromers) in CD_3OD. ∫ of TBAOH peaks =(3.3 ppm) 1 , (1.5 ppm) 4, (1 ppm) 3. Ratio TBAOH- target compound ~1:4.

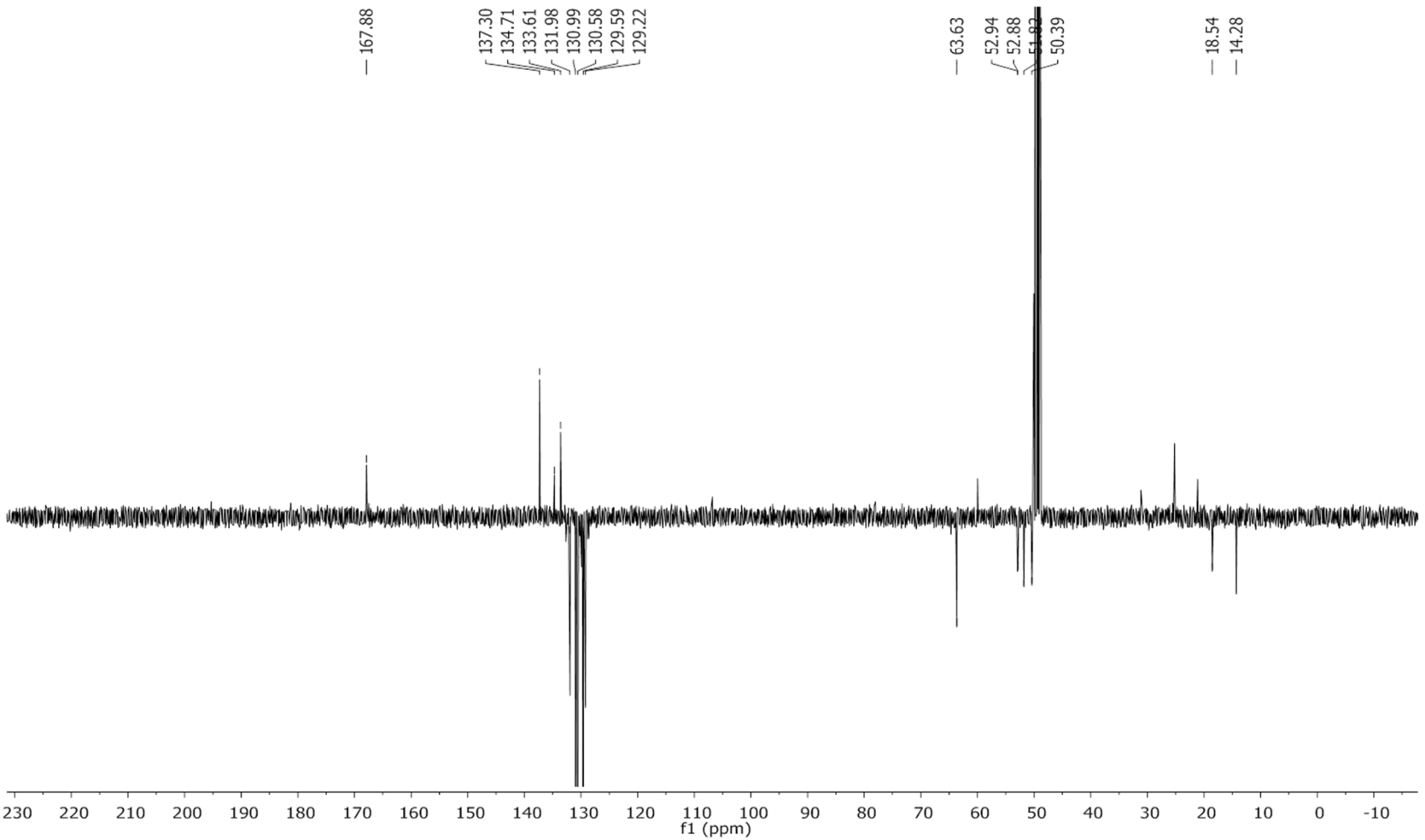

Figure N9, (b): ^{13}C NMR spectrum of *Table 3* compound **9** (as tetrabutylammonium salt) in CD_3OD.

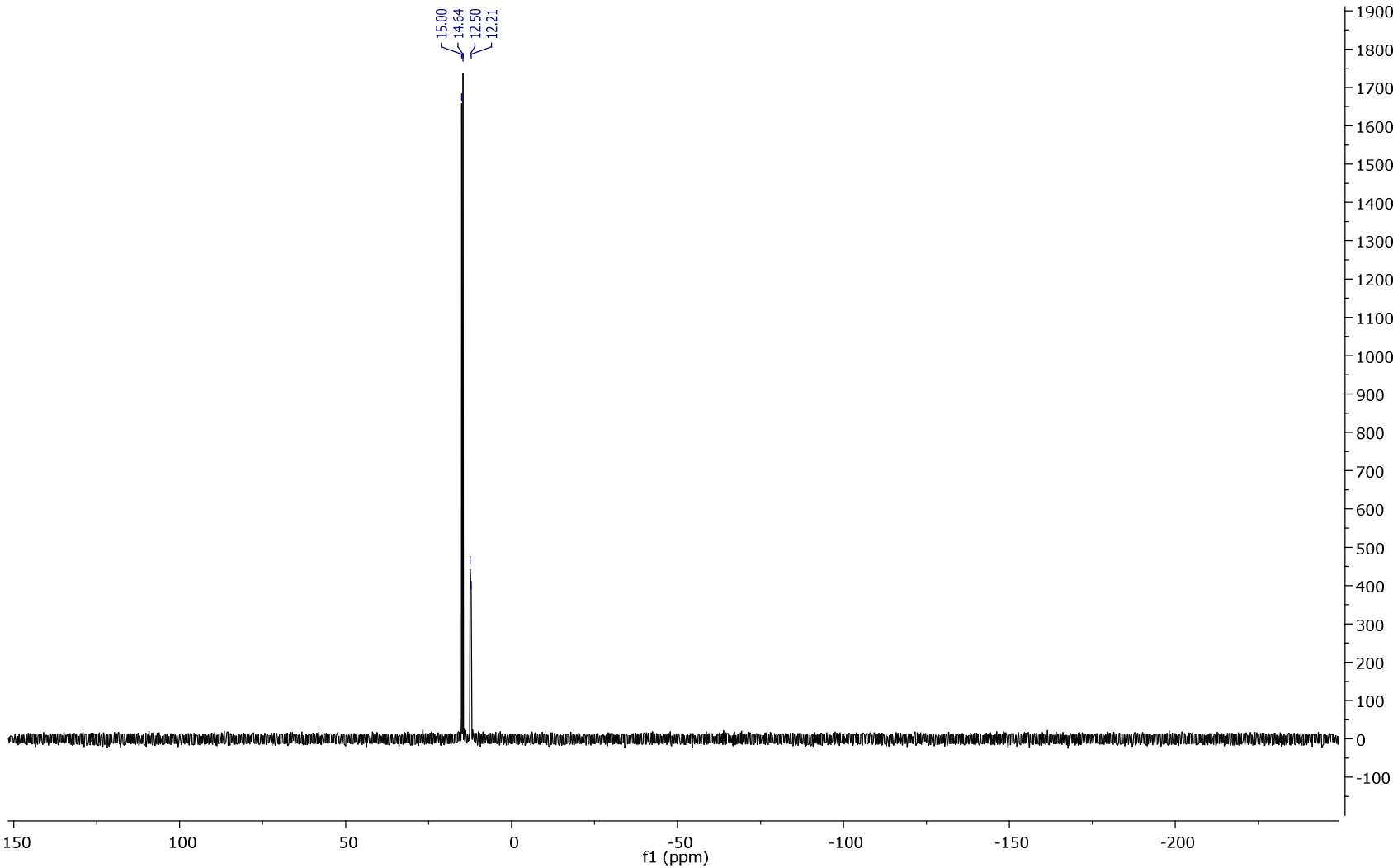

Figure N9, (c): ^{31}P NMR spectrum of *Table 3* compound **9** (as tetrabutylammonium salt) in CD_3OD.

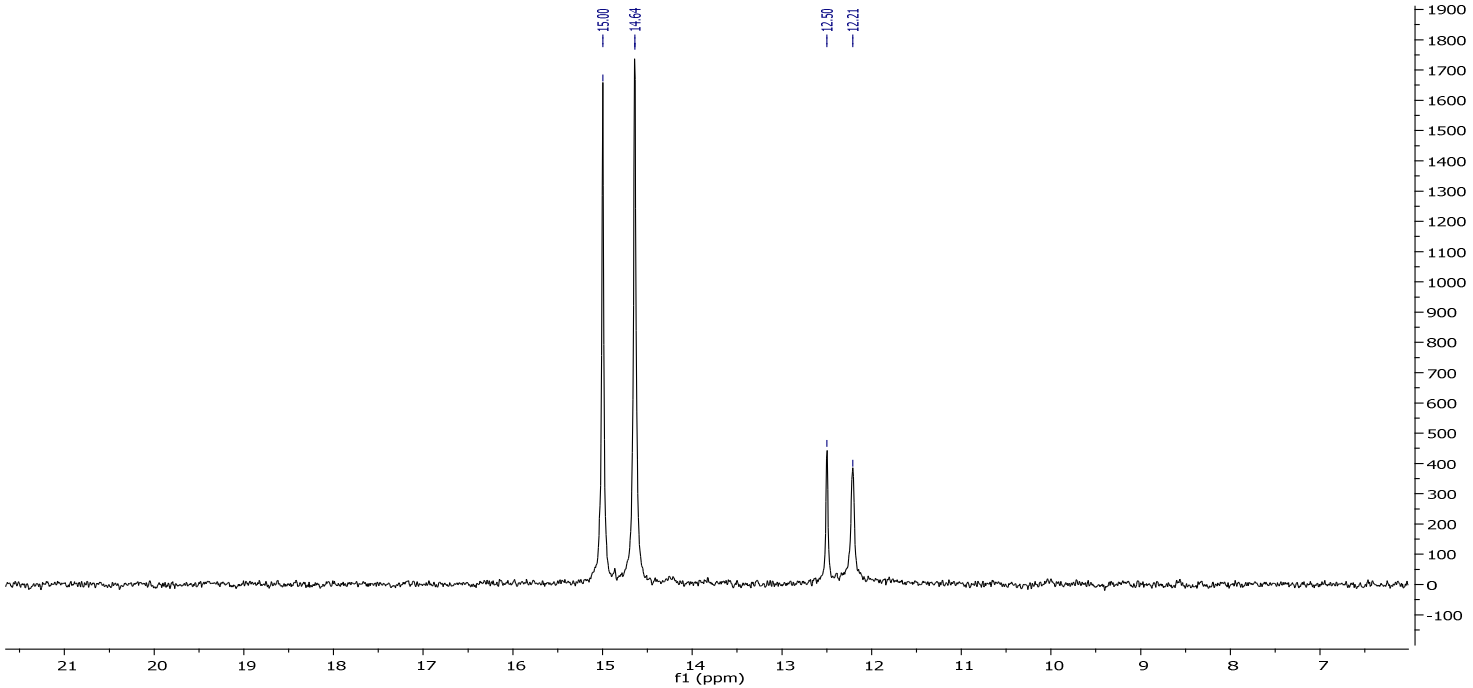

Figure N9, (d): ^{31}P NMR spectrum of Table 3 compound 9 (as tetrabutylammonium salt) in CD3OD. The 31P NMR spectrum reflects the presence of the pair of diastereomers in their approximate ratio 1:4 (ä 15 vs 12 ppm) and at the same time the coexistence of zwitterionic and tetrabutylammonium salt forms (ä for the first diastereomer: 15.00 and 14.64 and for the second: 12.50 – 12.21 ppm). Data reported in literature report that between phosphonic acid and their salts differences in chemical shifts are observed. For instance, methylphosphonic acid (δ 31.1) gives a diammonium salt with δ 19.31 and a tetramethylammonium salt with δ 20.11[3]. The aminophosphonic acid 1-amino 1-ethyl phosphonic acid when dissolved in water gives a zwitterion with δ 19.12, but in NaOH solution it has δ 17 for the dianion[4].

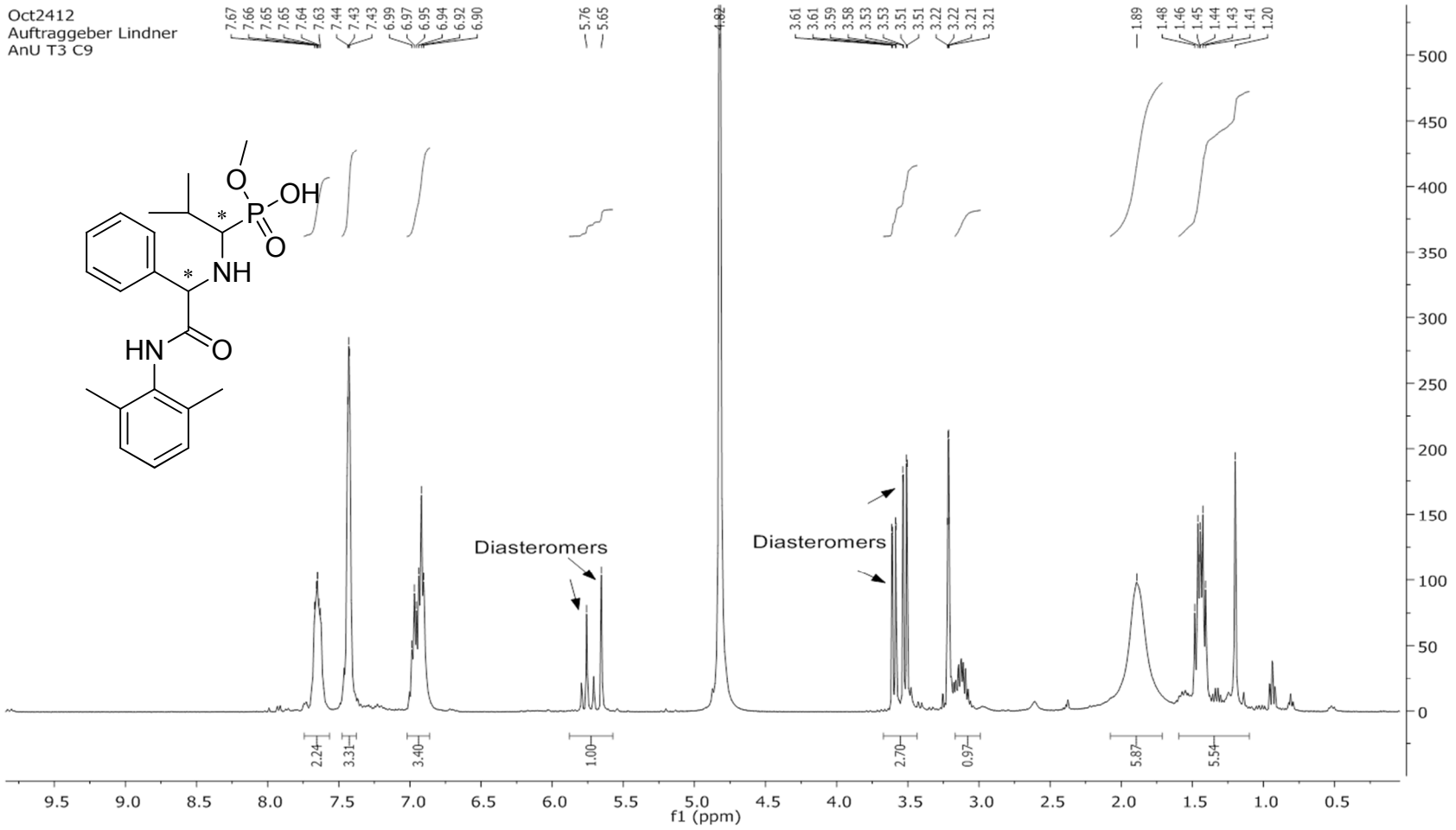

Figure N10, (a): ^{1}H NMR spectrum of *Table 3* compound **10** (mixture of diastereomers in a 1:3 ratio) in CD_3OD.

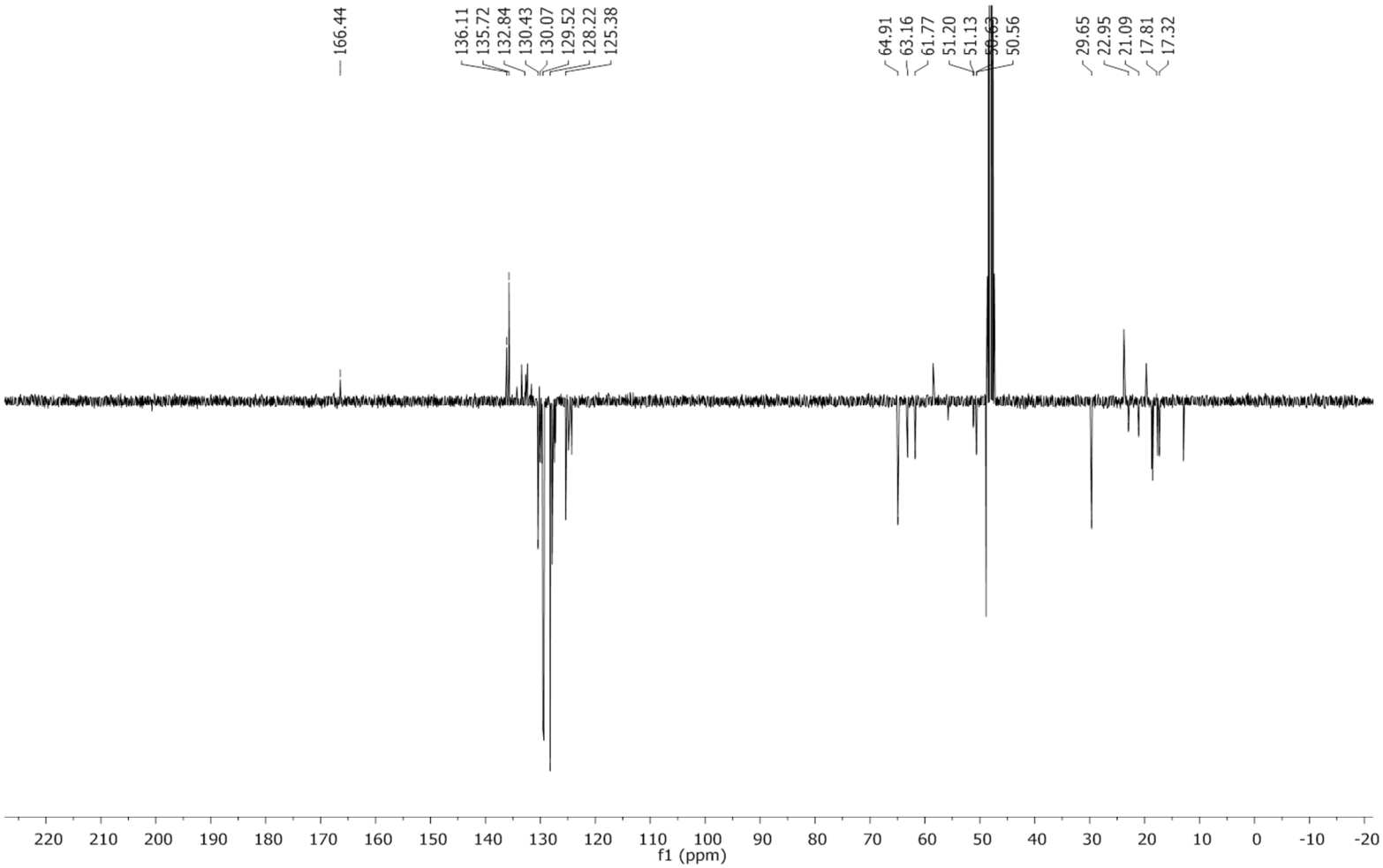

Figure N10, (b): ^{13}C NMR spectrum of *Table 3* compound **10** (mixture of diastereomers) in CD_3OD.

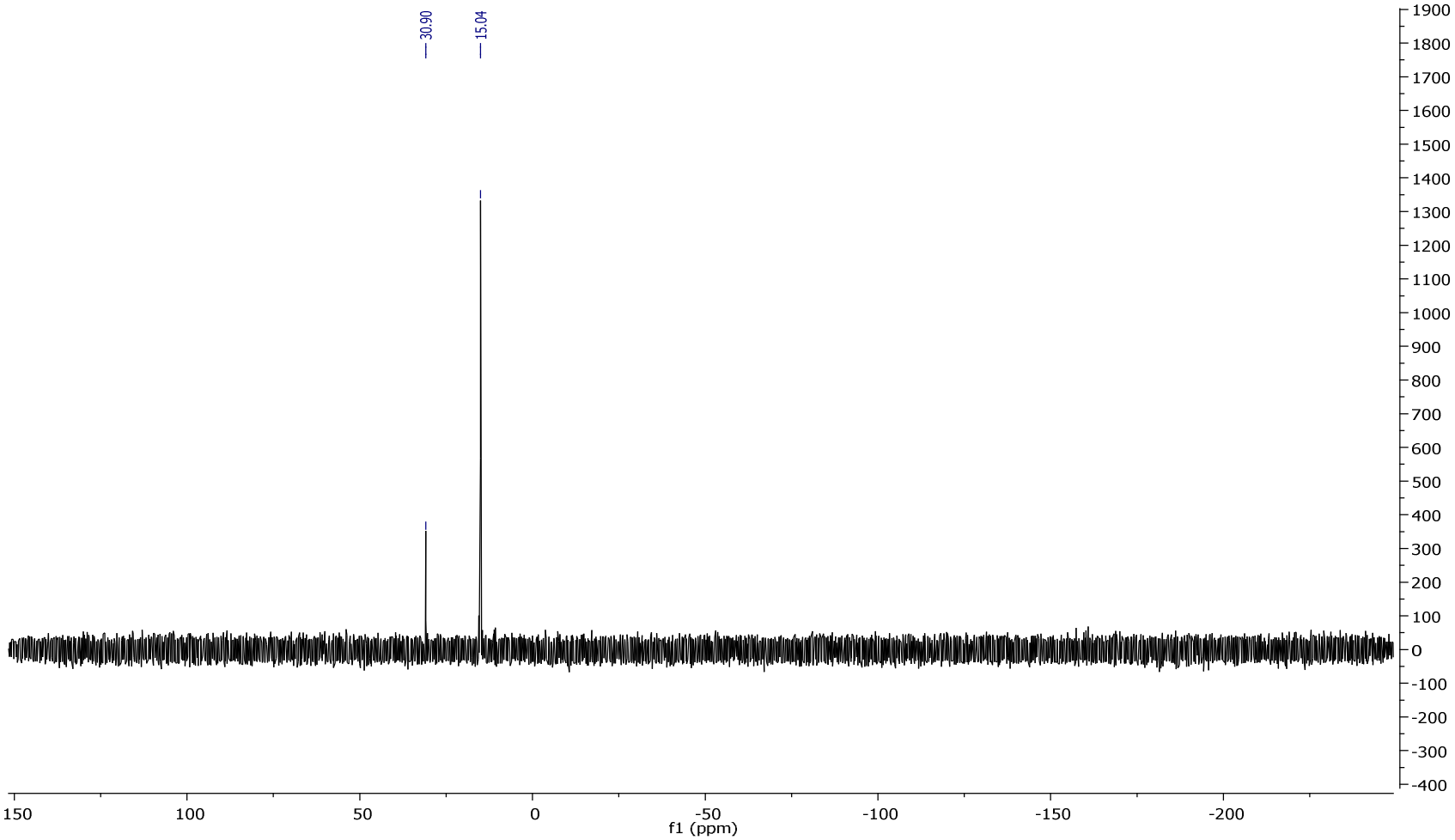

Figure N10, (c): ^{31}P NMR spectrum of Table 3 compound 10 (mixture of diastereomers) in CD3OD. The presence of a double peak in the ^{31}P NMR spectrum is a result of the presence of both of the diastereomeric forms of the target compound in the sample.

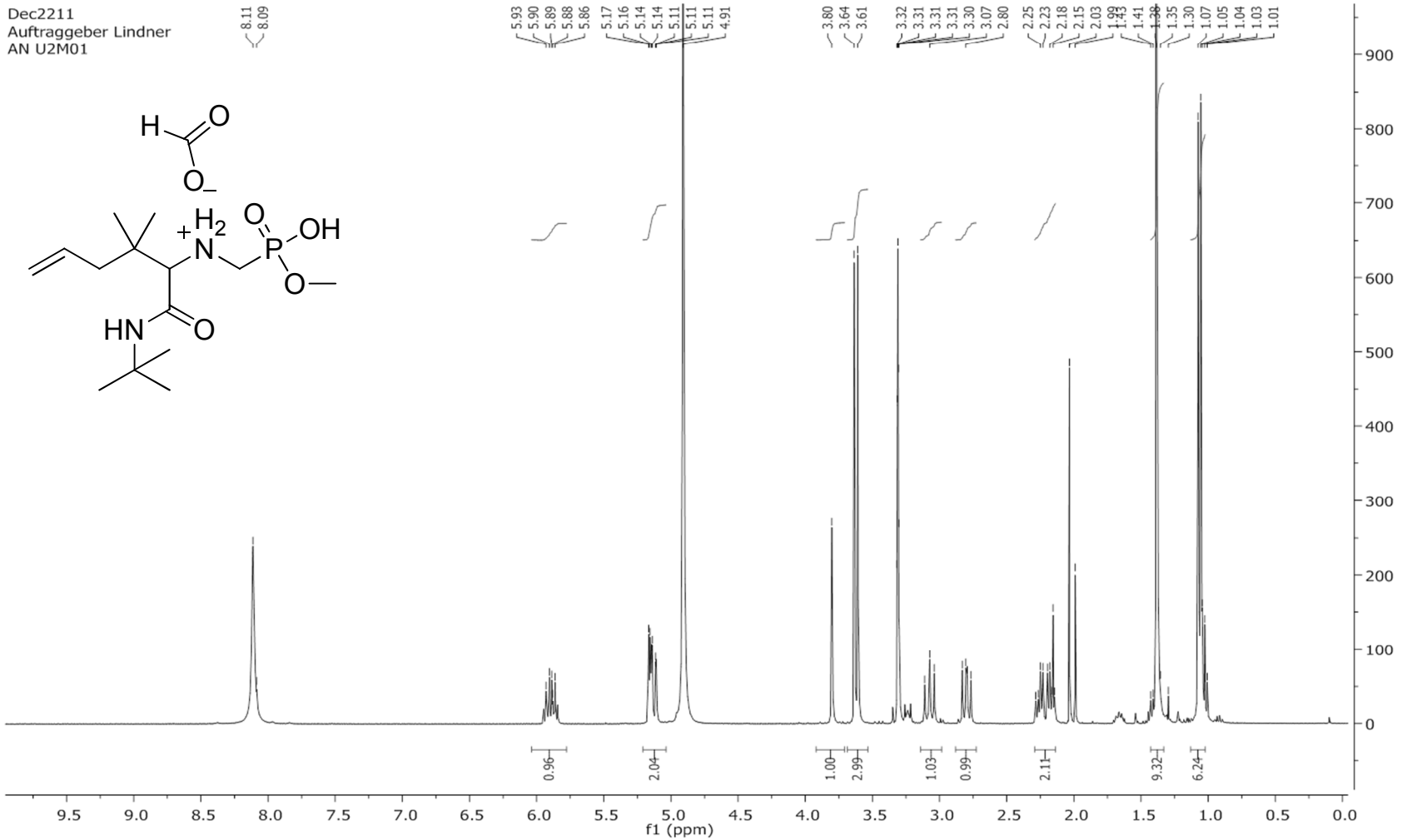

Figure N11, (a): ^{1}H NMR spectrum of *Table 3* compound **11** (as formate salt) in CD_3OD. ∫ of FA peak =(8.2 ppm) 3.

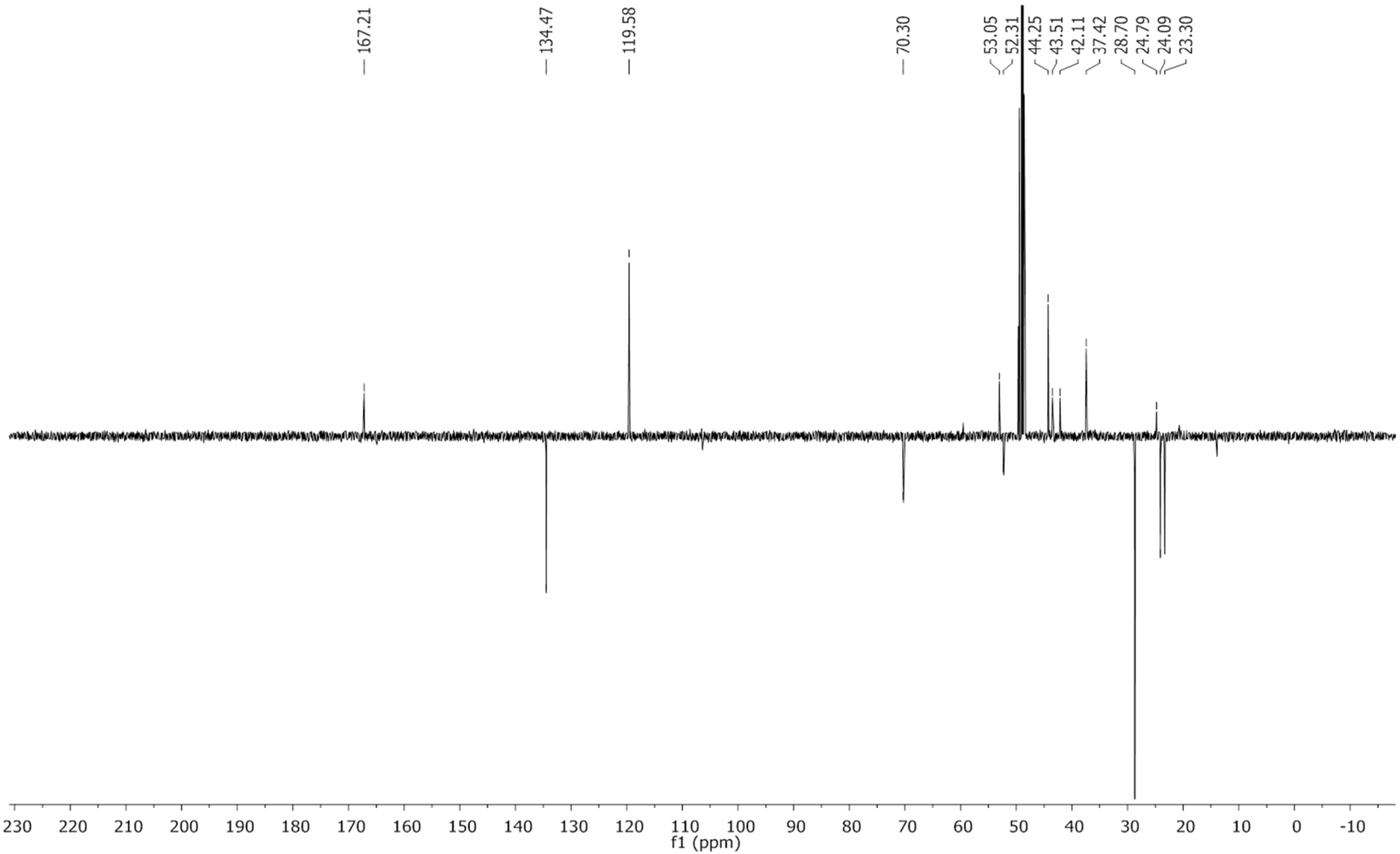

Figure N11, (b): ^{13}C NMR spectrum of *Table 3* compound **11** (as formate salt) in CD_3OD.

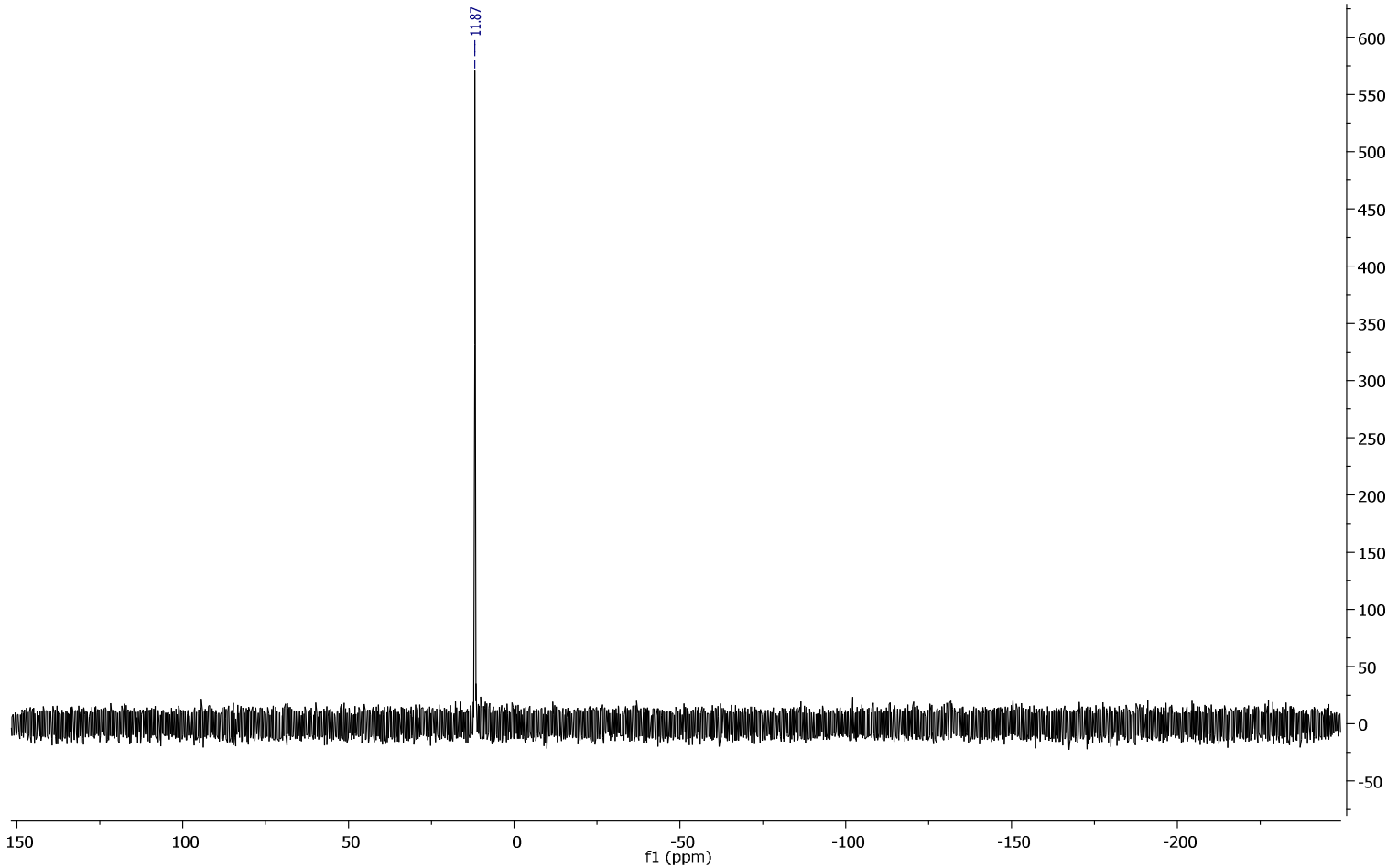

Figure N11, (c): ^{31}P NMR spectrum of *Table 3* compound **11** (as formate salt) in CD_3OD.

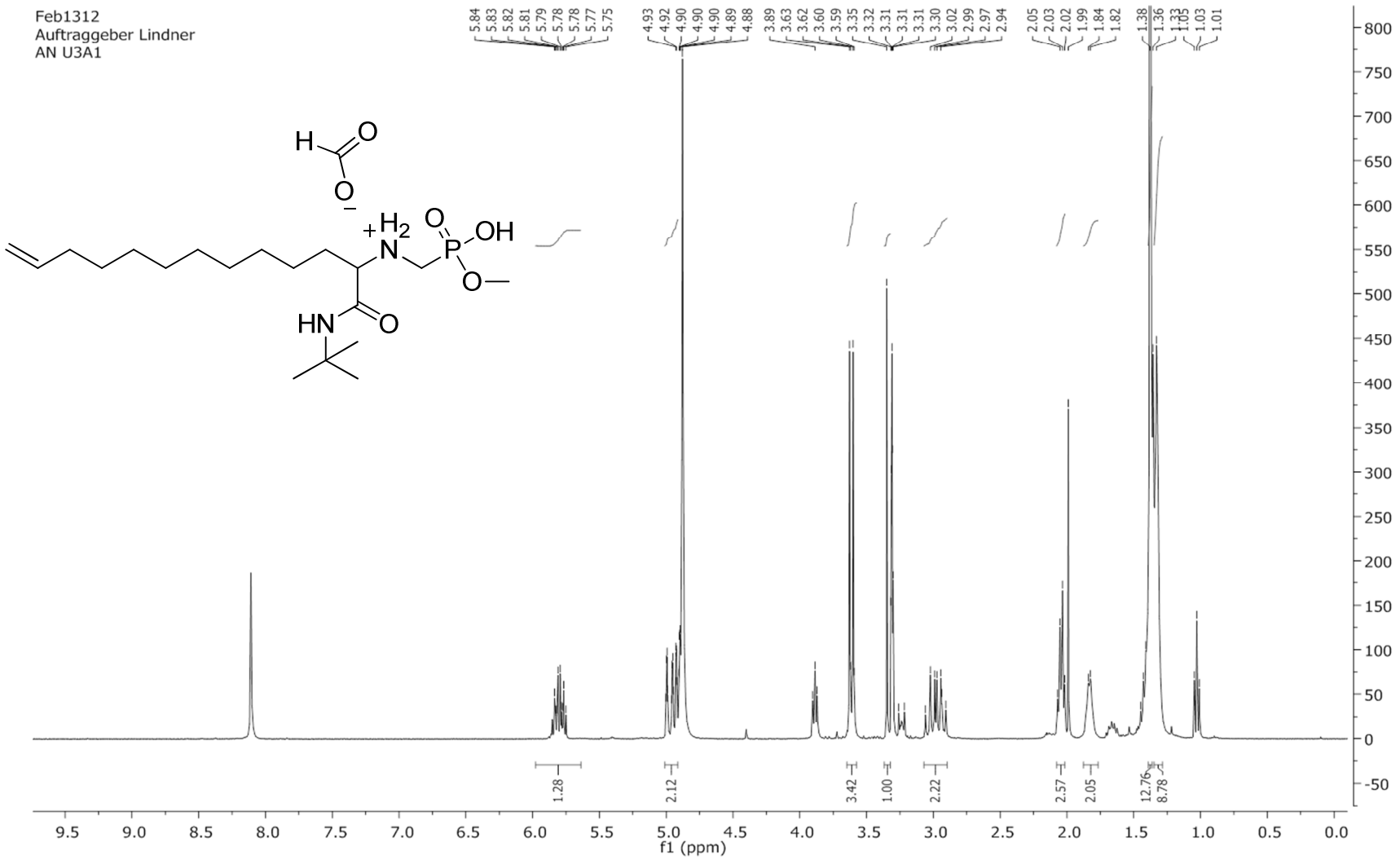

Figure N12, (a): ^{1}H NMR spectrum of *Table 3* compound **12** (as formate salt) in CD_3OD. ∫ of FA peak =(8.2 ppm) 2.6.

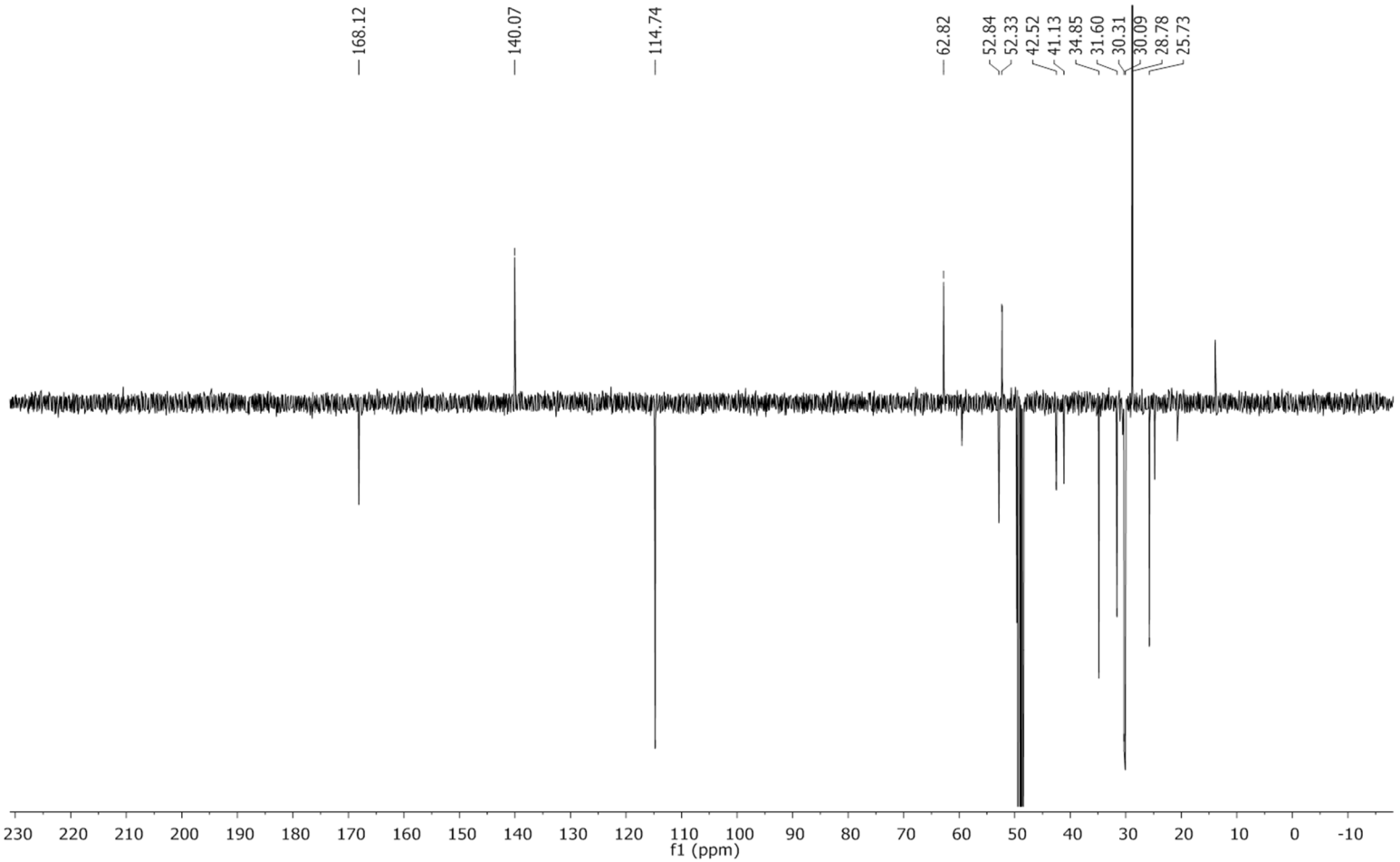

Figure N12, (b): ^{13}C-NMR spectrum of *Table 3* compound **12** (as formate salt) in CD_3OD.

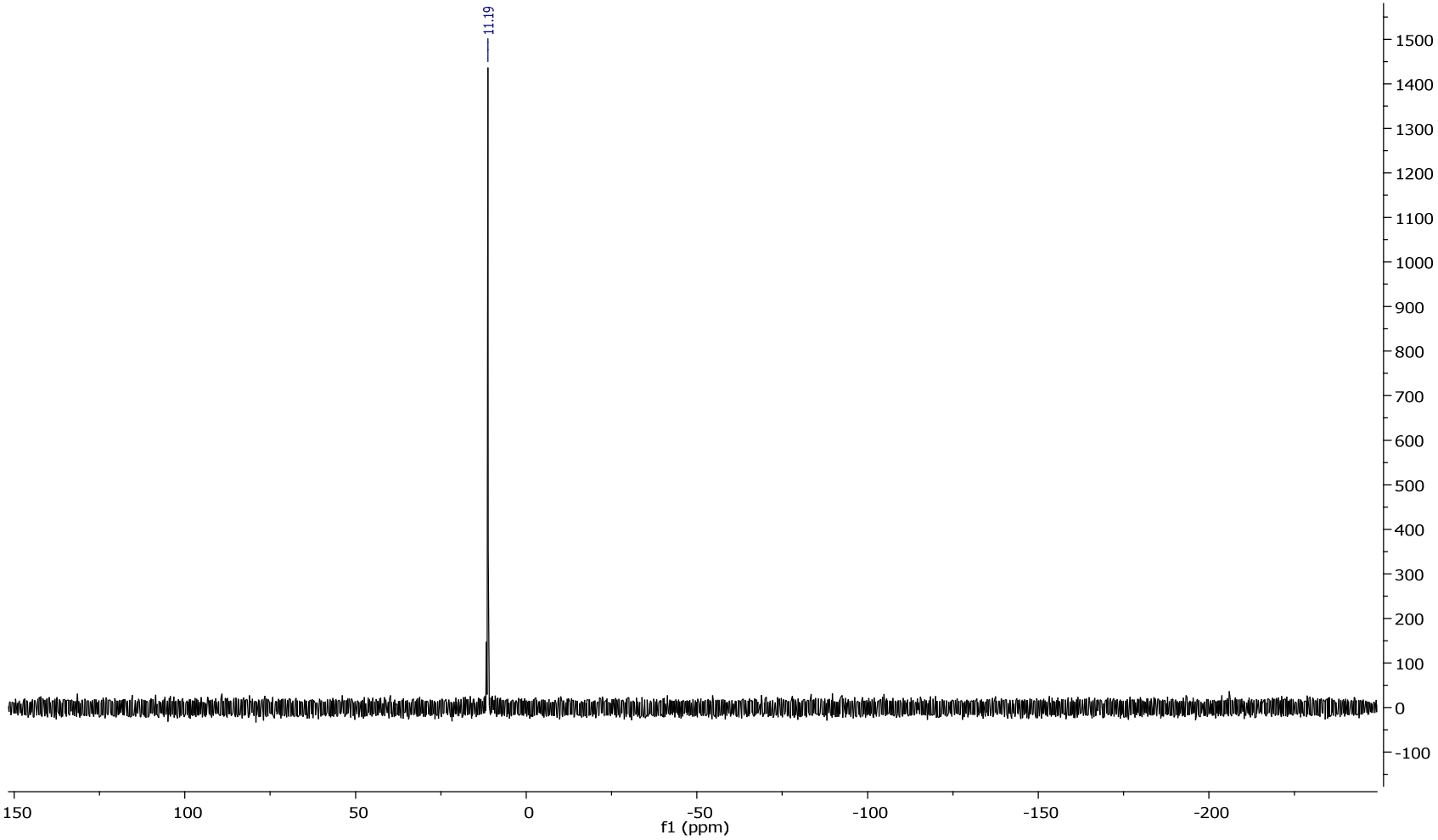

Figure N12, (c): ^{31}P-NMR spectrum of *Table 3* compound **12** (as formate salt) in CD_3OD.

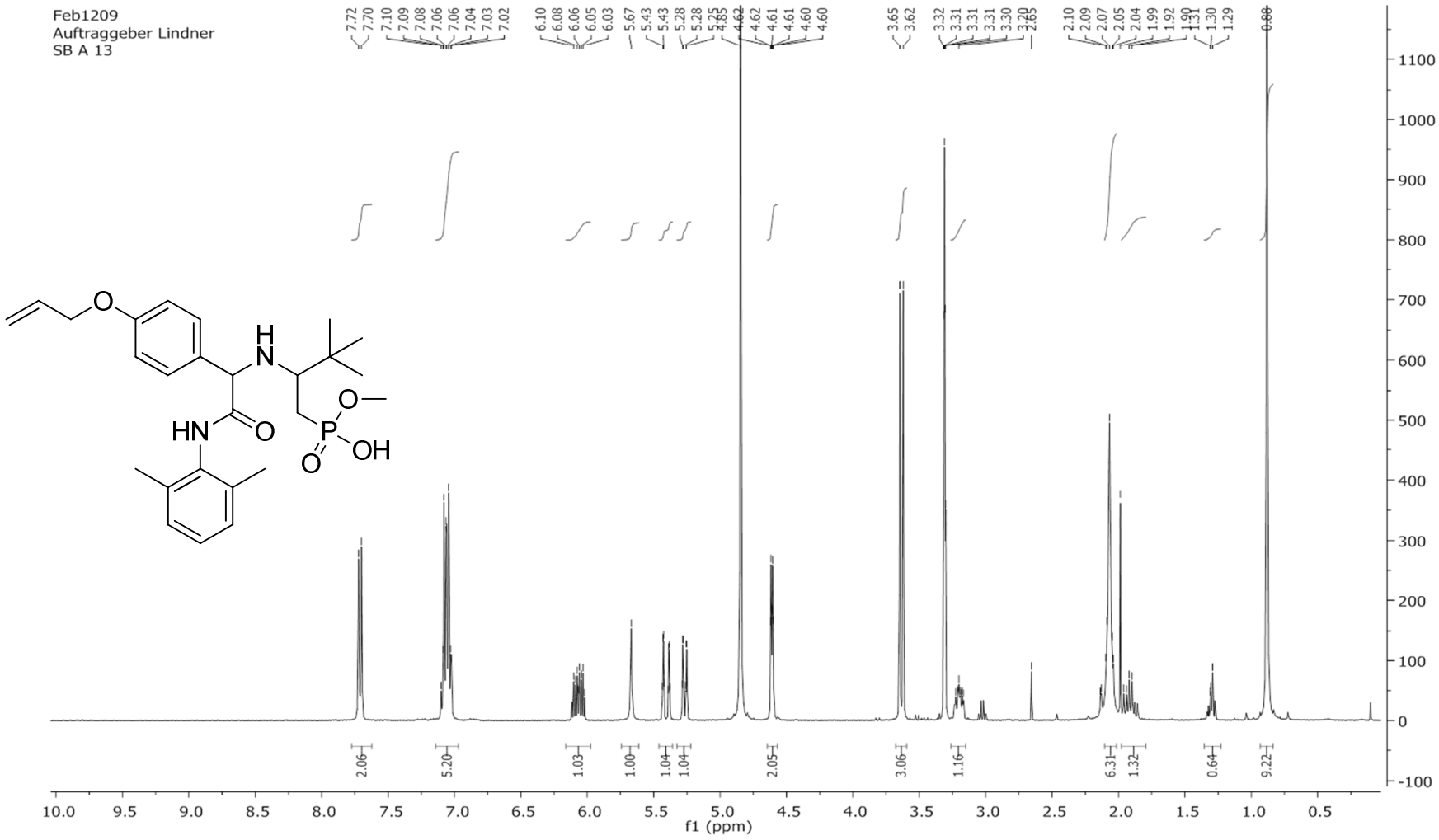

Figure N13, (a): ^{1}H NMR spectrum of *Table 3* compound **13** in CD_3OD.

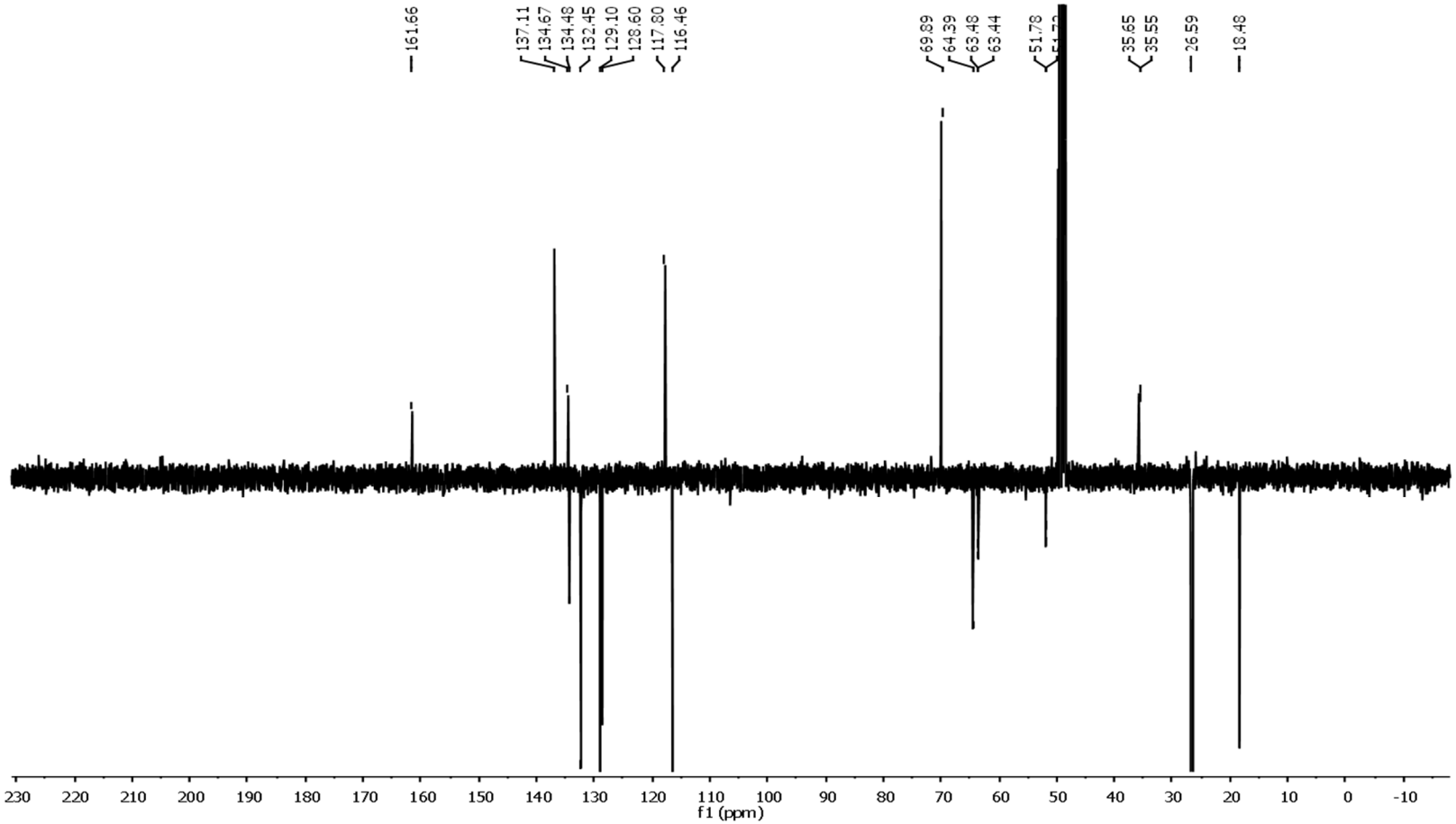

Figure N13, (b): ^{13}C NMR spectrum of *Table 3* compound **13** in CD_3OD.

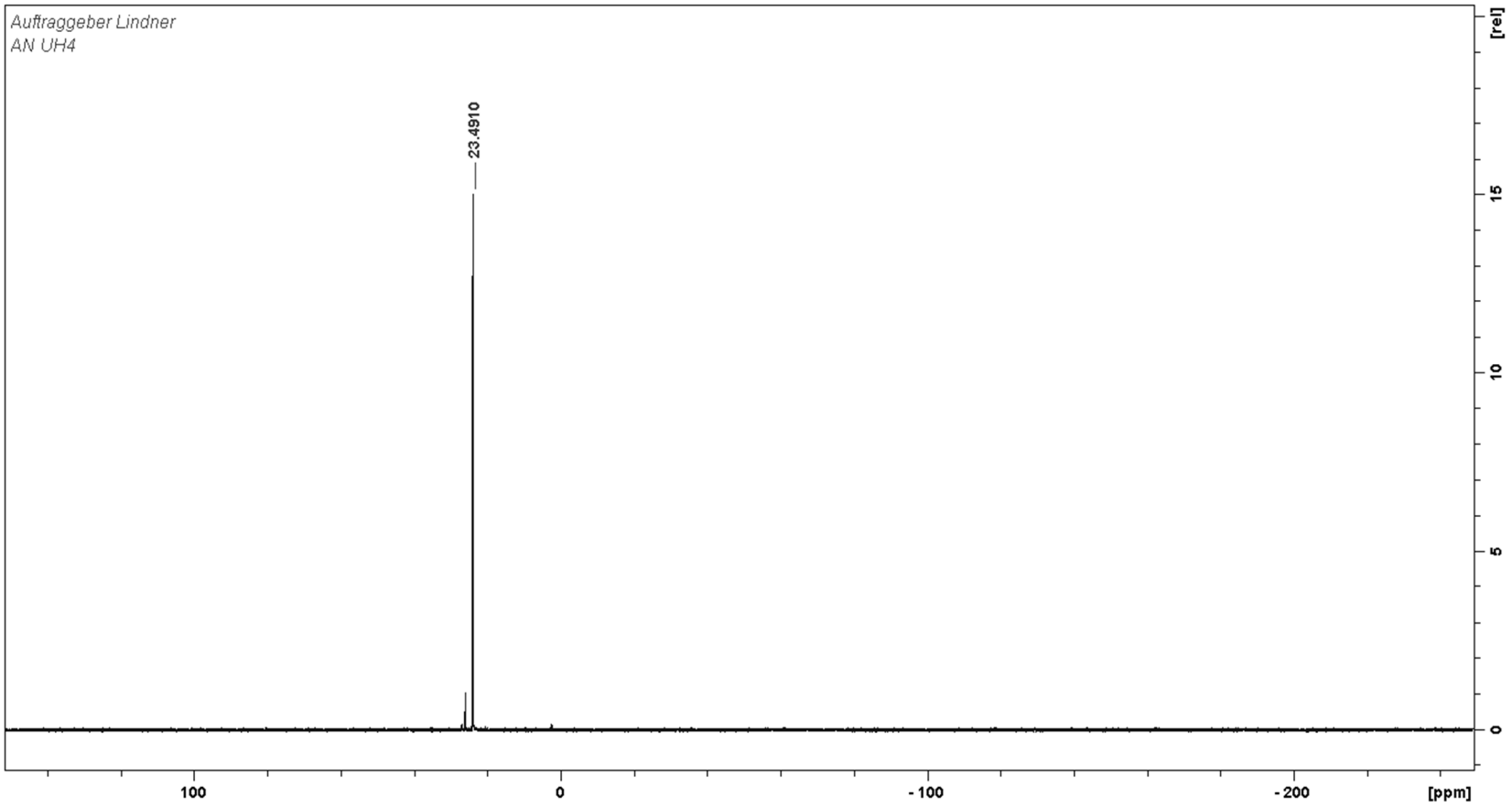

Figure N13, (c): ^{31}P NMR spectrum of *Table 3* compound **13** in CD_3OD.

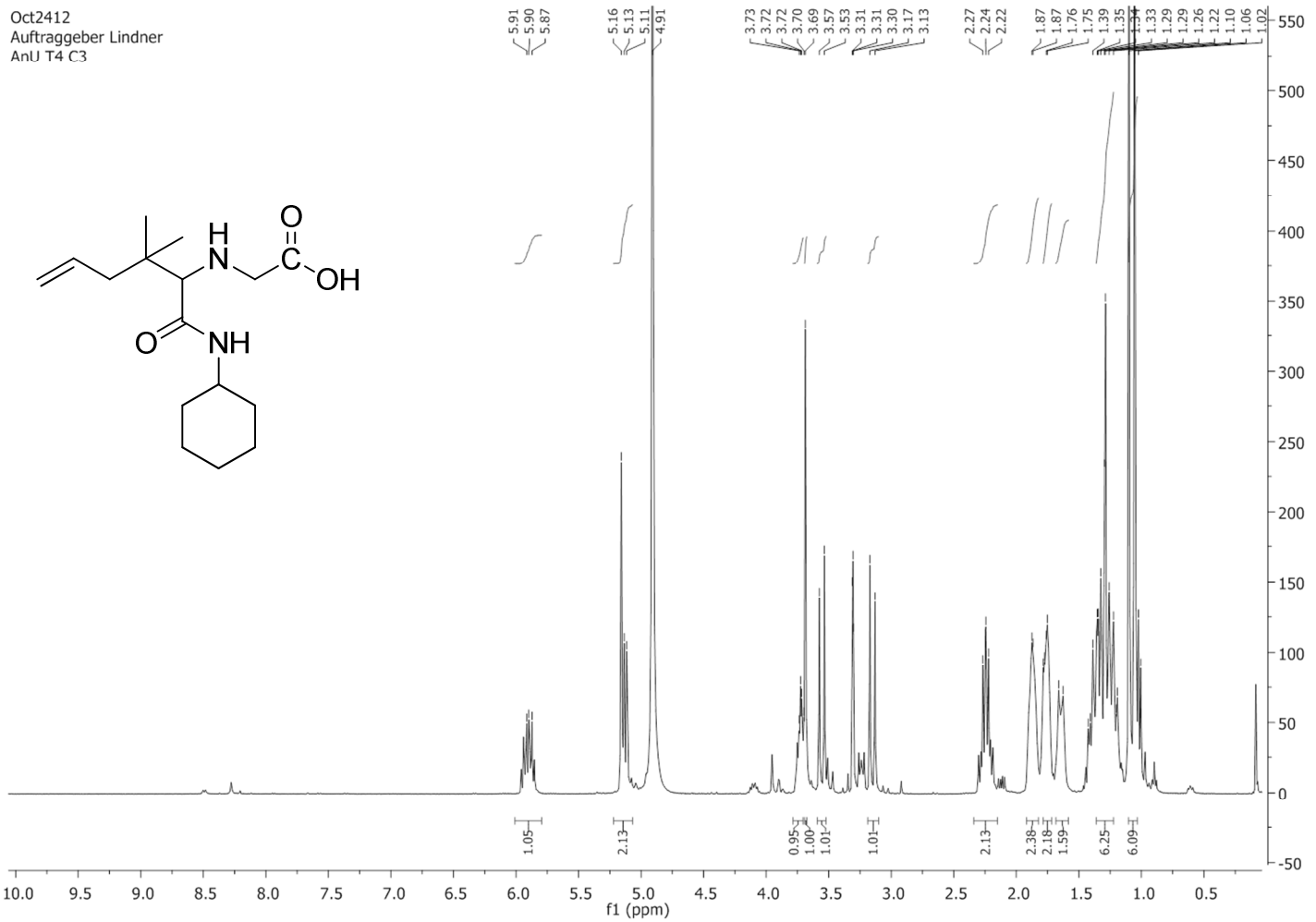

Figure N14, (a): ^{1}H NMR spectrum of *Table 4* compound **15** in CD_3OD.

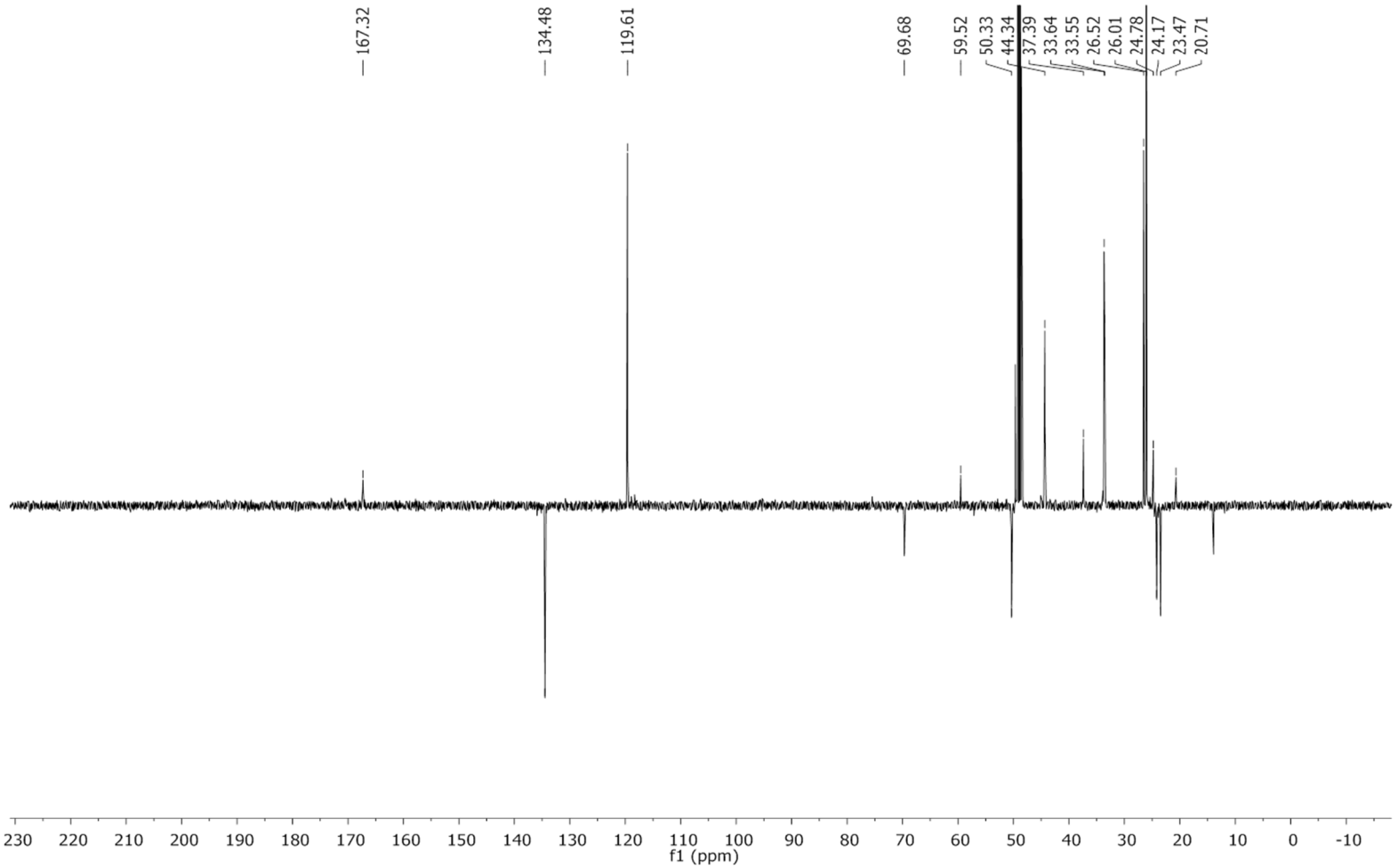

Figure N14, (b): ^{13}C NMR spectrum of *Table 4* compound **15** in CD_3OD.

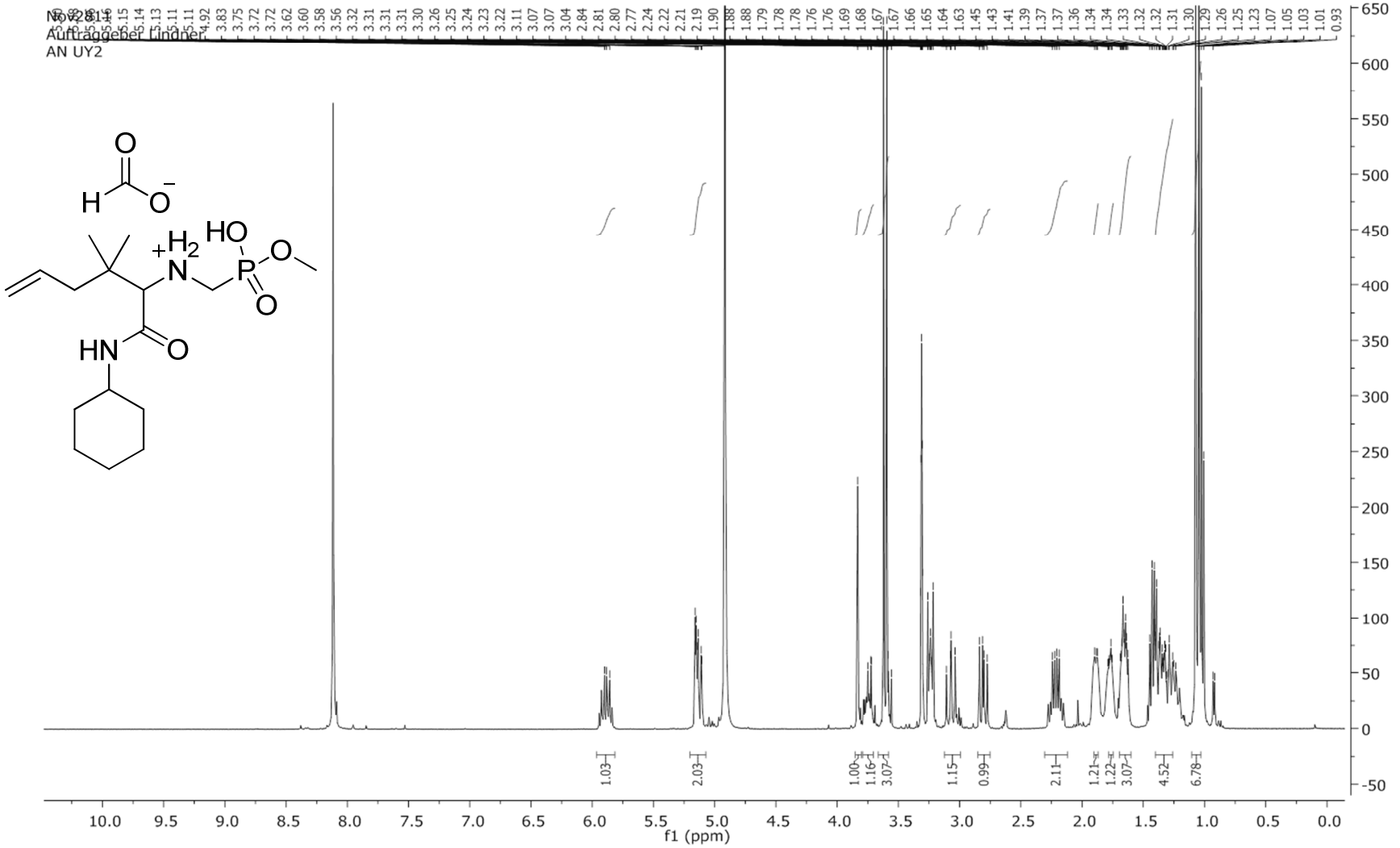

Figure N15, (a): ^{1}H NMR spectrum of *Table 4* compound **16** (as formate salt) in CD_3OD. ∫ of FA peak =(8.1 ppm) 4.

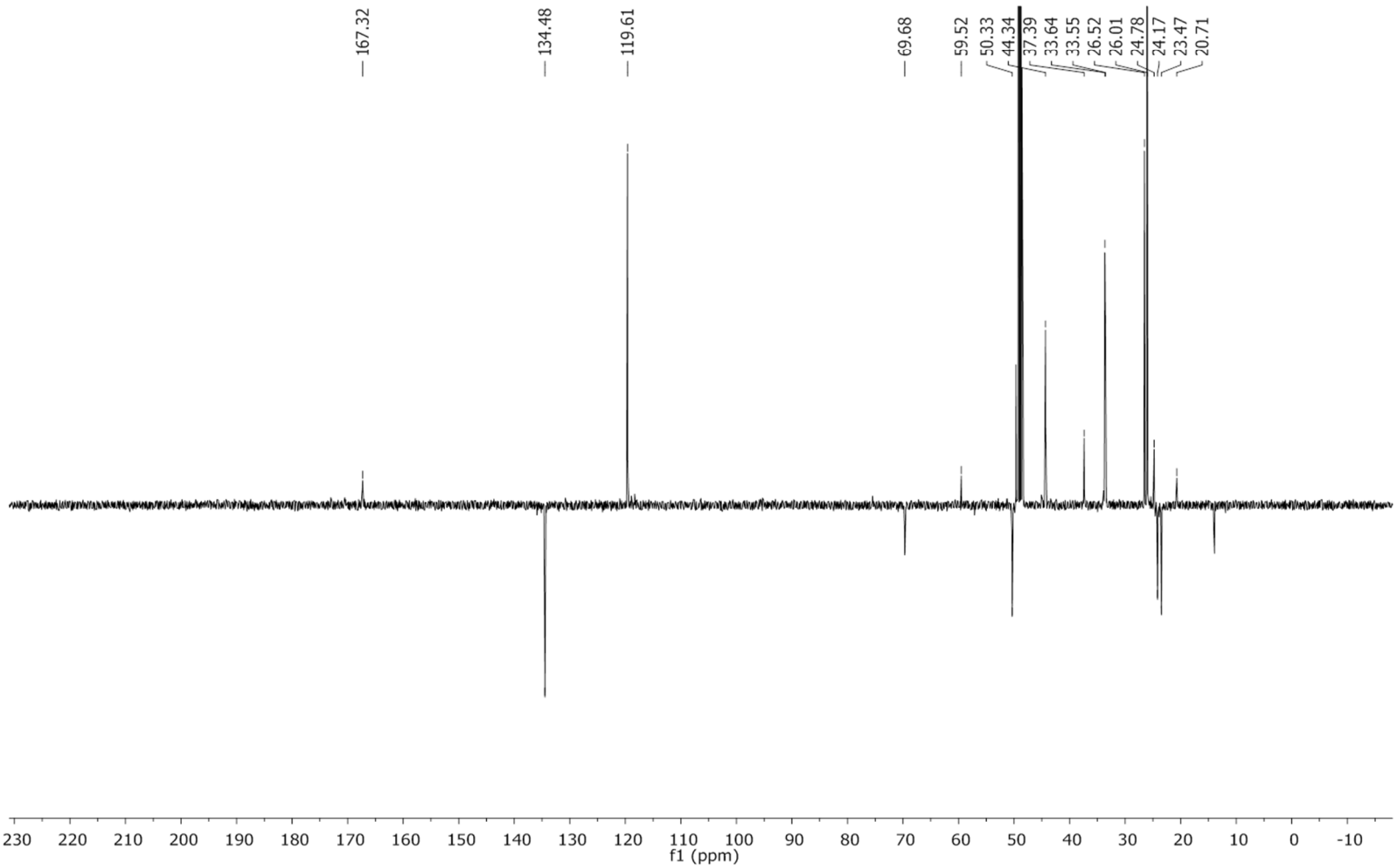

Figure N15, (b): ^{13}C NMR spectrum of *Table 4* compound **16** (as formate salt) in CD_3OD.

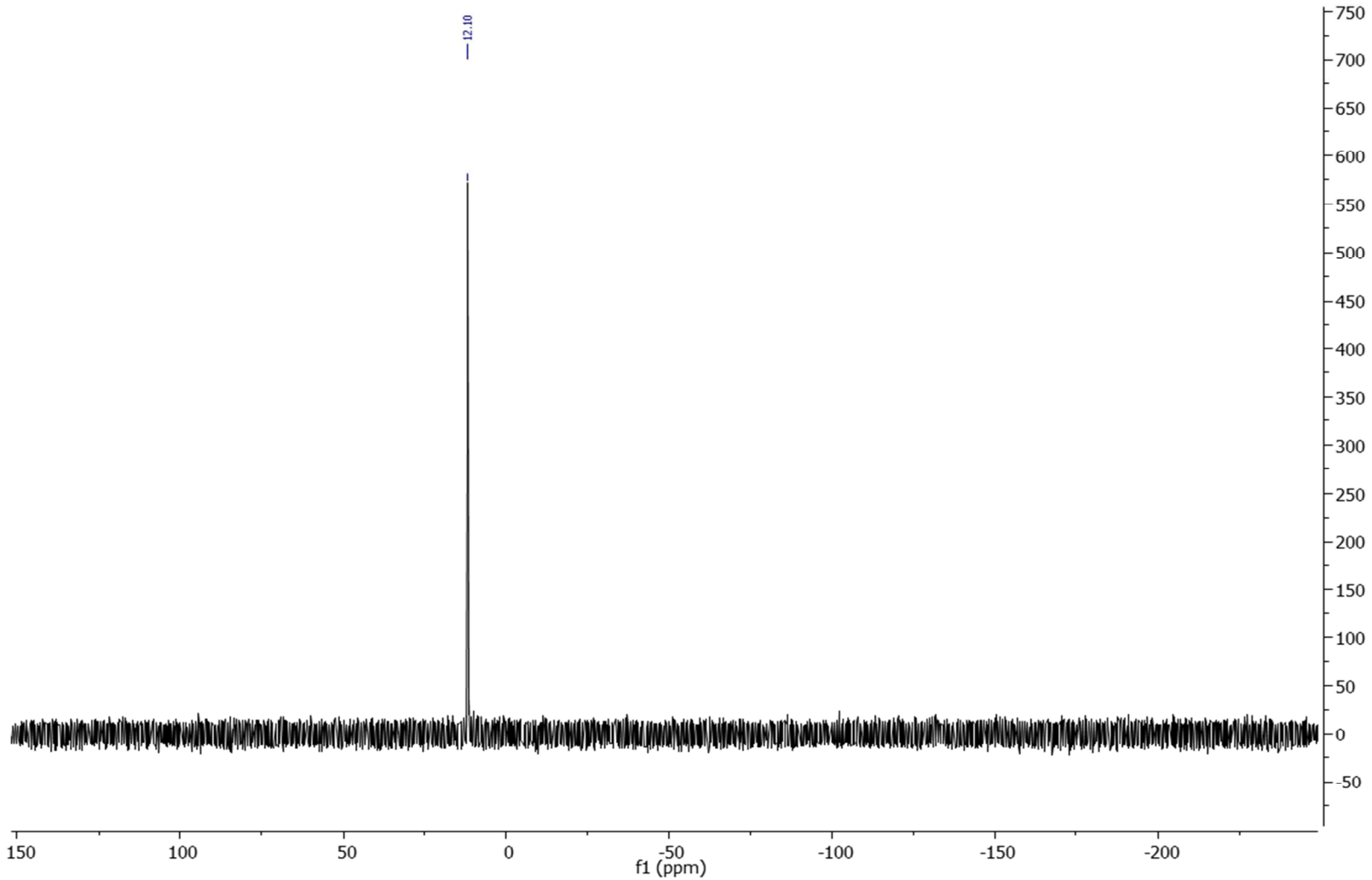

Figure N15, (c): ^{31}P NMR spectrum of *Table 4* compound **16** (as formate salt) in CD_3OD.

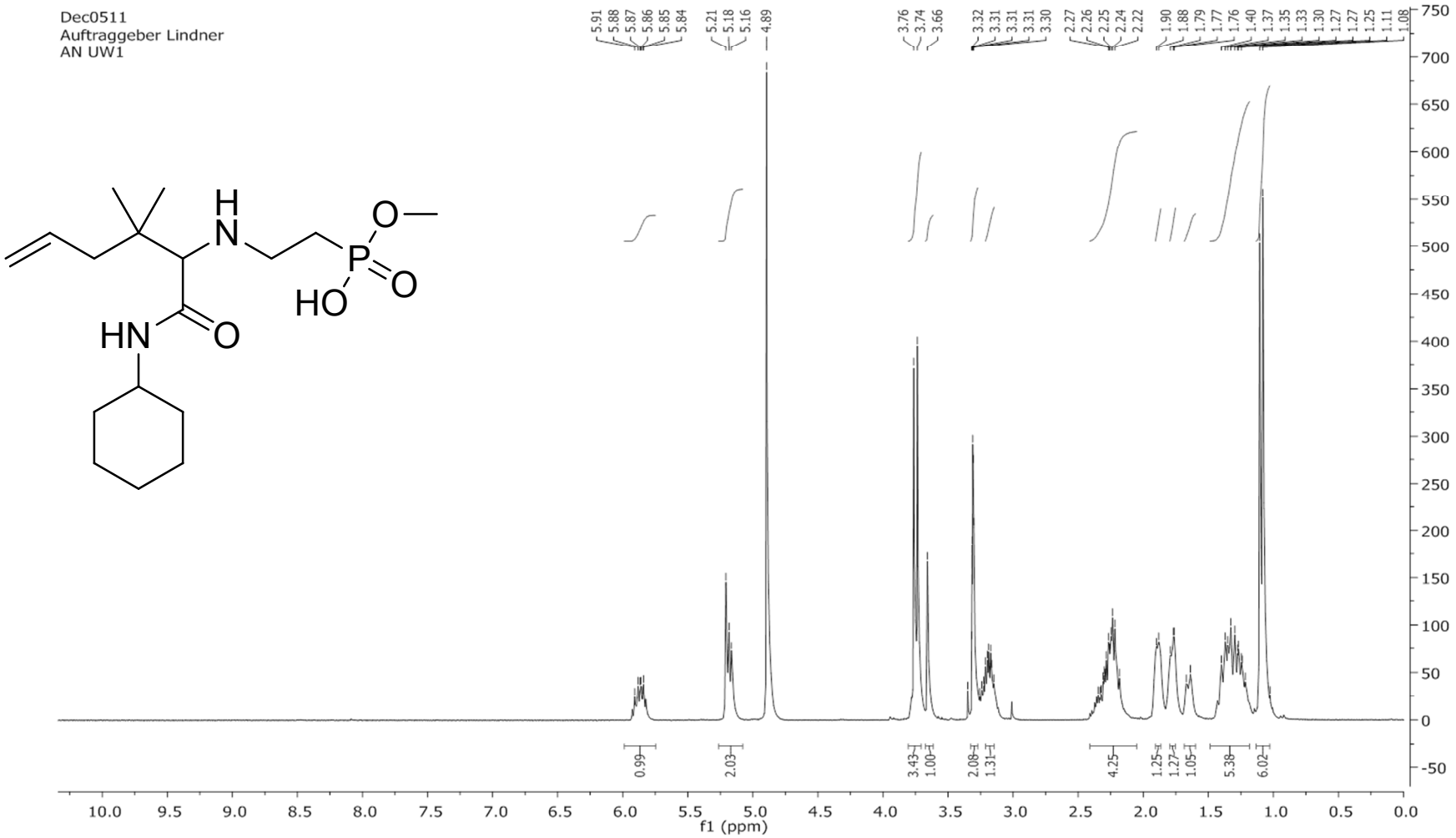

Figure N16, (a): ^{1}H NMR spectrum of *Table 4* compound **17** in CD_3OD.

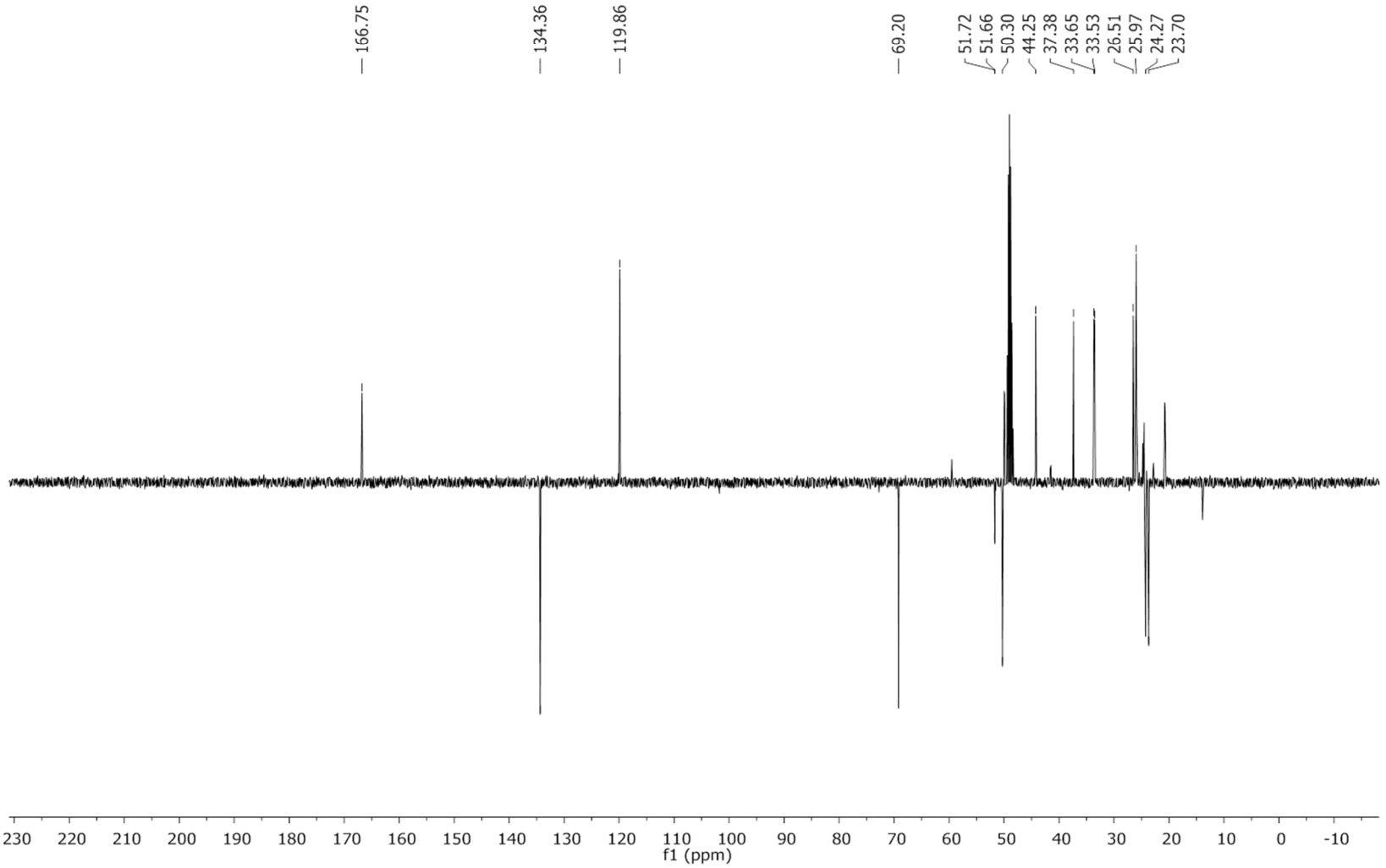

Figure N16, (b): ^{13}C NMR spectrum of *Table 4* compound **17** in CD_3OD.

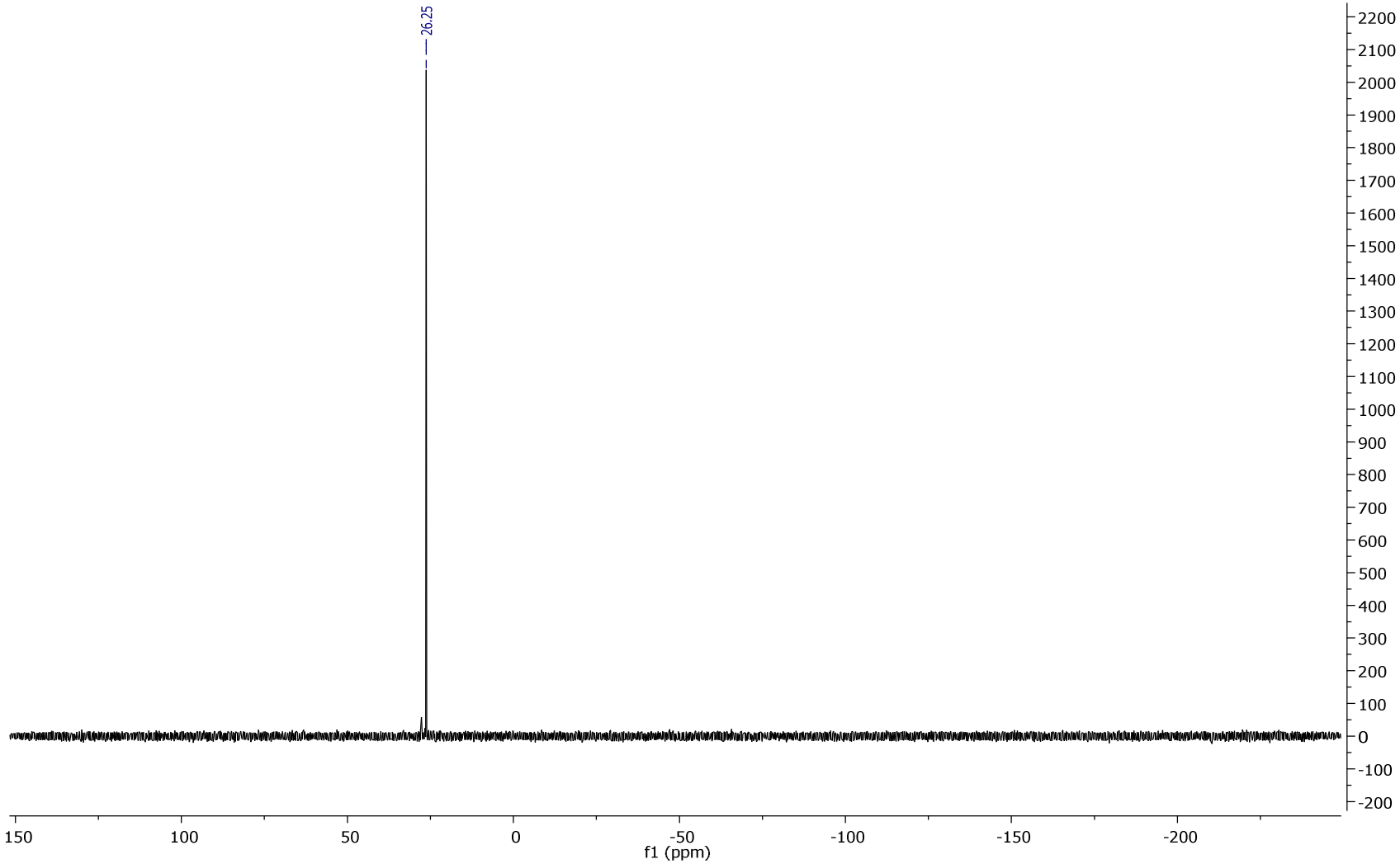

Figure N16, (c): ^{31}P NMR spectrum of *Table 4* compound **17** in D_2O.

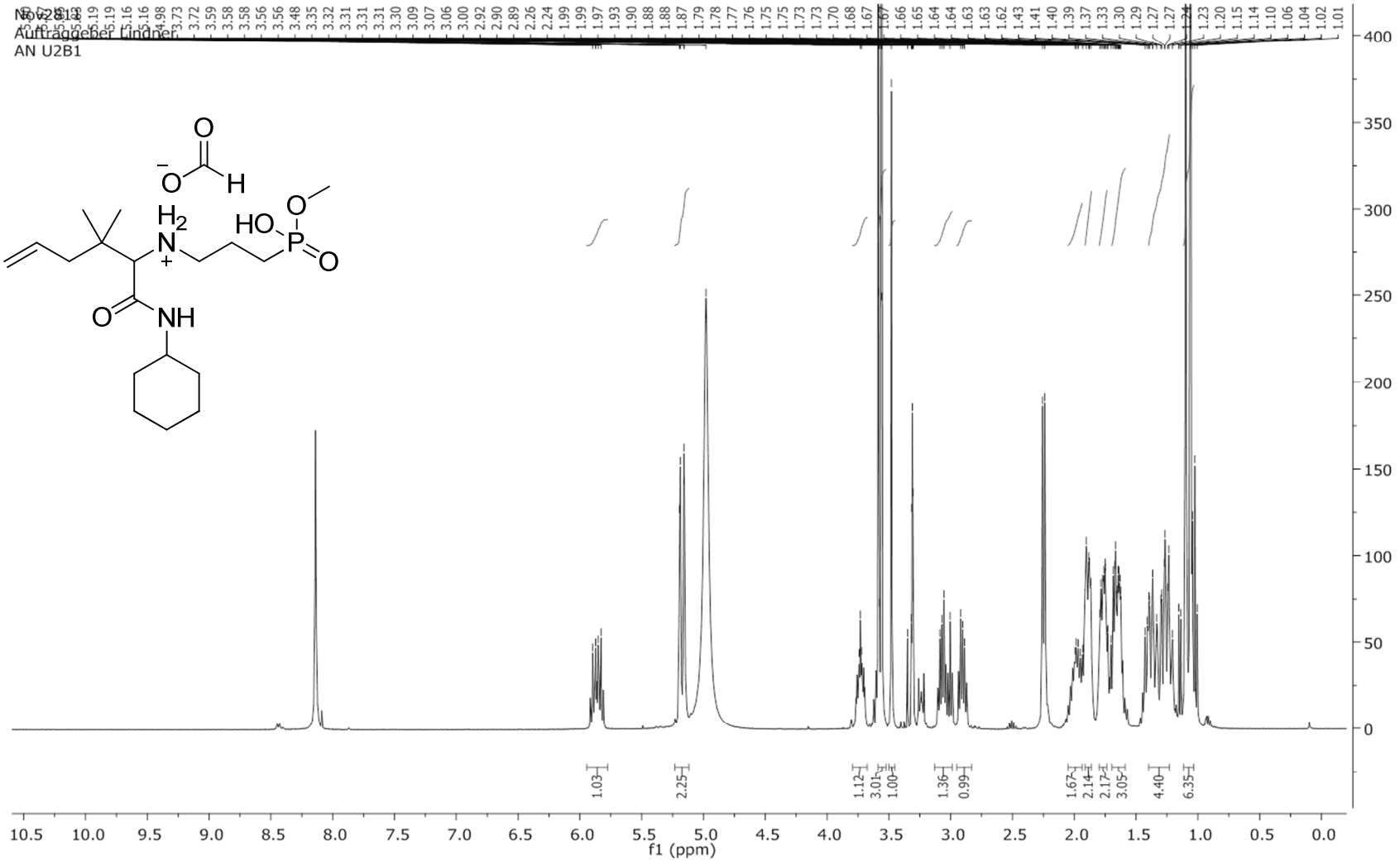

Figure N17, (a): ^{1}H NMR spectrum of *Table 4* compound **18** (as formate salt) in CD_3OD. ∫ of FA peak =(8.2 ppm) 1.1.

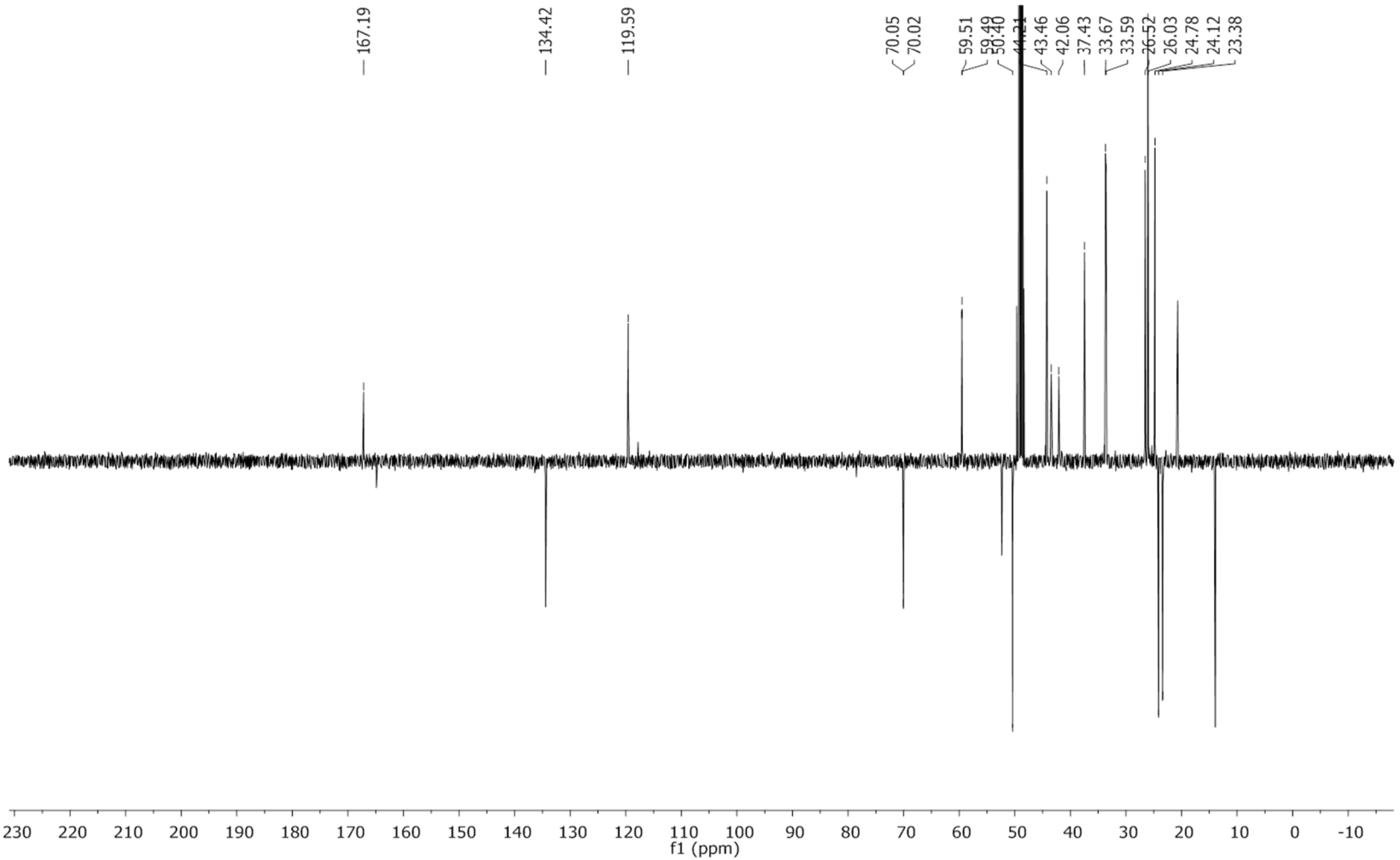

Figure N17, (b): ^{13}C NMR spectrum of *Table 4* compound **18** (as formate salt) in CD_3OD.

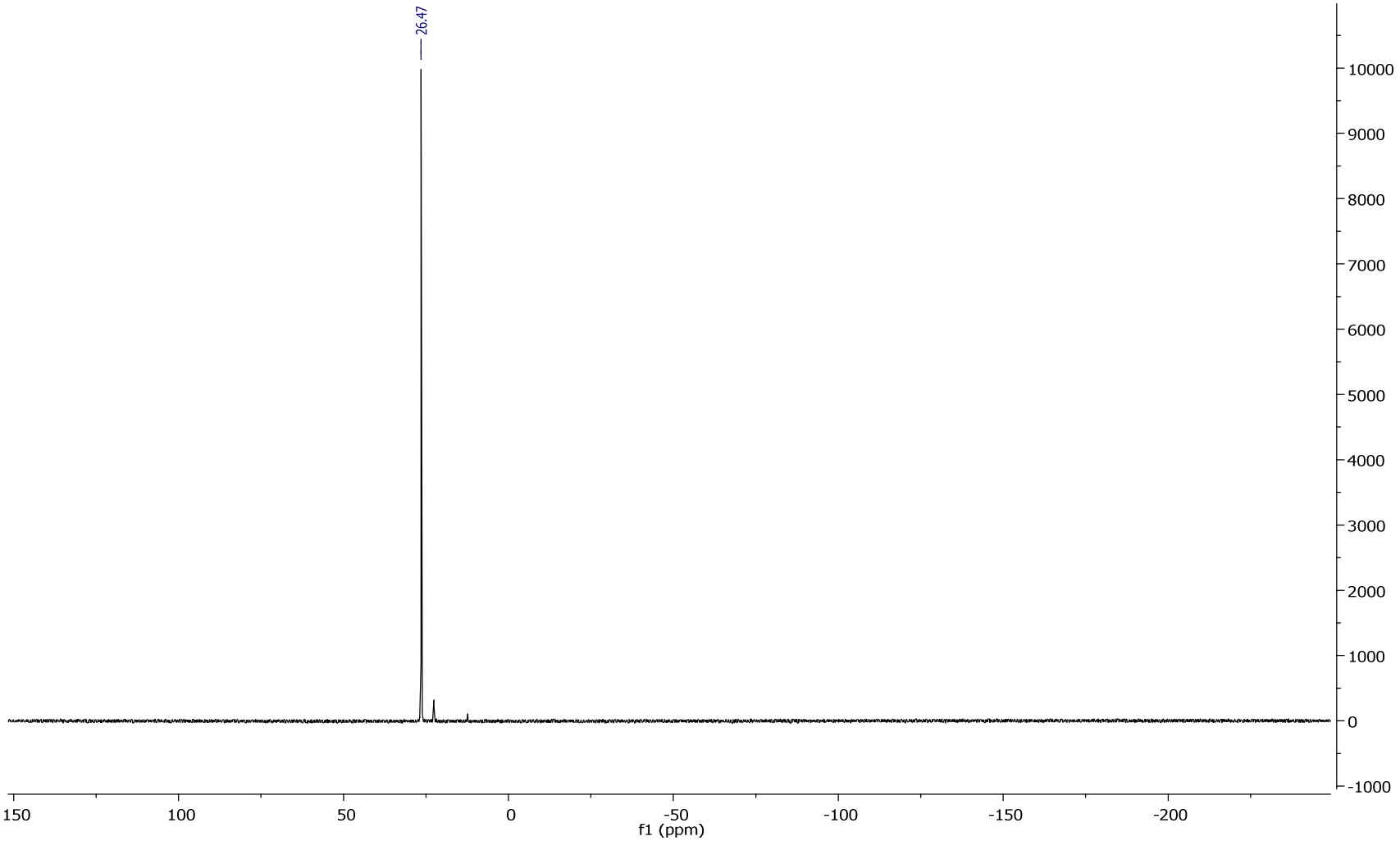

Figure N17, (c): ^{31}P NMR spectrum of *Table 4* compound **18** (as formate salt) in CD_3OD.

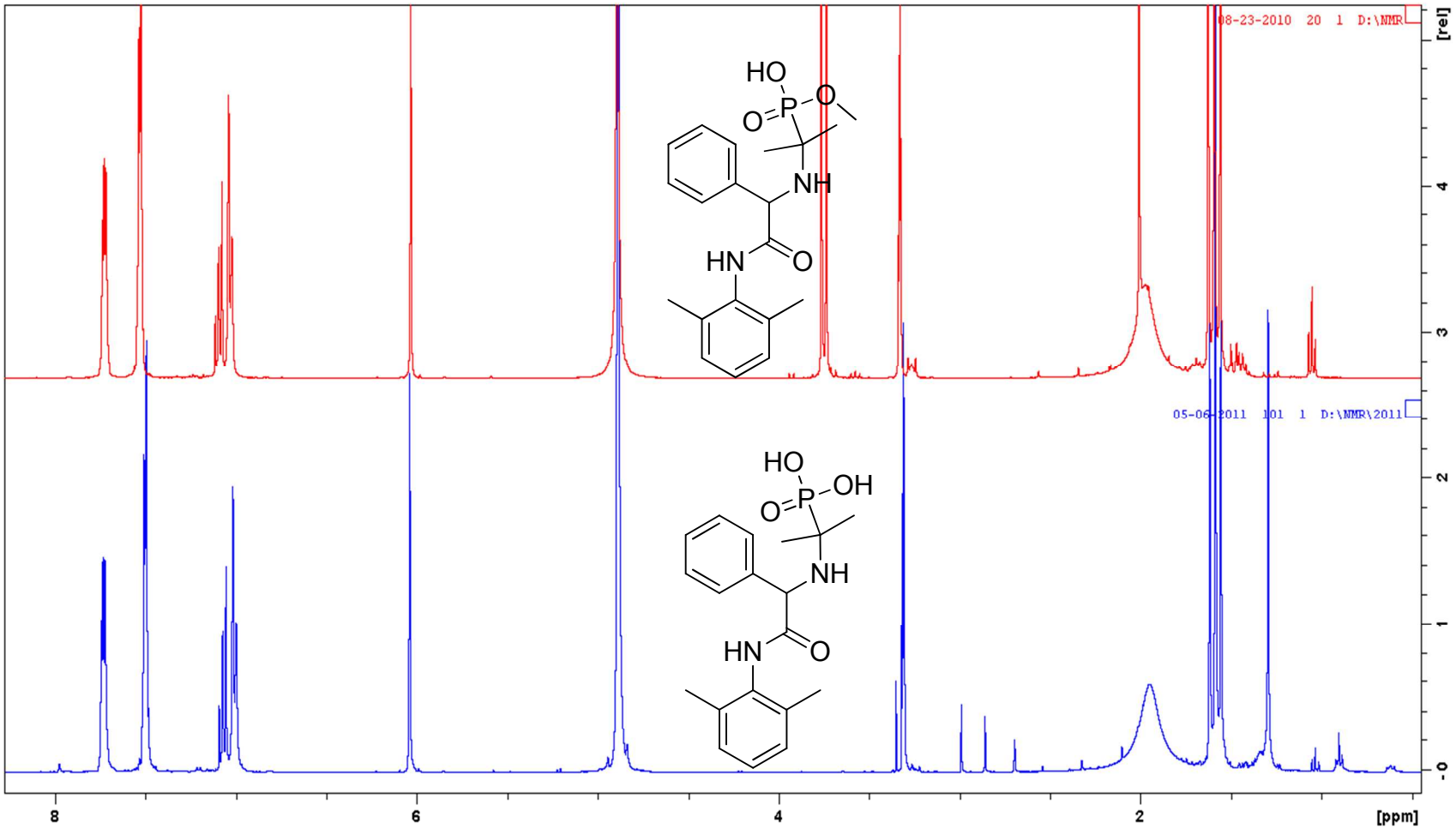

Figure N18: Overlay of ^{1}H NMR spectra of *Table 3* compound **1** (red trace, methyl phosphonate) and compound **19** (blue trace, phosphonic acid).

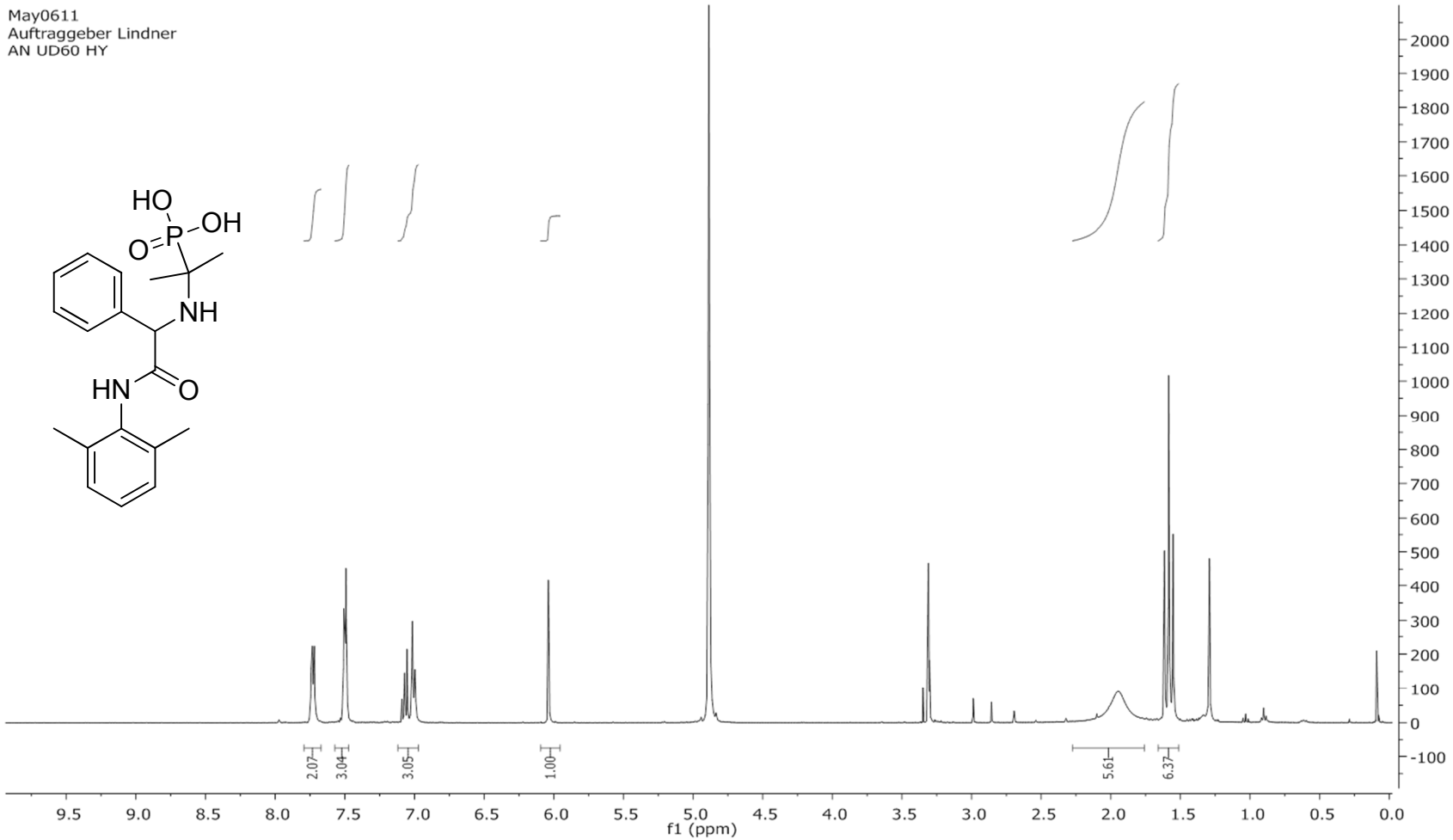

Figure N19, (a):[1]H NMR spectrum of compound **19** in CD_3OD (hydrolysis product of *Table 3* compound **1)**.

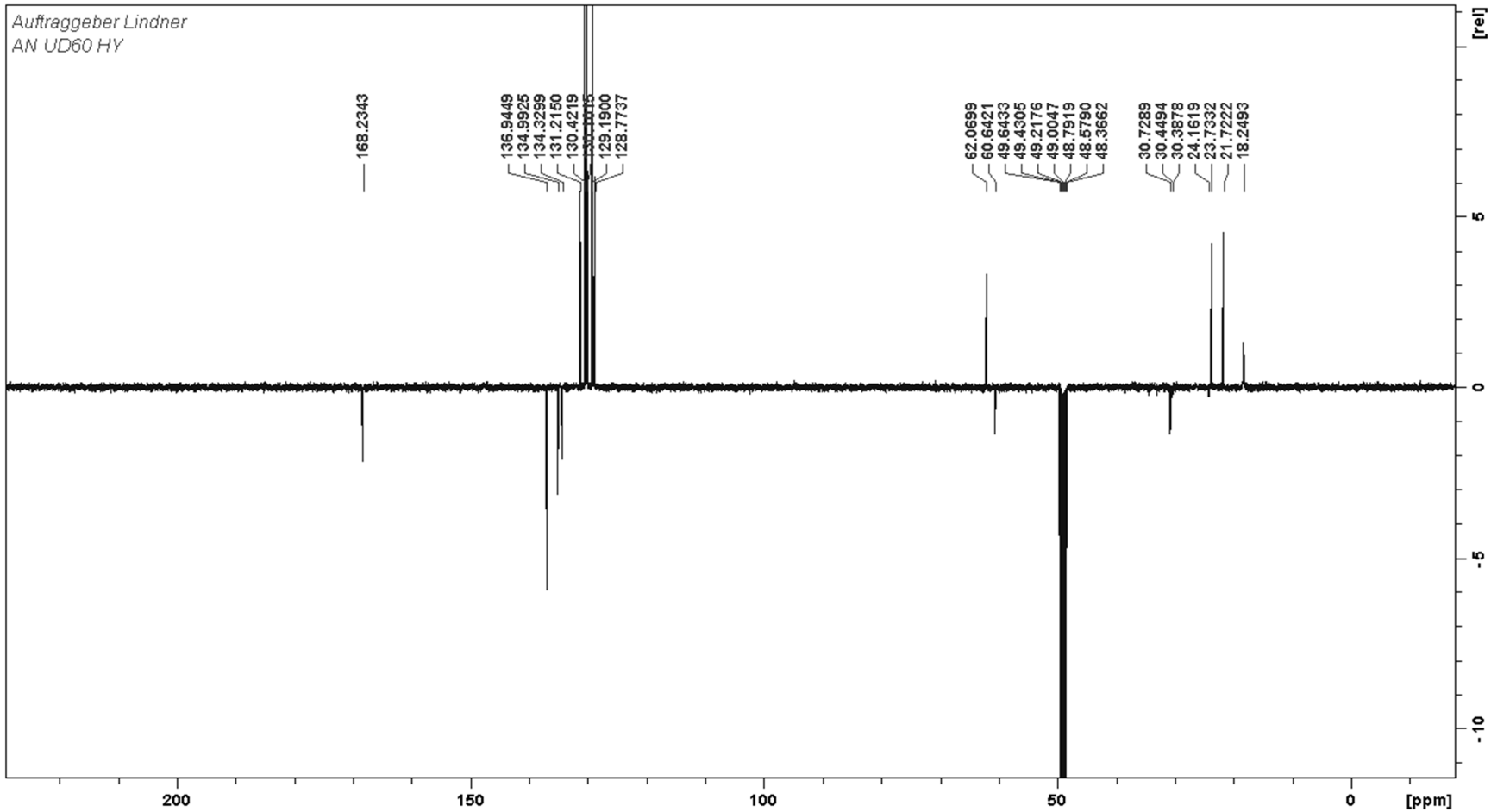

Figure N19, (b): ^{13}C NMR spectrum of compound **19** in CD_3OD (hydrolysis product of *Table 3* compound **1)**.

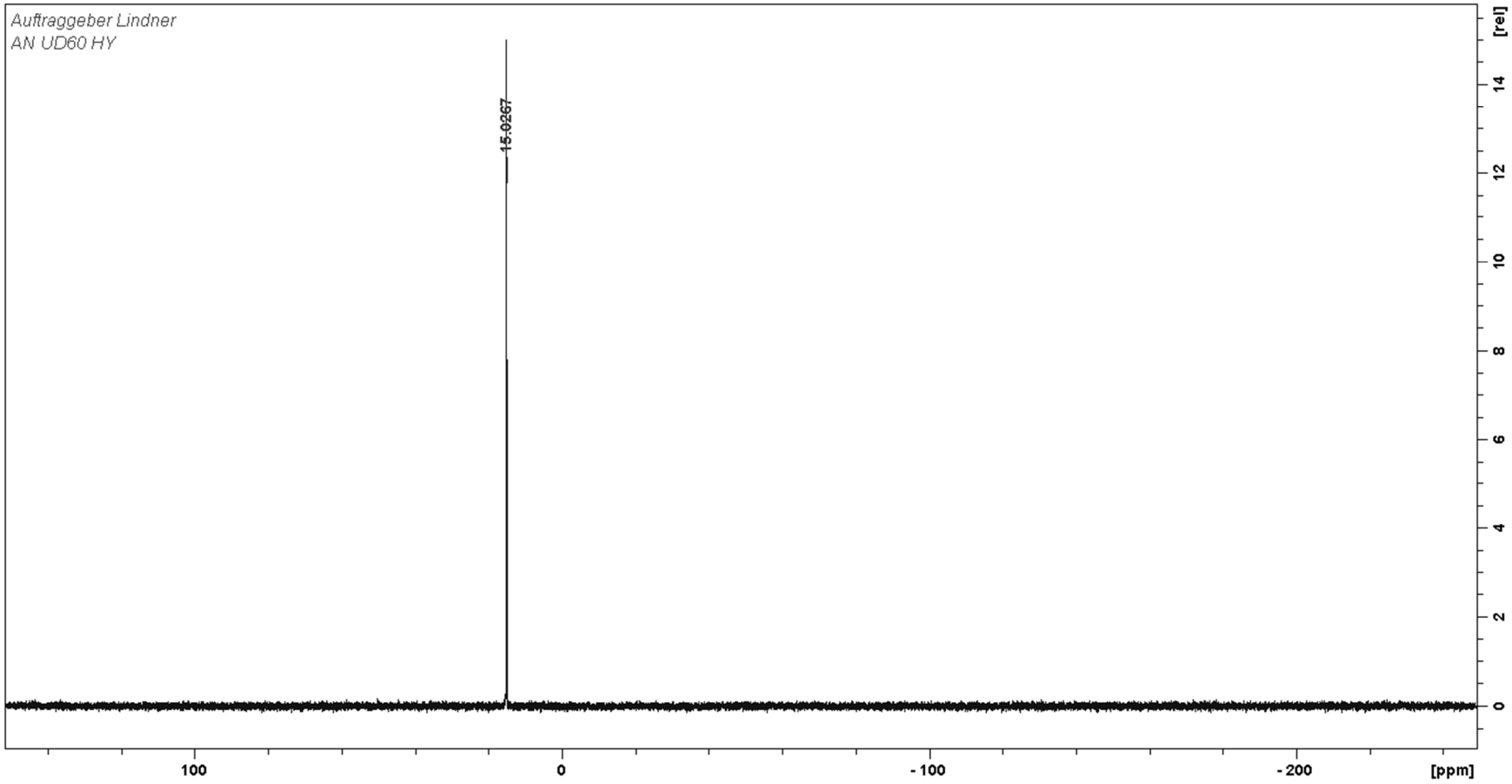

Figure N19, (c): ^{31}P NMR spectrum of compound **19** in CD_3OD (hydrolysis product of *Table 3* compound **1)**.

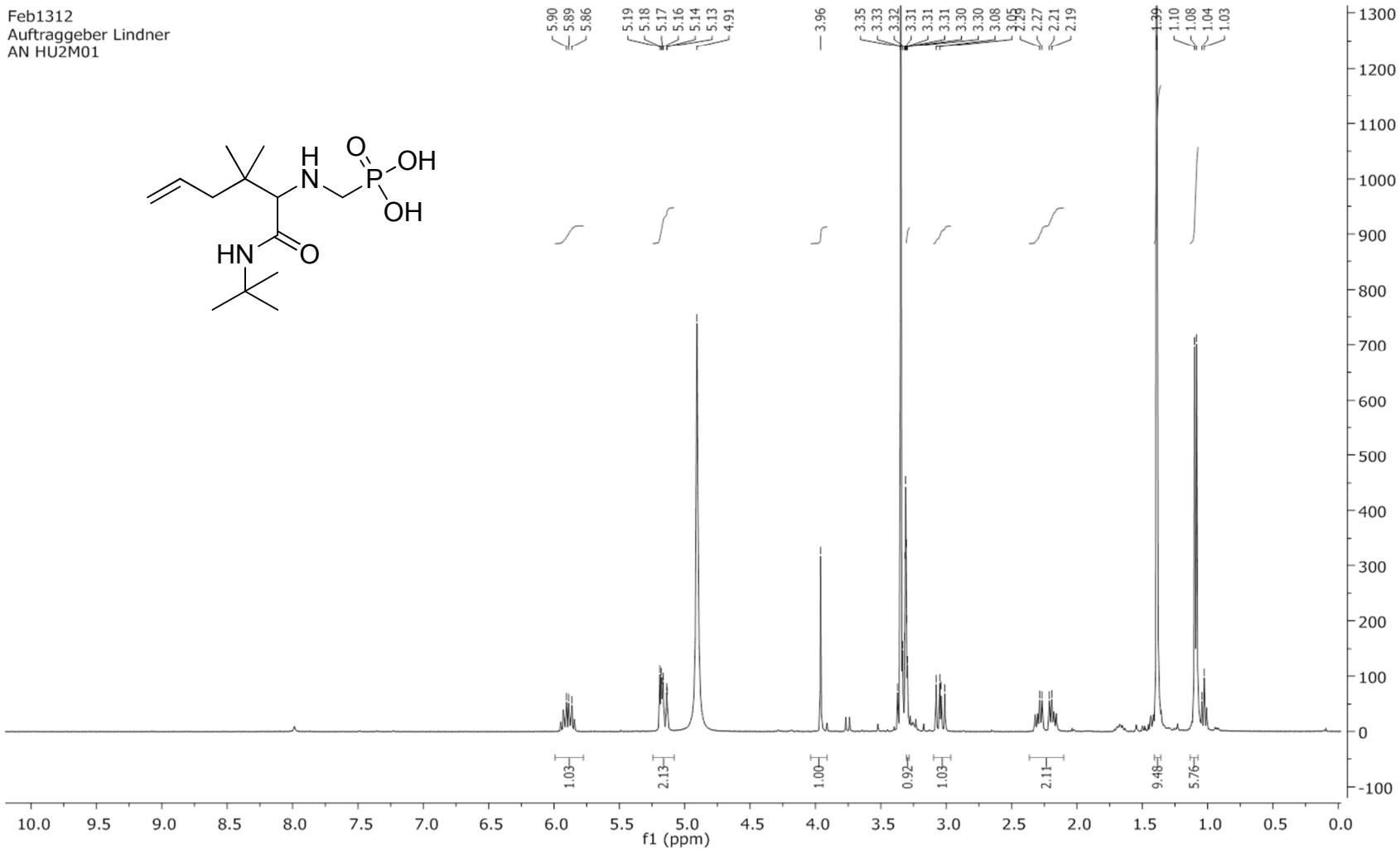

Figure N20, (a):[1]H NMR spectrum of compound **20** in CD_3OD (hydrolysis product of *Table 3* compound **11)**.

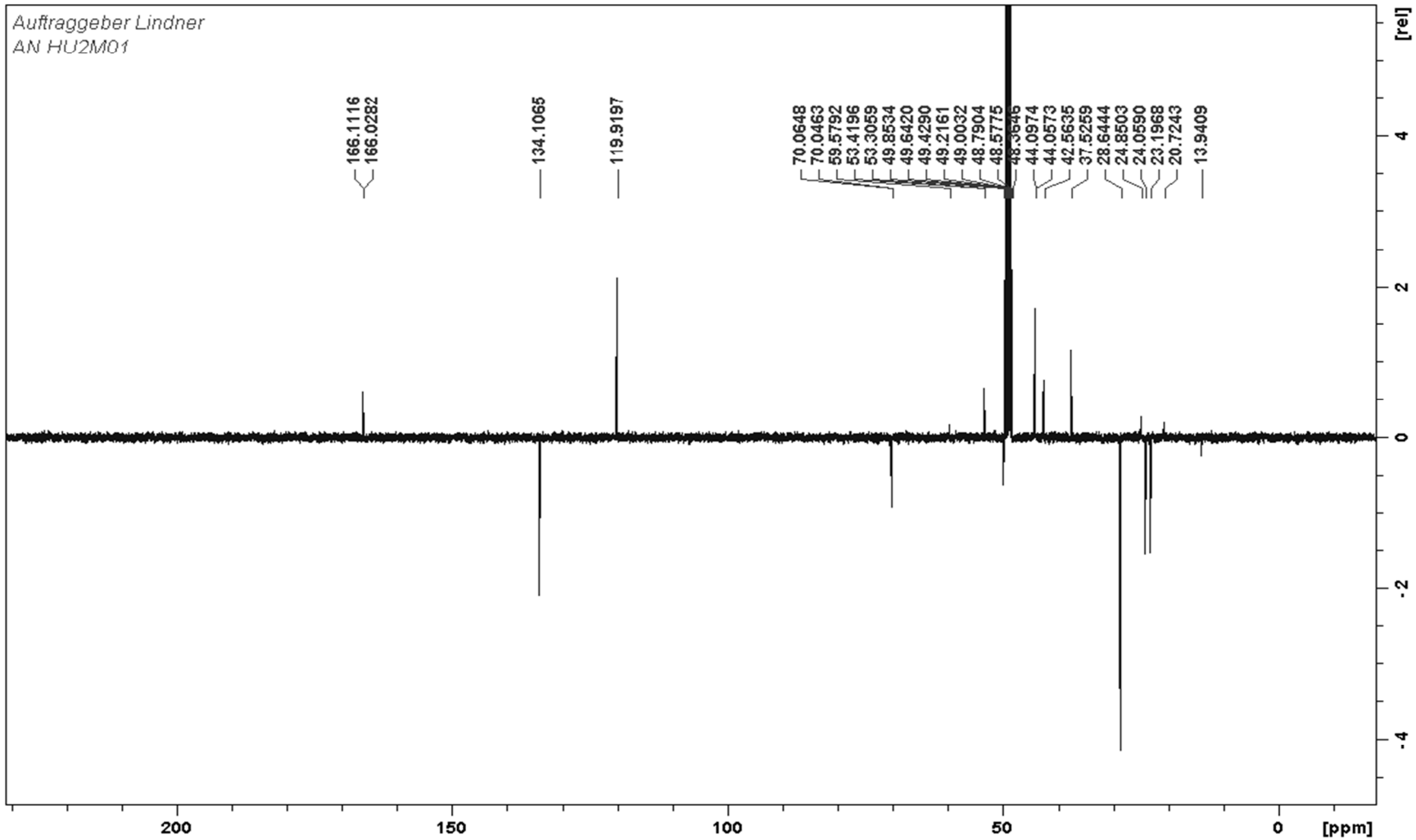

Figure N20, (b): ^{13}C NMR spectrum of compound **20** in CD_3OD (hydrolysis product of *Table 3* compound **11)**.

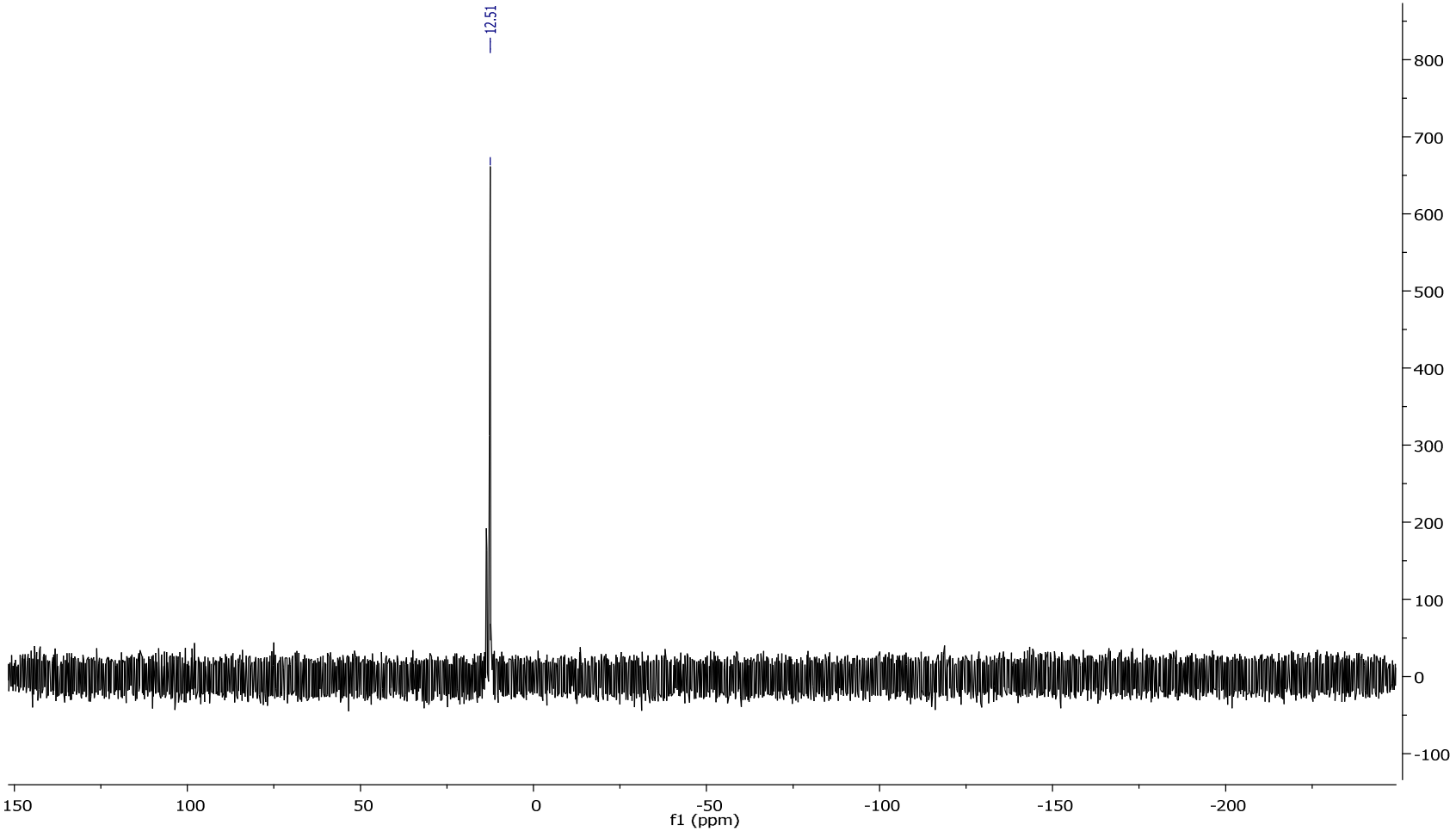

Figure N20, (c): ^{31}P NMR spectrum of compound **20** in CD_3OD (hydrolysis product of *Table 3* compound **11)**.

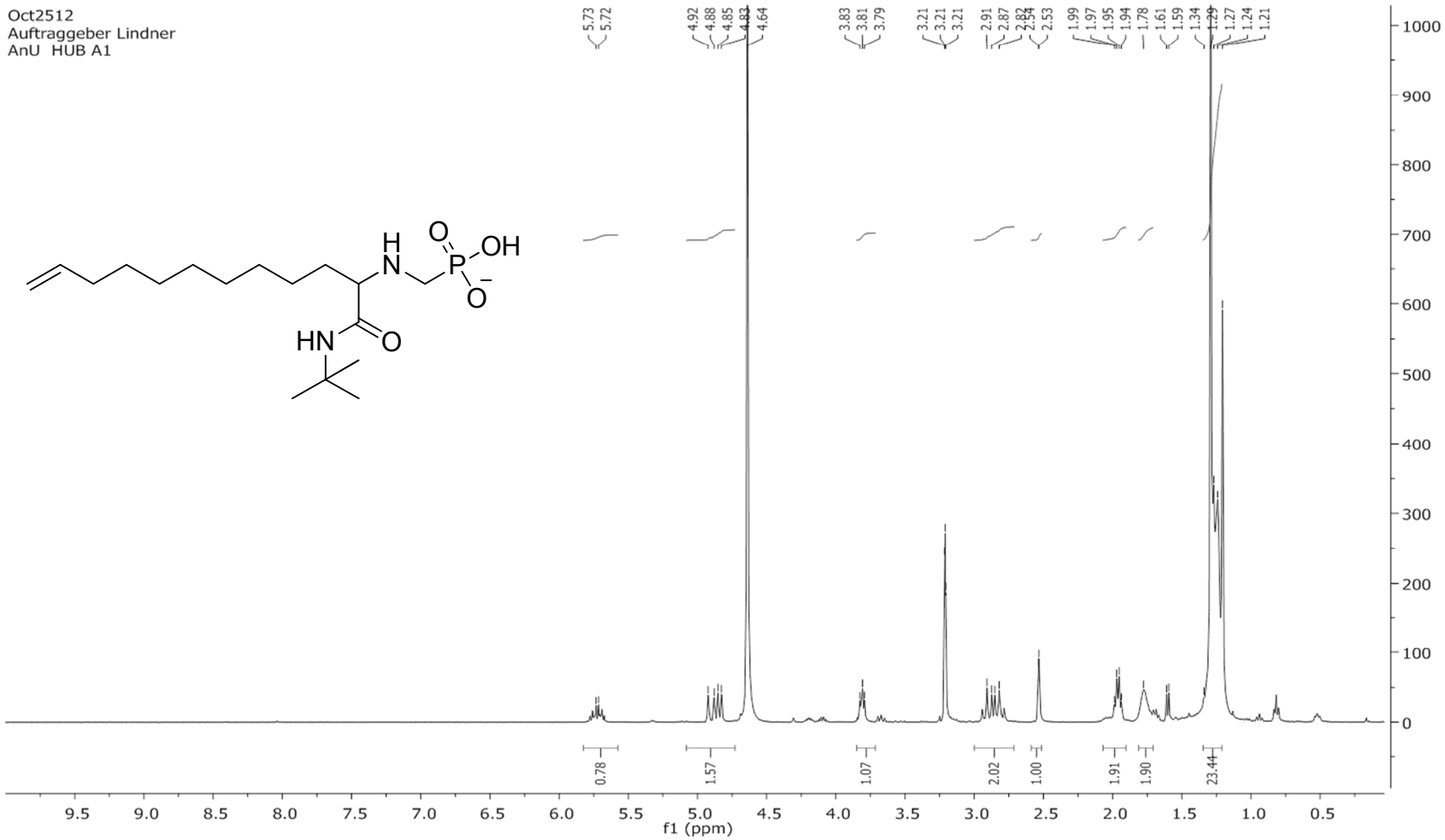

Figure N21, (a):^{1}H NMR spectrum of compound **21** in CD_3OD (hydrolysis product of *Table 3* compound **12)**.

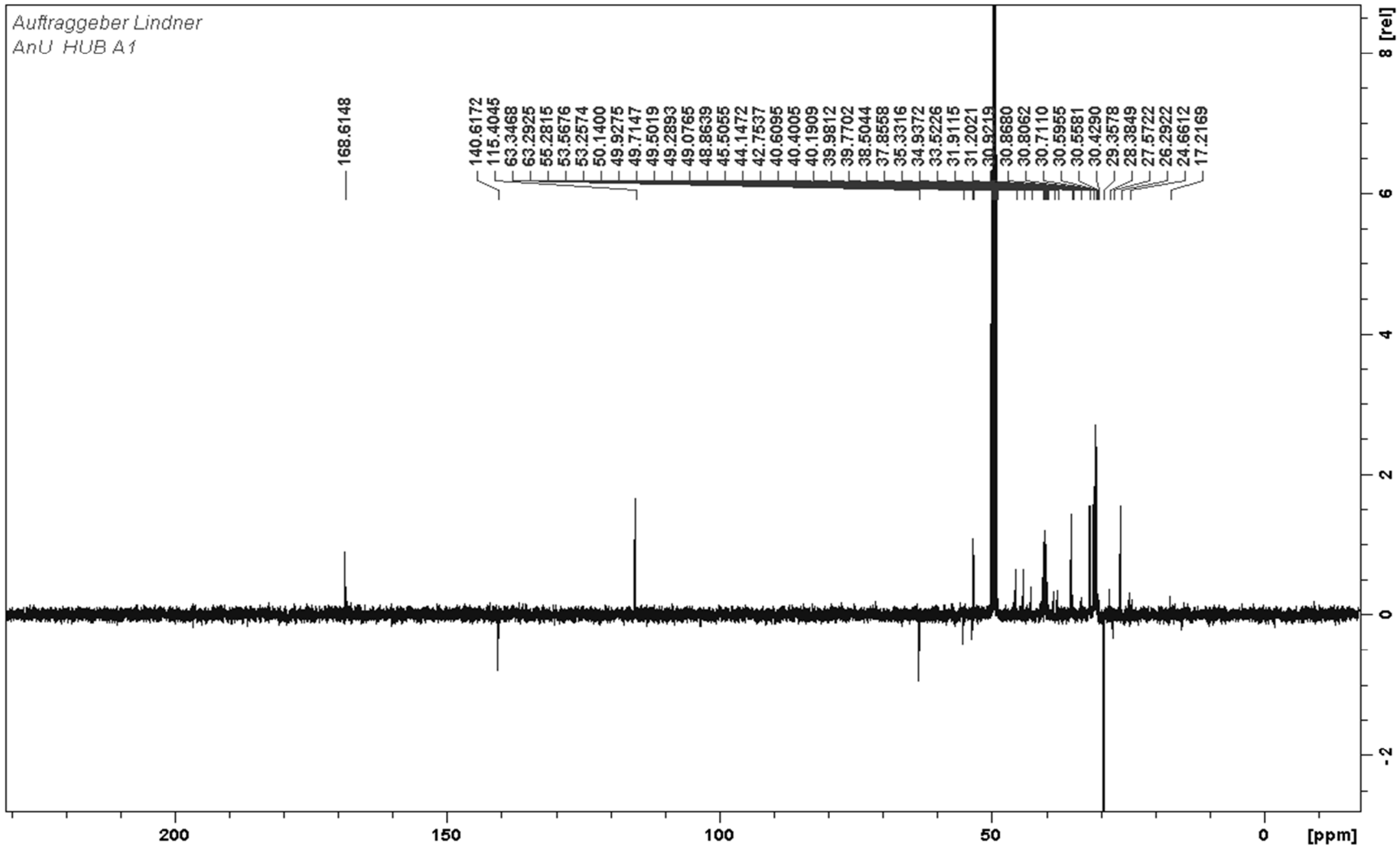

Figure N21, (b): ^{13}C NMR spectrum of compound **21** in CD_3OD (hydrolysis product of *Table 3* compound **12)**.

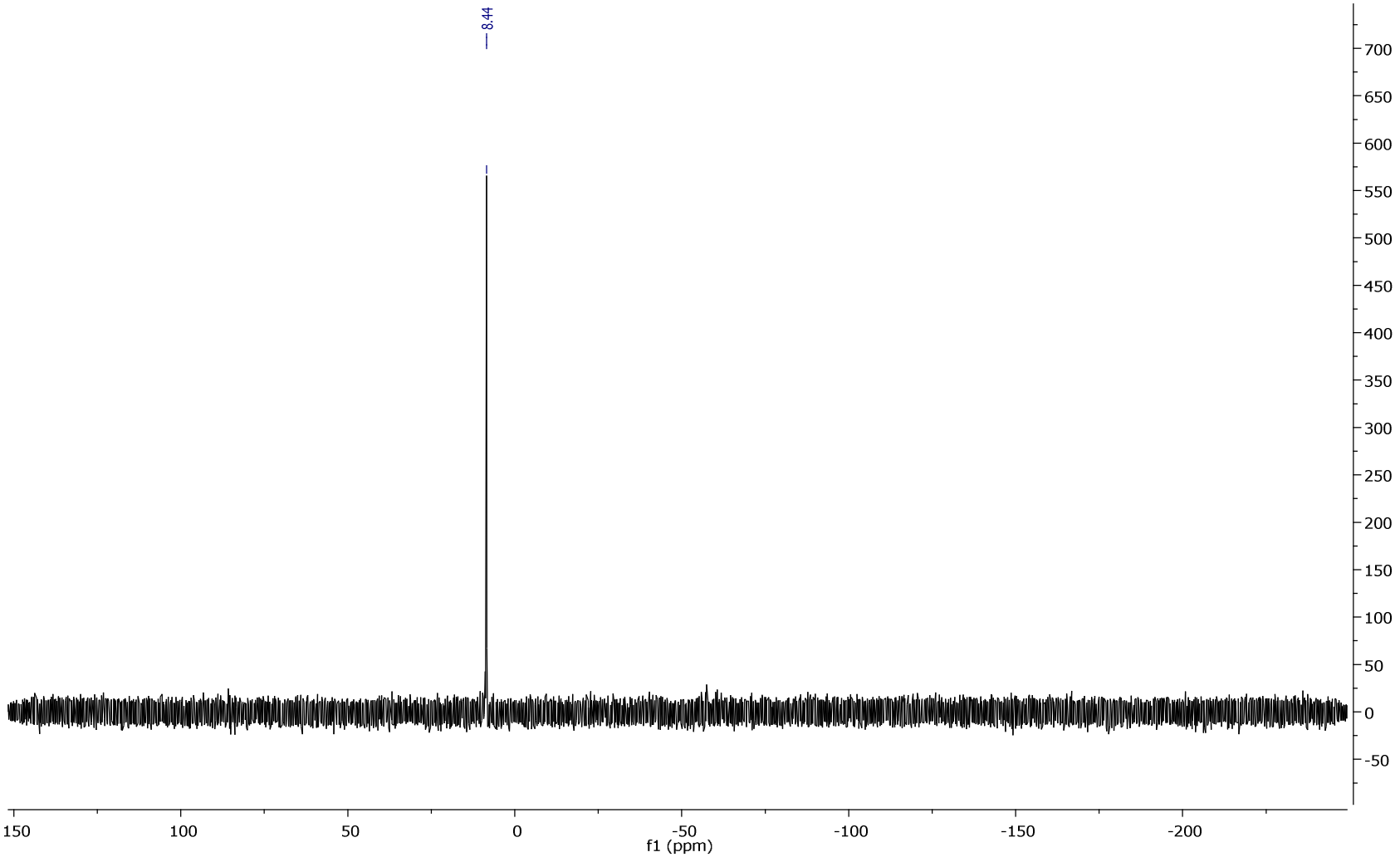

Figure N21, (c): ^{31}P NMR spectrum of compound **21** in CD_3OD (hydrolysis product of *Table 3* compound **12)**.

References

[1] A. F. G. Gargano, W. Lindner, M. Lämmerhofer, *Journal of Chromatography A* **2013**, *Accepted*.
[2] G. Auger, J. van Heijenoort, D. Blanot, C. Deprun, *Journal für Praktische Chemie/Chemiker-Zeitung* **1995**, *337*, 351-357.
[3] B. Costisella, H. Gross, *Journal für Praktische Chemie* **1977**, *319*, 8-16.
[4] L. D. Quin, G. S. Quin, *Comparative Biochemistry and Physiology Part B: Biochemistry and Molecular Biology* **2001**, *128*, 173-185.

[1] A. F. G. Gargano, W. Lindner, M. Lämmerhofer, *Journal of Chromatography A* **2013**, *Accepted*.
[2] G. Auger, J. van Heijenoort, D. Blanot, C. Deprun, *Journal für Praktische Chemie/Chemiker-Zeitung* **1995**, *337*, 351-357.
[3] B. Costisella, H. Gross, *Journal für Praktische Chemie* **1977**, *319*, 8-16.
[4] L. D. Quin, G. S. Quin, *Comparative Biochemistry and Physiology Part B: Biochemistry and Molecular Biology* **2001**, *128*, 173-185.

[1] A. F. G. Gargano, W. Lindner, M. Lämmerhofer, *Journal of Chromatography A* **2013**, *Accepted*.
[2] G. Auger, J. van Heijenoort, D. Blanot, C. Deprun, *Journal für Praktische Chemie/Chemiker-Zeitung* **1995**, *337*, 351-357.
[3] B. Costisella, H. Gross, *Journal für Praktische Chemie* **1977**, *319*, 8-16.
[4] L. D. Quin, G. S. Quin, *Comparative Biochemistry and Physiology Part B: Biochemistry and Molecular Biology* **2001**, *128*, 173-185.

[1] A. F. G. Gargano, W. Lindner, M. Lämmerhofer, *Journal of Chromatography A* **2013**, *Accepted*.
[2] G. Auger, J. van Heijenoort, D. Blanot, C. Deprun, *Journal für Praktische Chemie/Chemiker-Zeitung* **1995**, *337*, 351-357.
[3] B. Costisella, H. Gross, *Journal für Praktische Chemie* **1977**, *319*, 8-16.
[4] L. D. Quin, G. S. Quin, *Comparative Biochemistry and Physiology Part B: Biochemistry and Molecular Biology* **2001**, *128*, 173-185.